

INAOE • 2&4 September 2014

# The study of star-forming dwarf galaxies with IFS

Polychronis Papaderos

Centro de Astrofísica da Universidade do Porto (CAUP)  
 & Instituto de Astrofísica e Ciências do Espaço

# Spectroscopic surveys of emission-line & UV-excess galaxies

(a substantial fraction of which are star-forming dwarf galaxies – SFDGs)

PARTIAL LIST OF PREVIOUS SCHMIDT/OBJECTIVE-PRISM SURVEYS

Survey Name (1)	Type <sup>a</sup> (2)	Area (deg <sup>2</sup> ) (3)	Number of Objects (4)	Density (deg <sup>-2</sup> ) (5)	Completeness <sup>b</sup> Limit ( $m_B$ ) (6)	Ref. (7)
Haro .....	C	Lots	~ 40	Small	??	1
Kiso .....	C	5100	8162	1.60	16.0	2
Montreal.....	C	4400	469	0.11	14.8	3
→ Markarian .....	UV	15000	1500	0.10	15.2	4
→ Tololo .....	L	1225	201	0.16	...	5
→ UM .....	L	667	349	0.52	(16.9)	6
Wasilewski .....	L	825	96	0.18	(15.2)	7
→ POX .....	L	82	23	0.28	(16.0)	8
ESO—H $\alpha$ .....	L	400	113	0.28	...	9
UCM.....	L	471	263	0.56	(~ 16.5)	10
Hamburg .....	L	1248	196	0.16	...	11
Marseille .....	L	46.5	92	1.98	(~ 16.0)	12
Case .....	UV+L	1440	1551	0.94	16.0	13
→ SBS .....	UV+L	~ 990	~ 1300	1.31	(~ 17.0)	14
KISS—red .....	L	62.2	1128	18.14	(18.1)	15
KISS—blue.....	L	116.6	223	1.91	(18.2)	15

<sup>a</sup> (C) Color selected; (UV) UV-excess selected; (L) line selected.

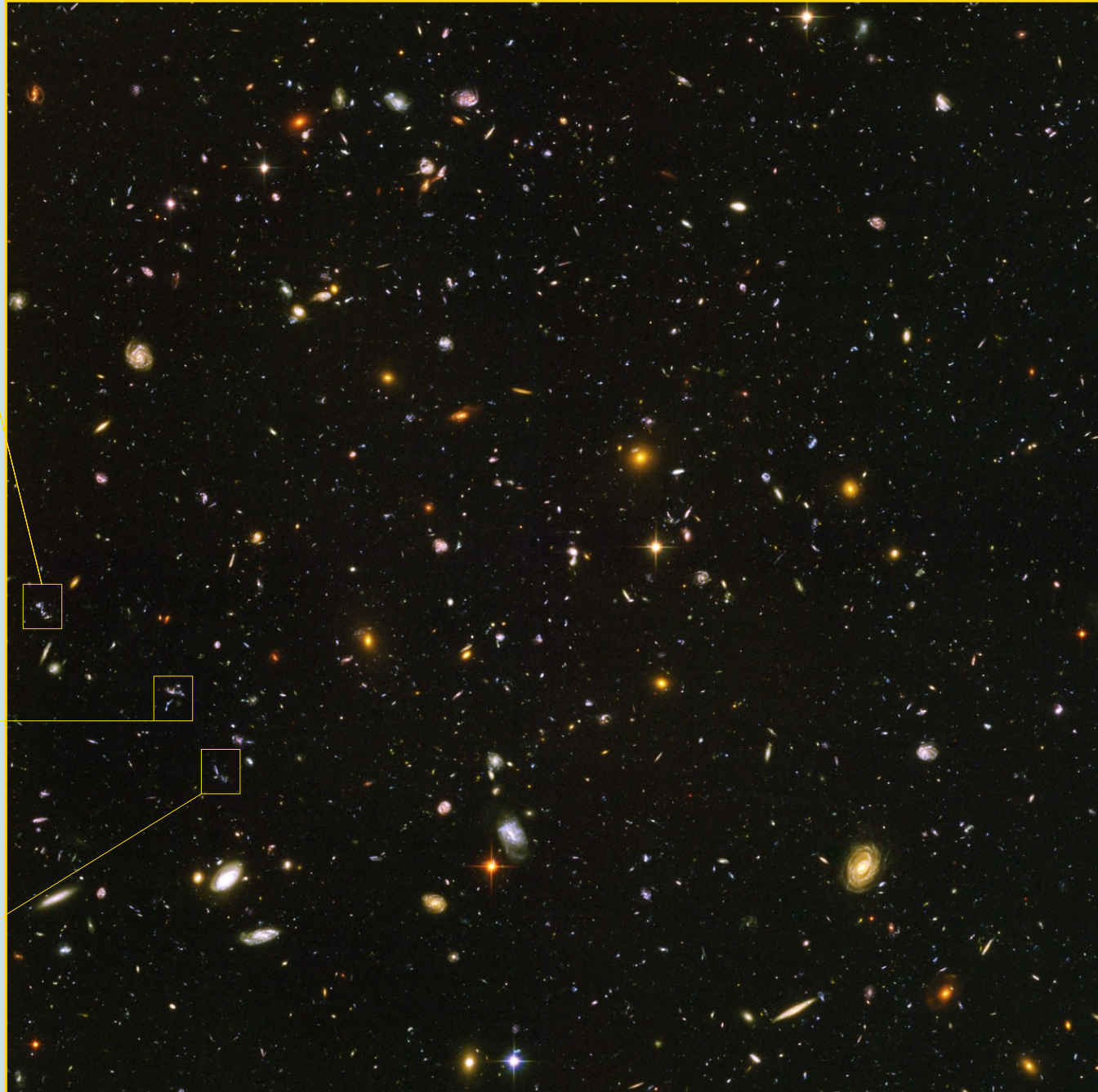
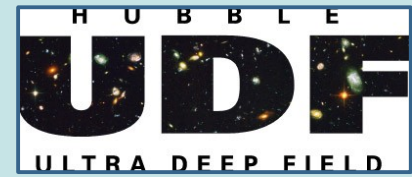
<sup>b</sup> Values in parentheses are median apparent magnitudes for that survey, not a completeness limit.

REFERENCES.—(1) Haro 1956; (2) Takase & Miyauchi-Isobe 1983; (3) Coziol et al. 1993, 1997; (4) Markarian 1967, Markarian et al. 1981; (5) Smith 1975, Smith et al. 1976; (6) MacAlpine et al. 1977, MacAlpine & Williams 1981; (7) Wasilewski 1983; (8) Kunth, Sargent, & Kowal 1981; (9) Wamsteker et al. 1985; (10) Zamorano et al. 1994, 1996; (11) Popescu et al. 1996; (12) Surace & Comte 1998; (13) Pesch & Sanduleak 1983, Stephenson et al. 1992; (14) Markarian et al. 1983, Markarian & Stepanian 1983, Stepanian 1994; (15) this paper, Salzer et al. 2000a, 2000b.



# Extragalactic systems in the distant universe

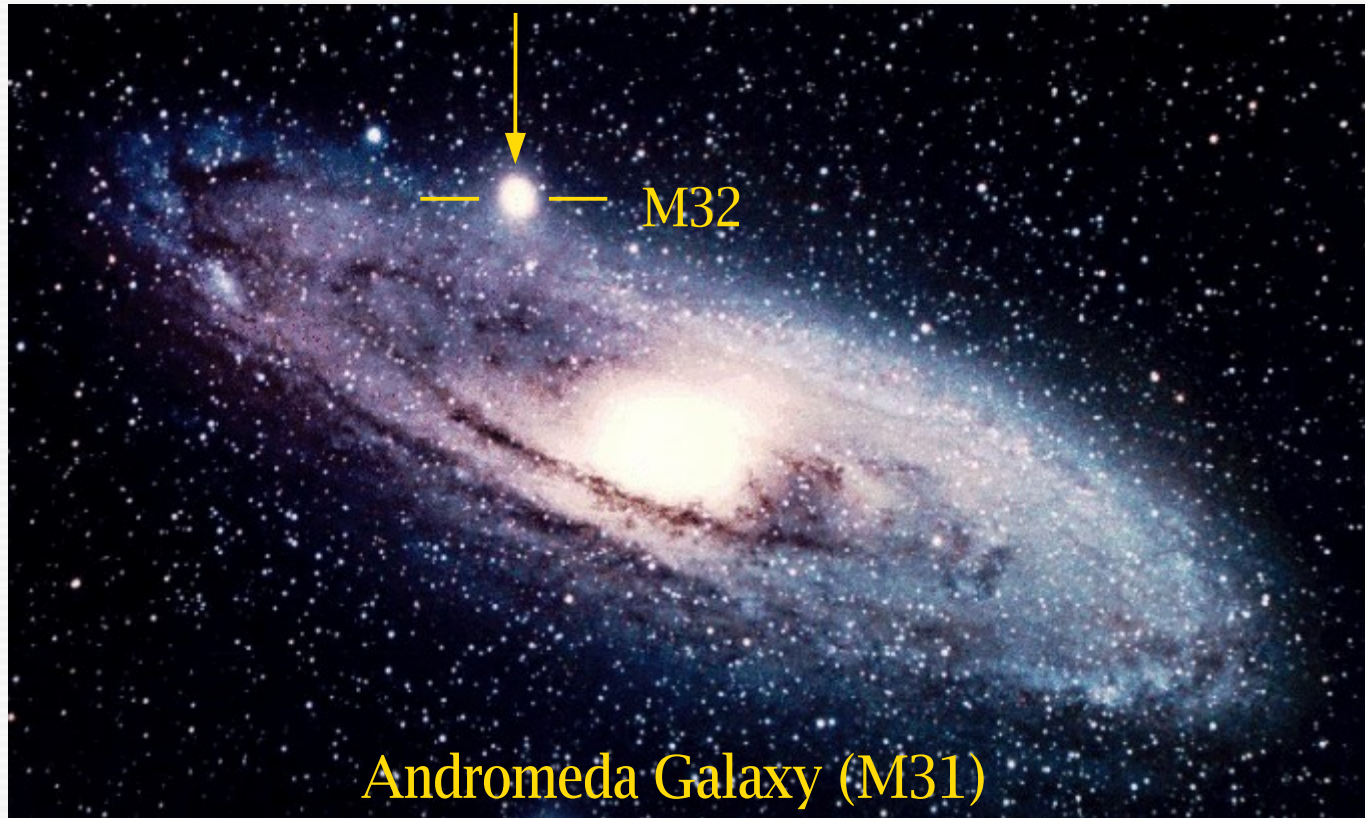
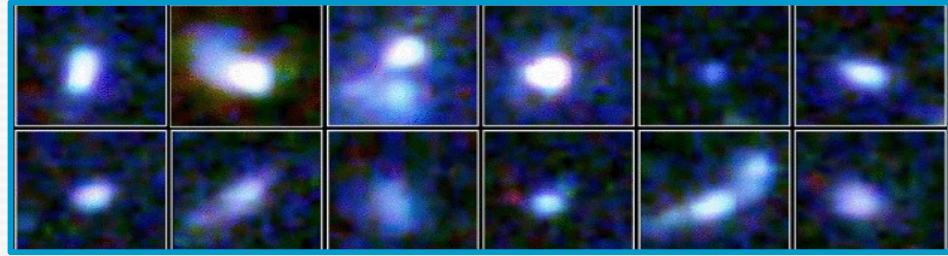
Blue, irregular sub-galactic units in the process of merging





# Compact low-mass starburst galaxies in the distant Universe

- compact narrow-emission line galaxies – **CNELGs**
- luminous blue compact galaxies – **LBCGs**
- green peas

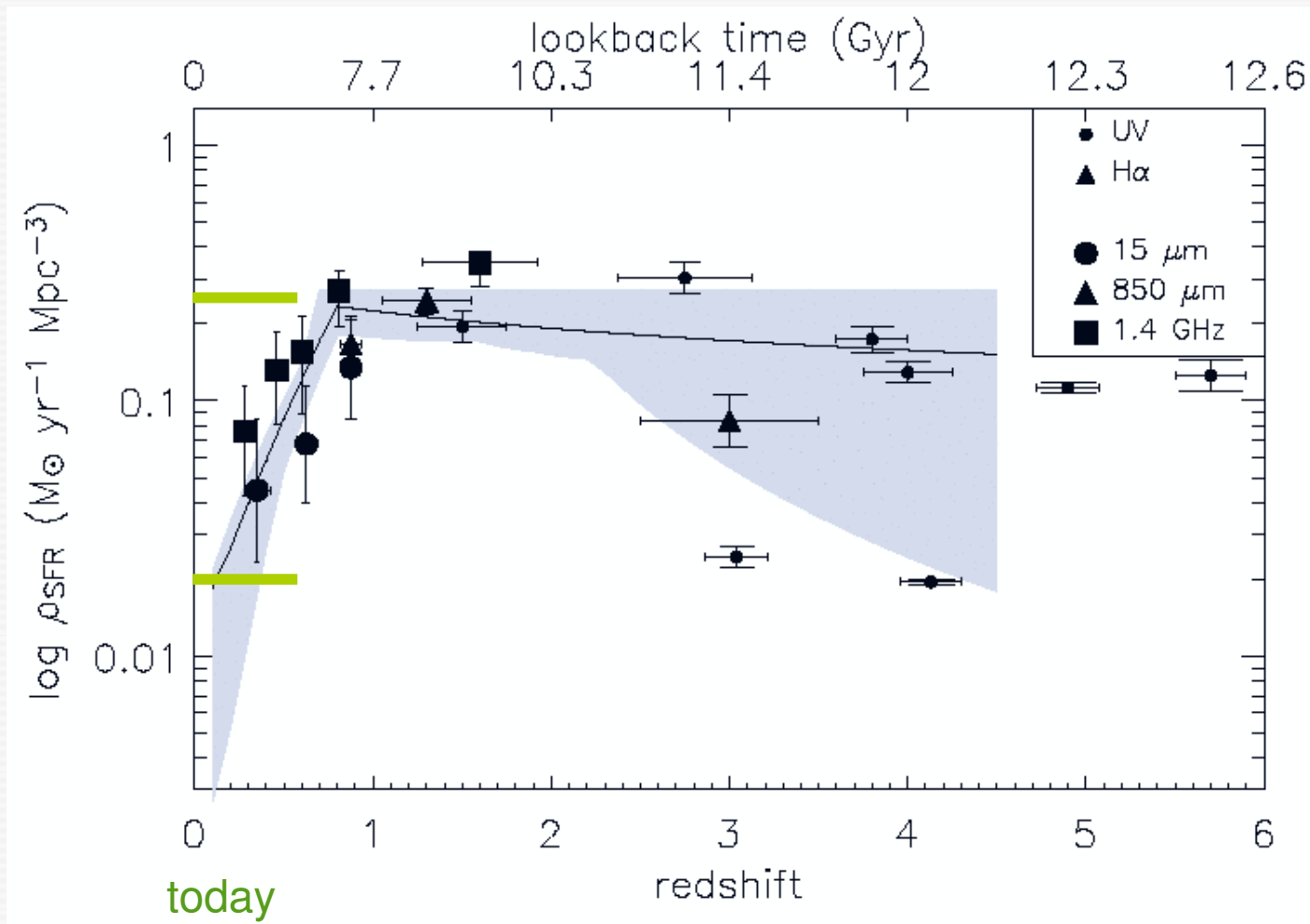


- Absolute Magnitude -10 (?) .. -19 B mag ; diameter: 0.5 ... 10 kpc (Milky Way  $\simeq$  30 kpc)
- Stellar mass  $M_*$ :  $10^6$  ...  $10^9 M_\odot$ ; i.e.  $\sim 1/10^4$  ...  $\sim 1/10$  of the mass of a spiral galaxy
- Typically irregular morphology
- blue colors  $\rightarrow$  intense, galaxy-wide star forming activity

1 kpc =  $3.1 \times 10^{19}$  m



# Evolution of the cosmic star formation rate (SFR) density

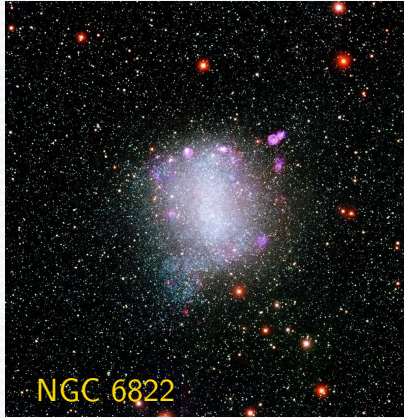


Elbaz et al. (2004)

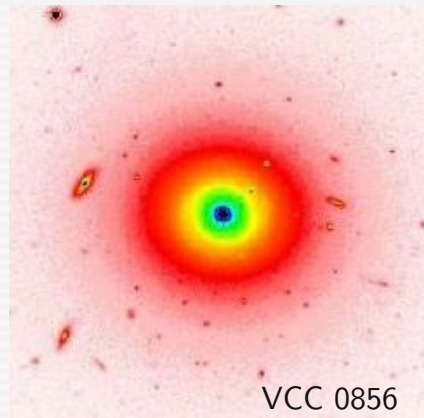
- i) Star-forming dwarf galaxies account for  $\sim 1/3$  of the cosmic SFR density at  $z \sim 1$  (cf Guzman et al. 1998)
- ii) From  $z=1$  to  $z=0$  (today) the cosmic star formation rate density has decreased by an order of magnitude. Normal galaxies underwent their major formation phase several Gyr ago. Galaxies with high **specific star formation rate** ( $\text{sSFR} = \text{SFR}/M_{\star}$ ), such as **starburst dwarf galaxies** are comparatively rare in the local Universe.

# Dwarf Galaxies in the local universe

↑ gas content  
metallicity  
↓ color: rel. blue

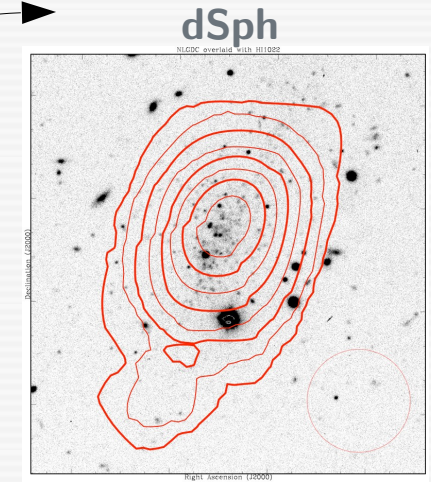


Dwarf Irregular (dI)

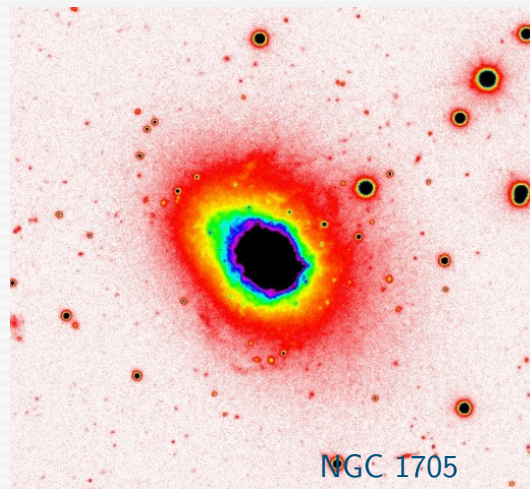


Dwarf Elliptical (dE)

↑ gas content  
metallicity  
↓ color: red



dSph



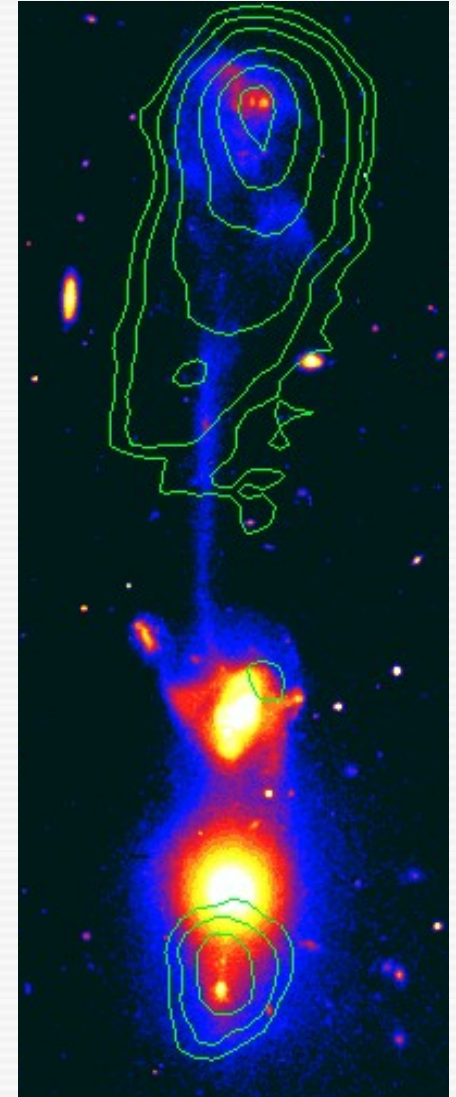
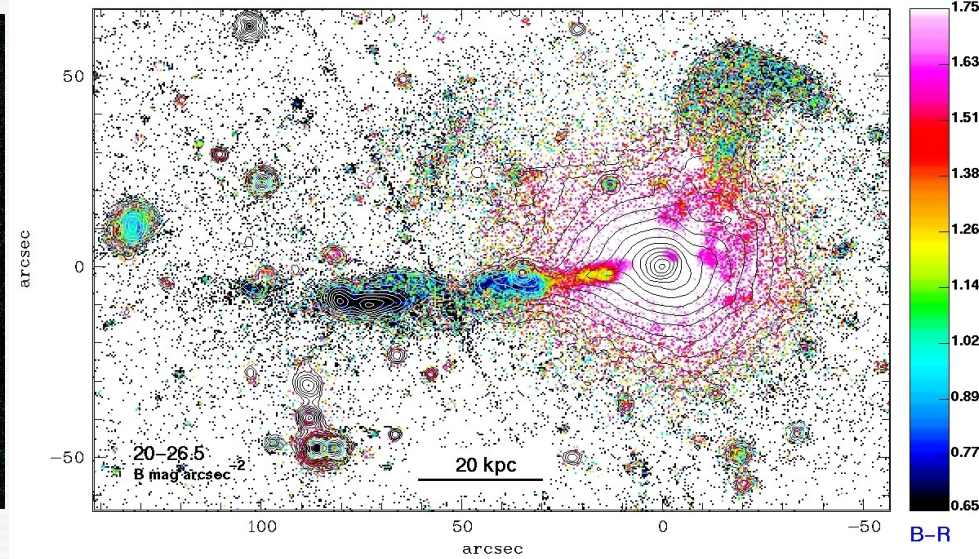
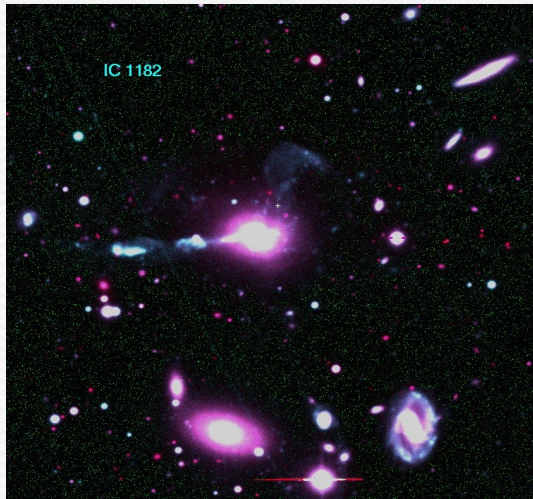
Blue Compact Dwarf (BCD/HII)  
(morphologically heterogeneous)

↑ gas content  
oxygen abundance  
↓ color: blue

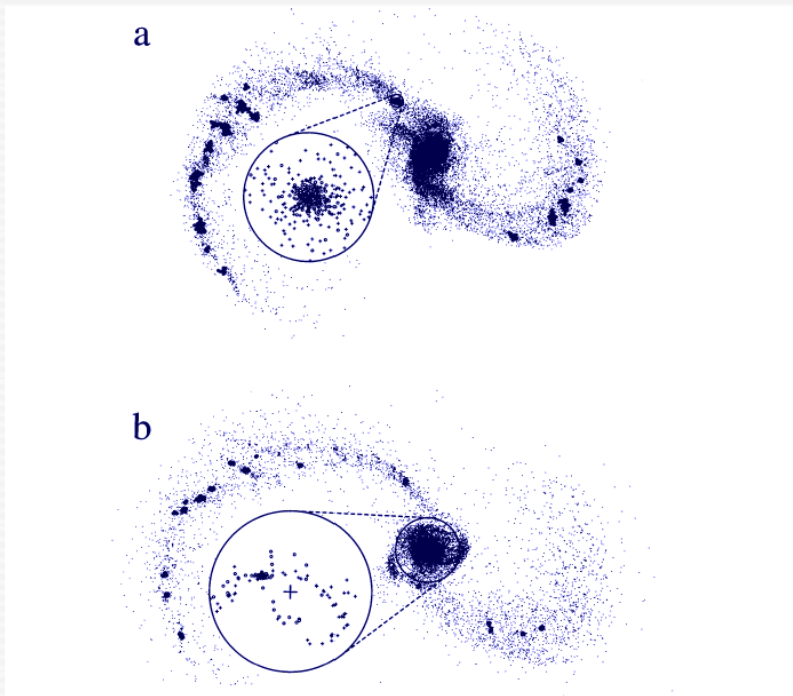
- Other recently discovered types of dwarf galaxies
- Ultra-faint dwarfs
  - Ultra-compact dwarfs
  - Tidal Dwarf Galaxies



# Tidal Dwarf Galaxies



Duc et al. (1997)



Barnes & Hernquist (1996)

Formation of low-mass self-gravitating entities out of tidally ejected matter in interacting/merging galaxy pairs.



# Why to study dwarf galaxies?

- ☐ ... dominate by number &  $\exists$  many nearby systems ←
- ☐ Building blocks of normal galaxies
- ☐ Most important sources of re-ionization
- ☐ Wide range in burst parameter, star formation rate (SFR) & specific SFR
- ☐ Most metal-poor galaxies known (the best local analogs of the first galaxies formed)
- ☐ "Simple" & dust-poor (i.e. low intrinsic extinction)

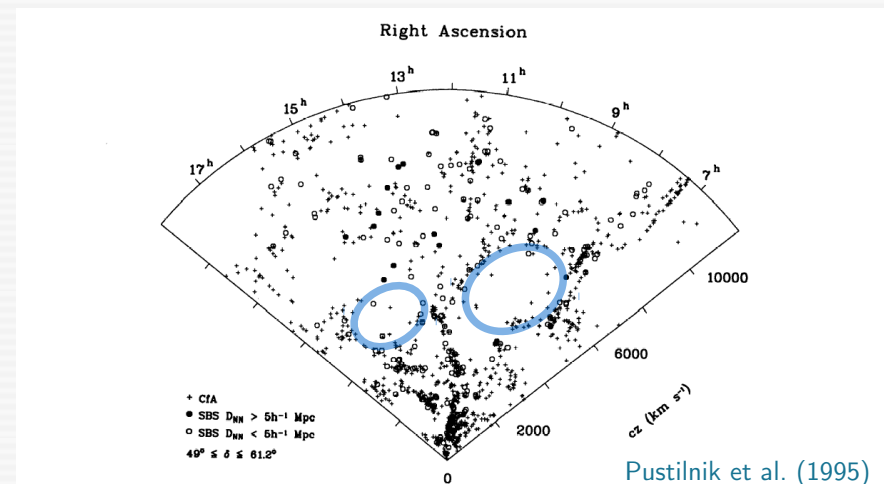
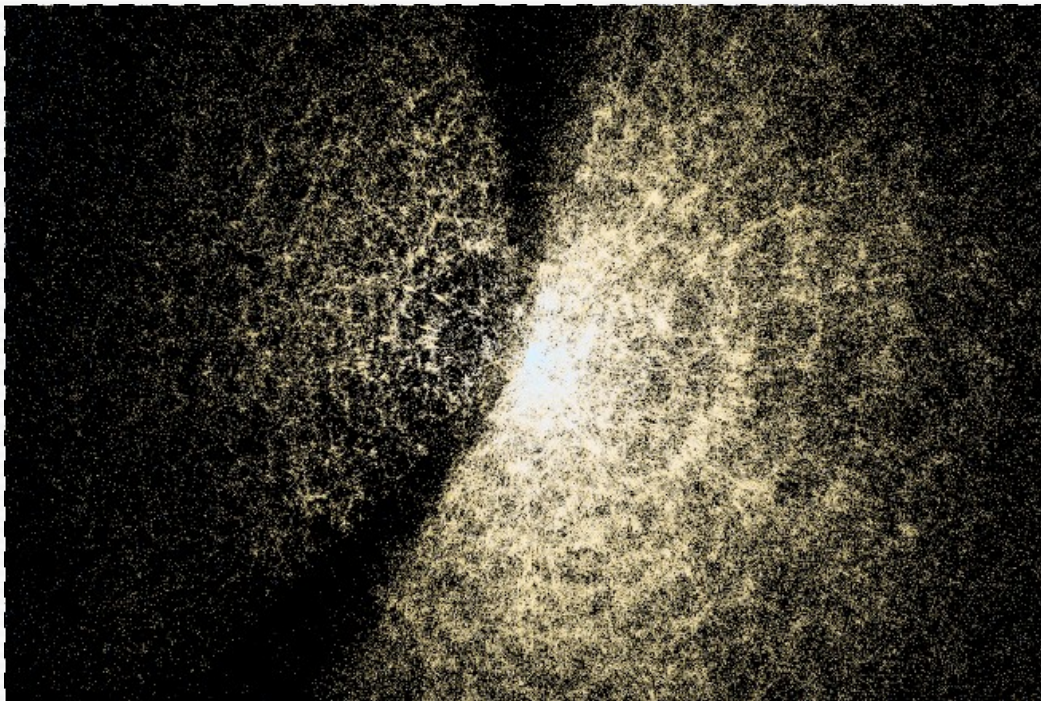
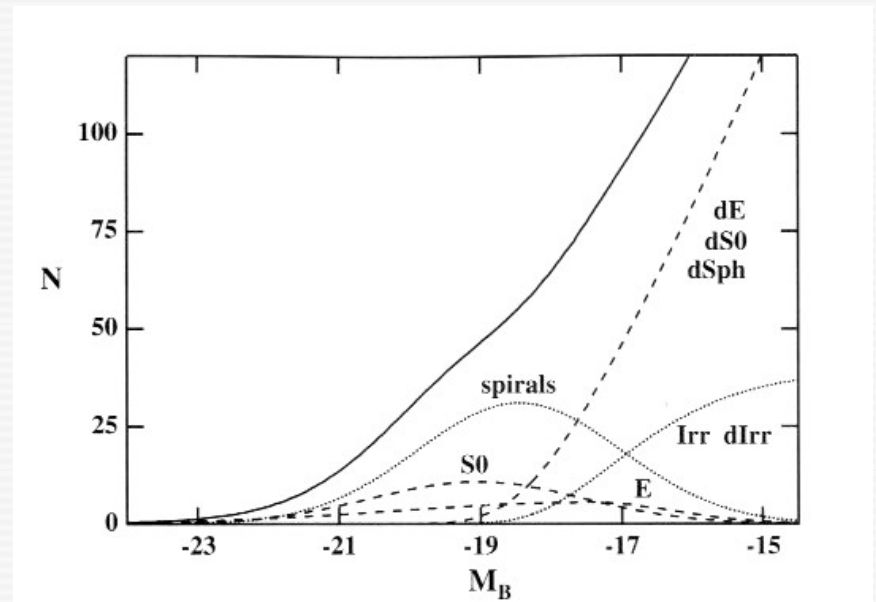


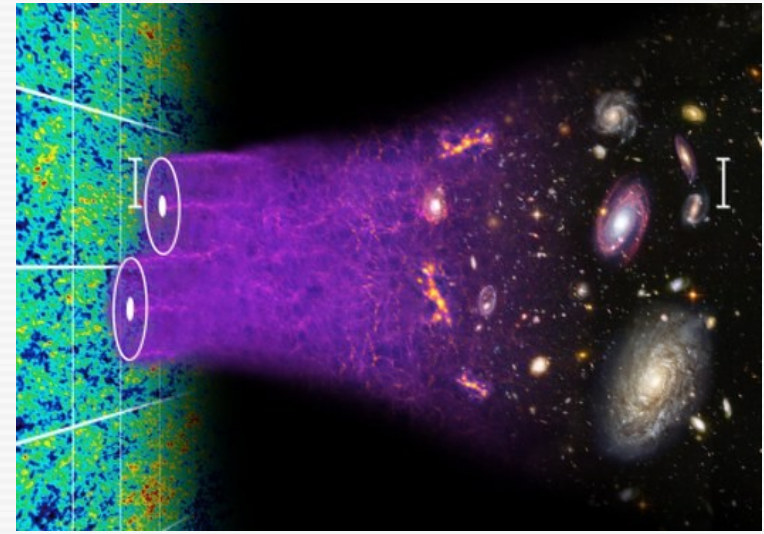
FIG. 2.—Heliocentric velocity vs. right ascension wedge diagram for the SBS zone ( $49^\circ \leq \delta \leq 61.2^\circ$ ). Bright CIA galaxies are shown as crosses, SBS BCGs without a bright neighbor within  $5 h^{-1} \text{ Mpc}$  are shown as filled circles, and SBS BCGs with a bright neighbor within  $5 h^{-1} \text{ Mpc}$  are shown as open circles.

Pustilnik et al. (1995)

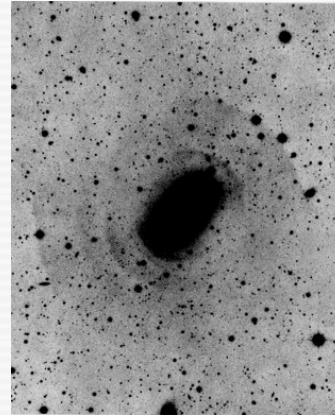


# Why to study dwarf galaxies?

- They dominate by number & are nearby
- Building blocks of normal galaxies
- Most important sources of re-ionization
- Wide range in burst parameter, star formation rate (SFR) & specific SFR
- Most metal-poor galaxies known (the best local analogs of the first galaxies formed)
- "Simple" & dust-poor (i.e. low intrinsic extinction)



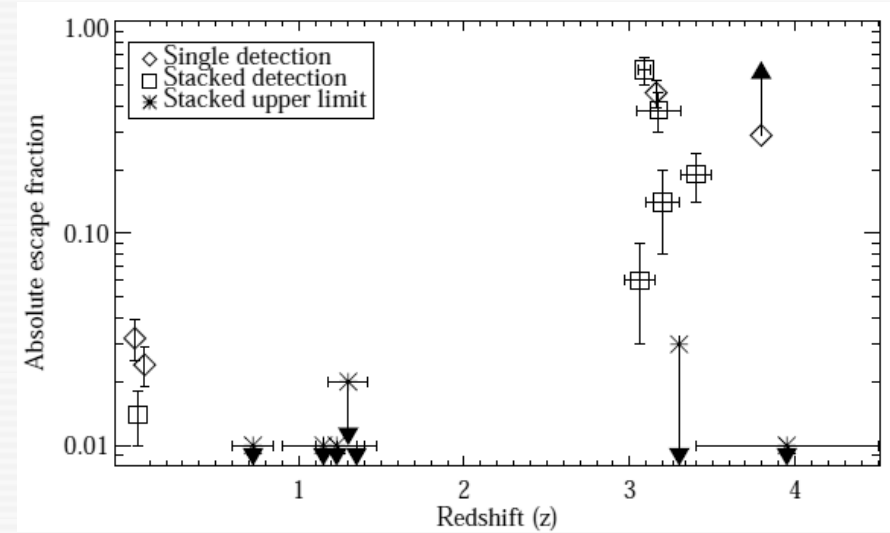
Martinez-Delgado et al. (2010)



Ripples and shells in (giant) ellipticals (example: NGC 5128; Centaurus A): relics from the infall of satellite galaxies

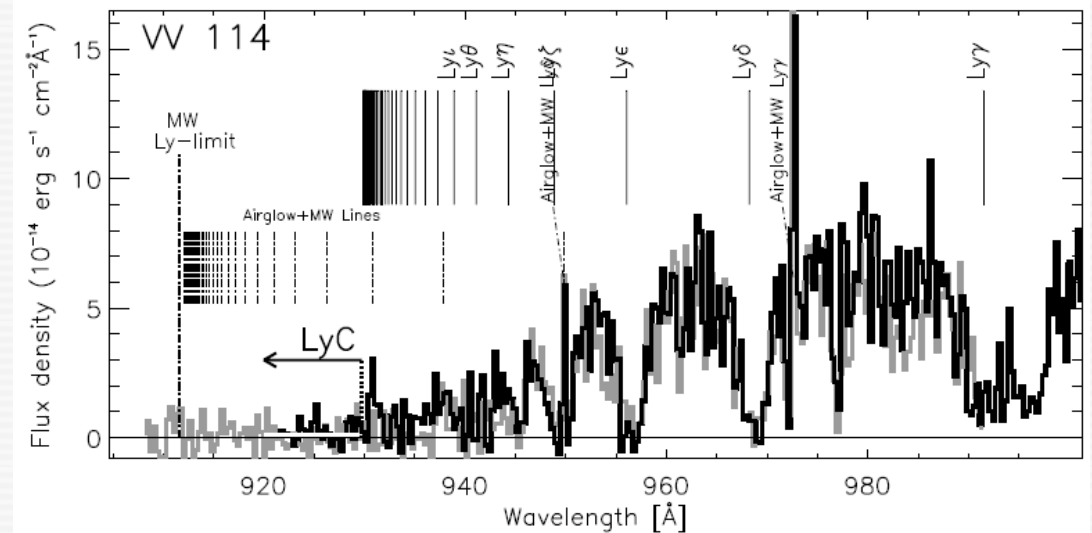
# Why to study dwarf galaxies?

- They dominate by number & nearby
- Building blocks of normal galaxies
- **Most important sources of re-ionization** ←
- Wide range in burst parameter, star formation rate (SFR) & specific SFR
- Most metal-poor galaxies known (the best local analogs of the first galaxies formed)
- "Simple" & dust-poor (i.e. low intrinsic extinction)



Bergvall et al. (2013)


- Reionization has probably been powered by massive stars / **low-mass proto-galaxies** and was finalized one Gyr ( $z \sim 6$ ) after the BB
- By then QSOs appeared (but their volume density sharply decreases for  $z > 3$ )
- Lyman continuum photon (LyC) escape from forming dwarf galaxies (!)
- Connection between **LyC** escape and **Lyman  $\alpha$**  photon emission



Leitet et al. (2013)

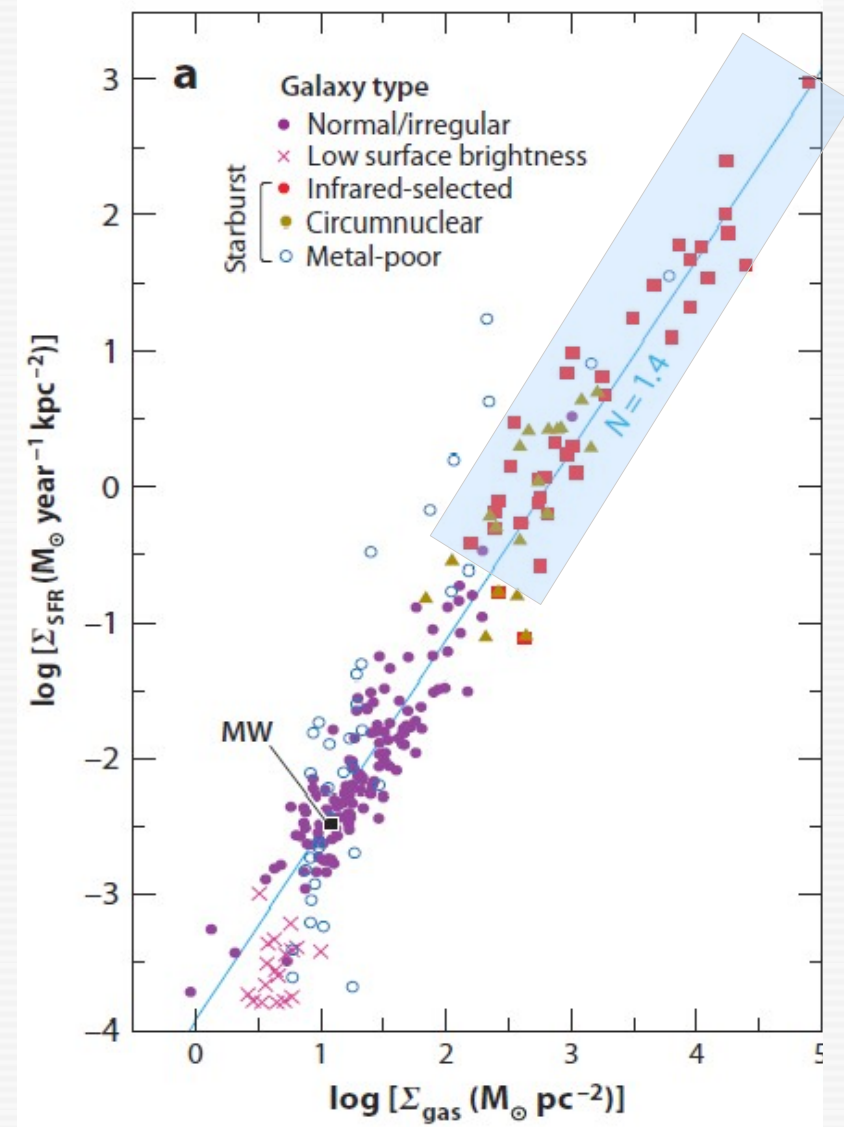


# Why to study dwarf galaxies?

- They dominate by number & nearby
- Building blocks of normal galaxies
- Most important sources of re-ionization
- Wide range in burst parameter, star formation rate (SFR) & specific SFR 
- Most metal-poor galaxies known (the best local analogs of the first galaxies formed)
- "Simple" & dust-poor (i.e. low intrinsic extinction)



HST image of the starburst component of the blue compact dwarf (BCD) galaxy He 2-10

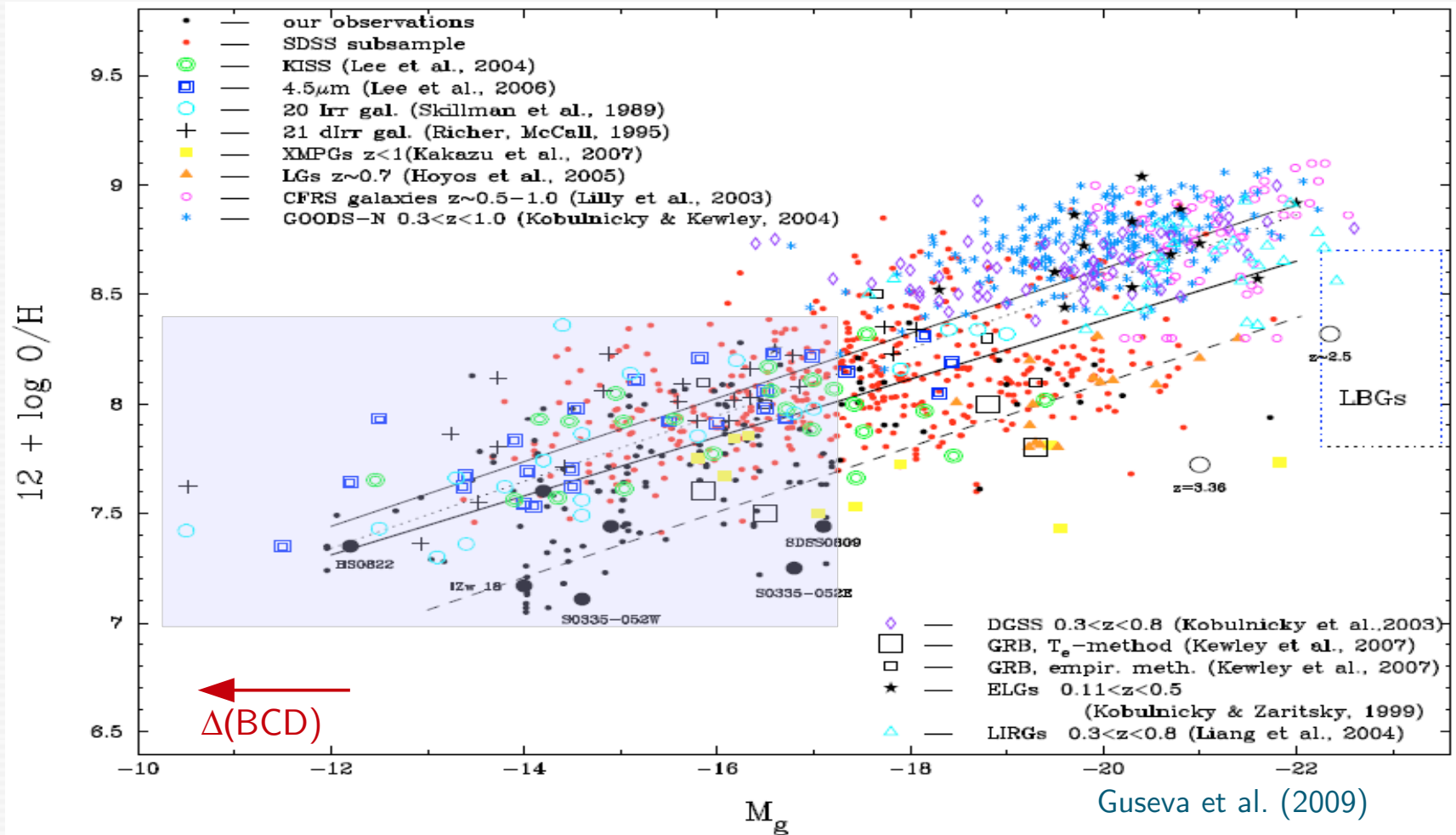


Kennicutt & Evans (2012)

# Why to study dwarf galaxies?

- They dominate by number & nearby
- Building blocks of normal galaxies
- Most important sources of re-ionization
- Wide range in burst parameter, star formation rate (SFR) & specific SFR
- Most metal-poor galaxies known (the best local analogs of the first galaxies formed) ←
- "Simple" & dust-poor (i.e. low intrinsic extinction)

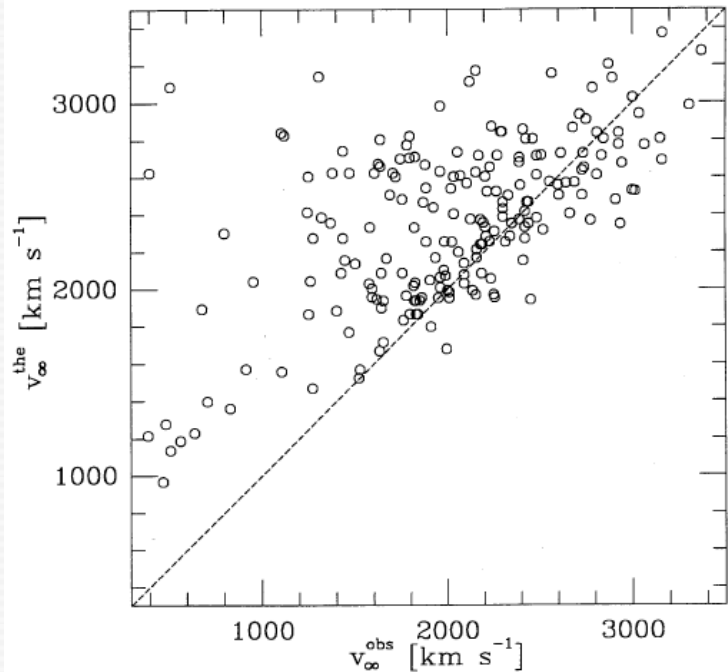
Luminosity-metallicity relation for star-forming galaxies





# Why to study dwarf galaxies?

- They dominate by number & nearby
- Building blocks of normal galaxies
- Most important sources of re-ionization
- Wide range in burst parameter, star formation rate (SFR) & specific SFR
- Most metal-poor galaxies known (the best local analogs of the first galaxies formed) ←
- "Simple" & dust-poor (i.e. low intrinsic extinction)



Prinja et al. (1990)

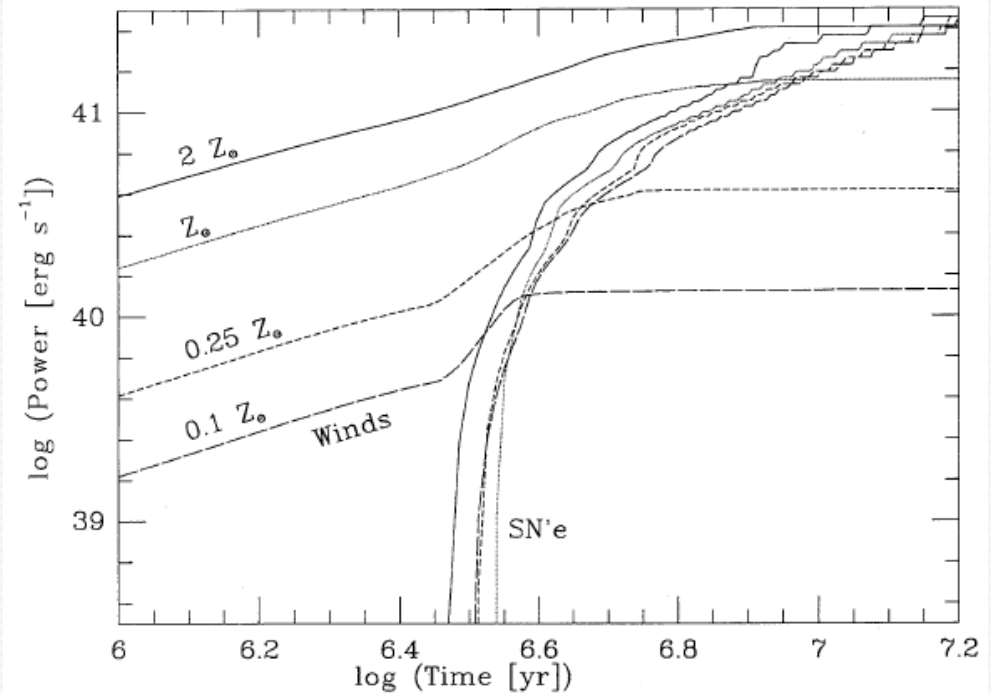


FIG. 10.—Wind power of massive stars forming continuously with  $\text{SFR} = 1 M_{\odot} \text{ yr}^{-1}$  ( $\alpha = 2.35$ ,  $M_{\nu} = 120 M_{\odot}$ ,  $M_l = 1 M_{\odot}$ ). Models for four different metallicities are plotted. The power released by SNs is included. The same line type has been used for winds and SNs of the same  $Z$ .

a →

$$\log [\dot{M}(M_{\odot} \text{ yr}^{-1})] = -24.06 + 2.45 \log [L(L_{\odot})] - 1.10 \log [M(M_{\odot})] + 1.31 \log [T_{\text{eff}}(\text{K})] + 0.80 \log [Z(Z_{\odot})];$$

b →

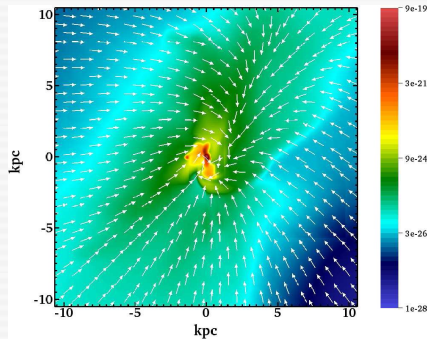
$$\log [v_{\infty}(\text{kms}^{-1})] = 1.23 - 0.30 \log [L(L_{\odot})] + 0.55 \log [M(M_{\odot})] + 0.64 \log [T_{\text{eff}}(\text{K})] + 0.13 \log [Z(Z_{\odot})].$$

Leitherer et al. (1992)

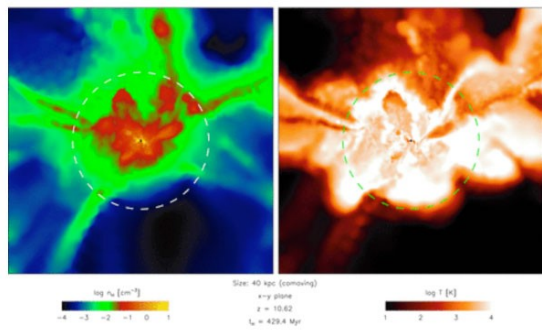
a: Mass loss rate    b: Stellar wind velocity

# Why to study dwarf galaxies?

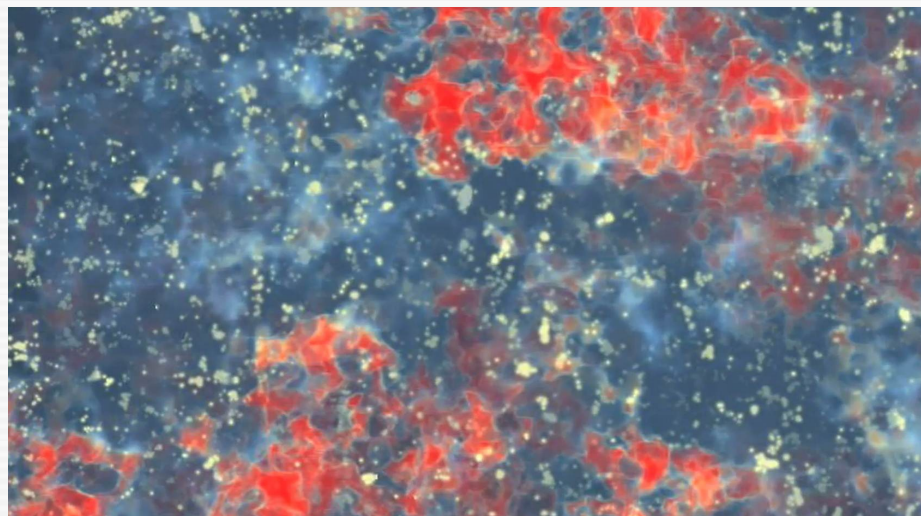
- They dominate by number & nearby
- Building blocks of normal galaxies
- Most important sources of re-ionization
- Wide range in burst parameter, star formation rate (SFR) & specific SFR
- Most metal-poor galaxies known (the best local analogs of the first galaxies formed) ←
- "Simple" & dust-poor (i.e. low intrinsic extinction)



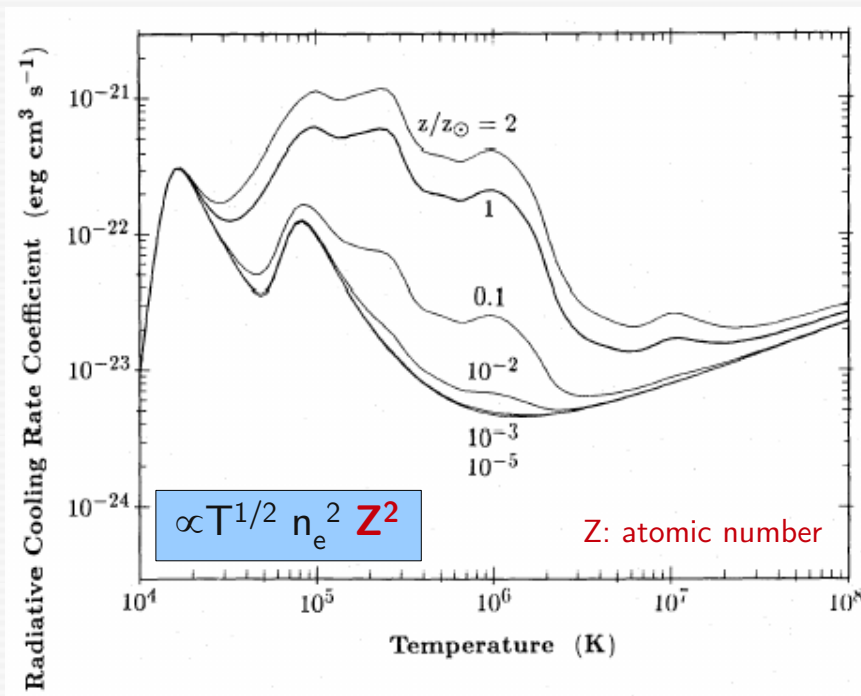
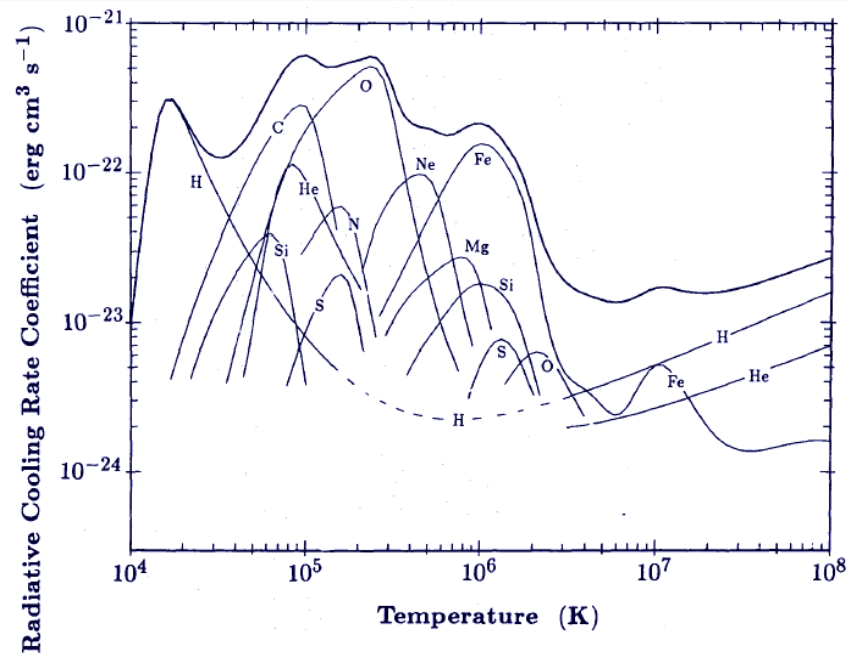
Latif et al. (2011)



Brohm et al. (2012)



Expected SKA image at  $z=10-20$  (imprint of first stars or galaxies)



Böhringer & Hensler (1987)



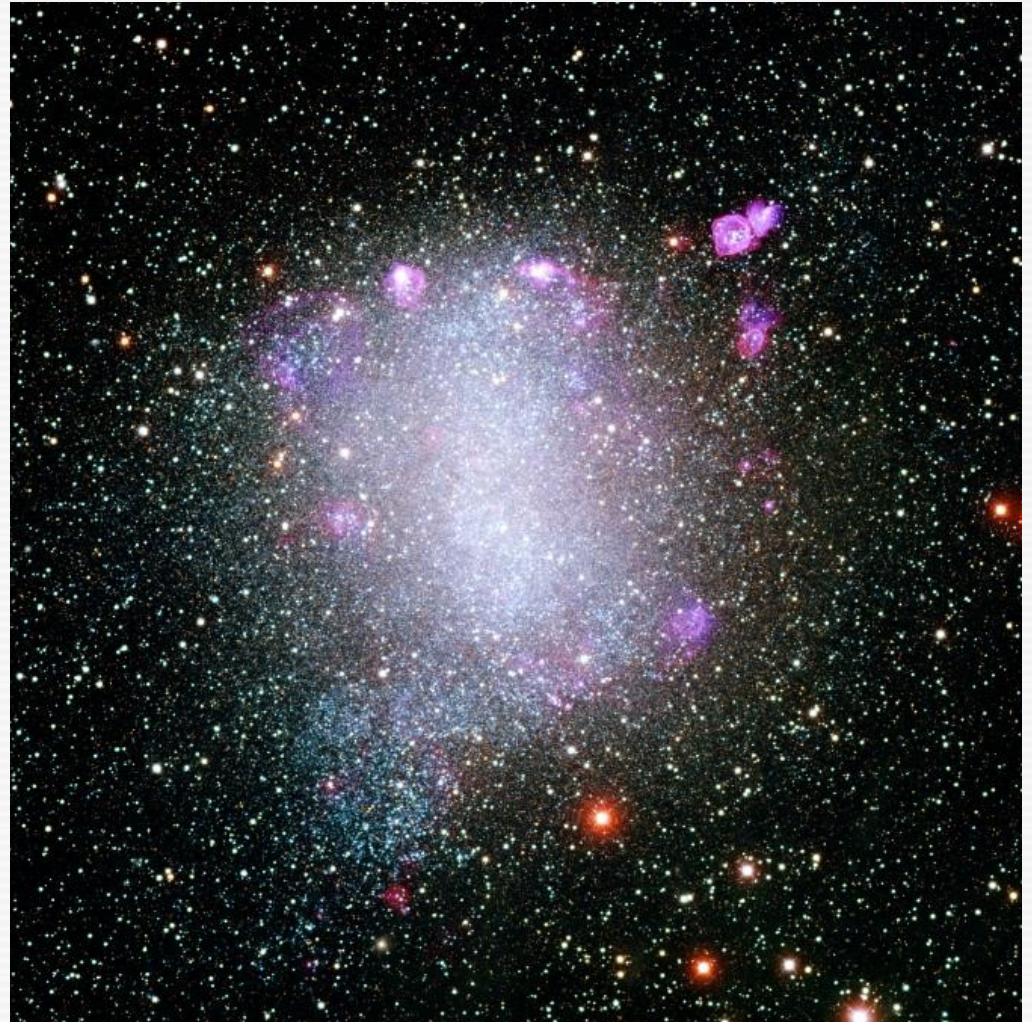
# Why to study dwarf galaxies?

- They dominate by number & nearby
- Building blocks of normal galaxies
- Most important sources of re-ionization
- Wide range in burst parameter, star formation rate (SFR) & specific SFR
- Most metal-poor galaxies known (the best local analogs of the first galaxies formed)
- "Simple" & dust-poor (i.e. low intrinsic extinction) ←



Arp 220 (ULIRG)

≠



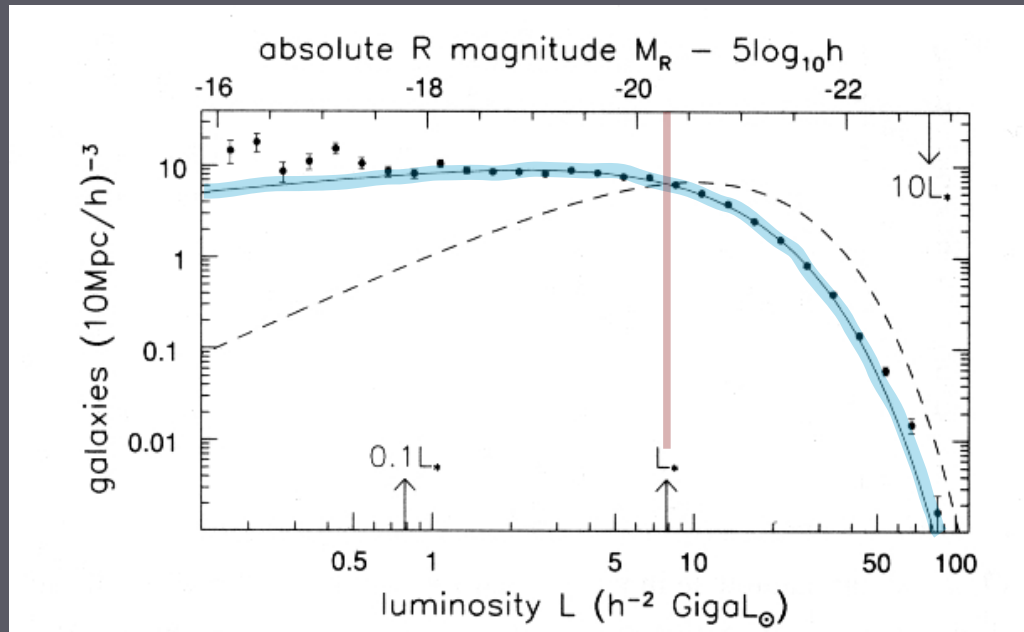
NGC 6822 (dwarf irregular)

## (some) Questions

- Star formation- and chemical enrichment history of SFDGs (and dwarf galaxies in general)
- Dynamical evolution of SFDGs
- Origin and implications of starburst activity in SFDGs
- Evolutionary connections between SFDGs (i.e. **late-type dwarfs**, such as dIs and BCD/HII galaxies) and **early-type** (dEs, dSphs) DGs
- Role of the environment
- Connection between evolutionary status, metallicity and morphology



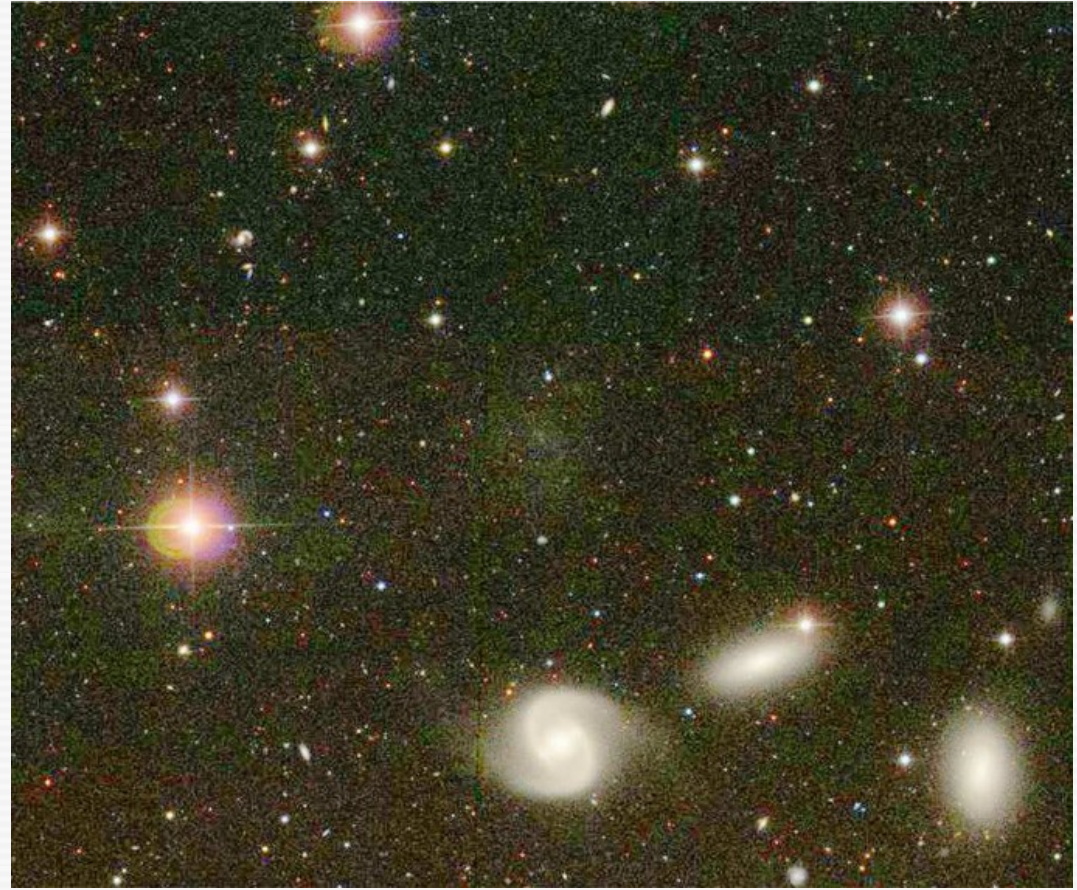
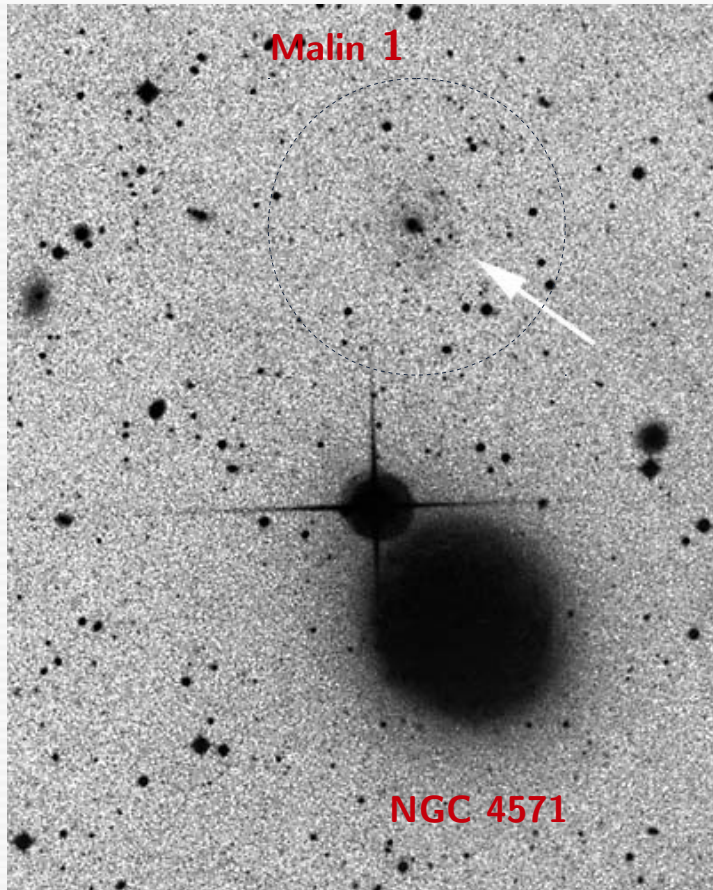
# Observational biases in studies of DGs



a) Malmquist bias

b) the surface brightness bias

# The surface brightness bias



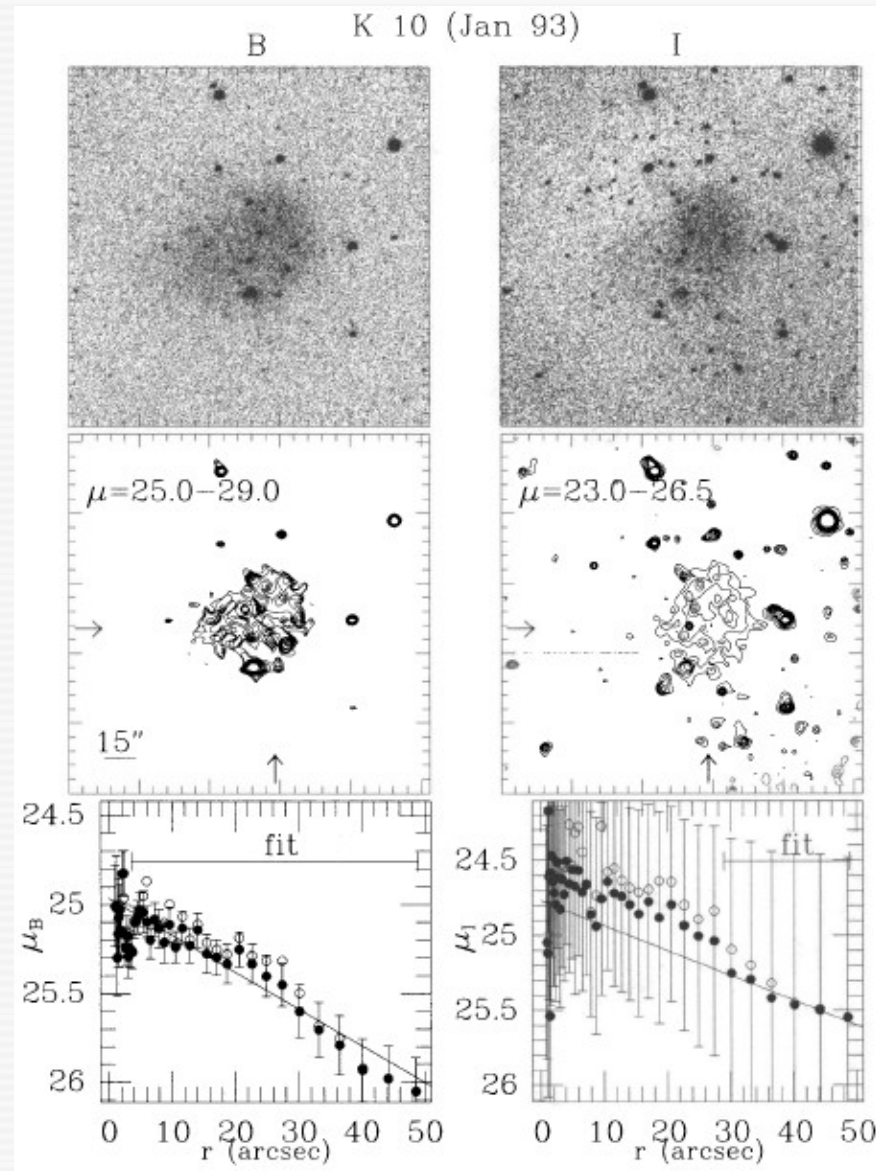
VCC 1052 (from Sandage & Binggeli 1983,  
see also Kormendy & Bender 2012)

**Low-surface brightness (LSB)** galaxies are probably numerous but difficult to detect (*consequently, their statistics are strongly biased*).

Typical central surface brightness:  $\mu_0 \geq 23.5\text{-}25.0 \text{ mag arcsec}^{-2}$  i.e.  $\times 10$  fainter than the night sky (!)



# The surface brightness bias



Patterson & Thuan (1996)

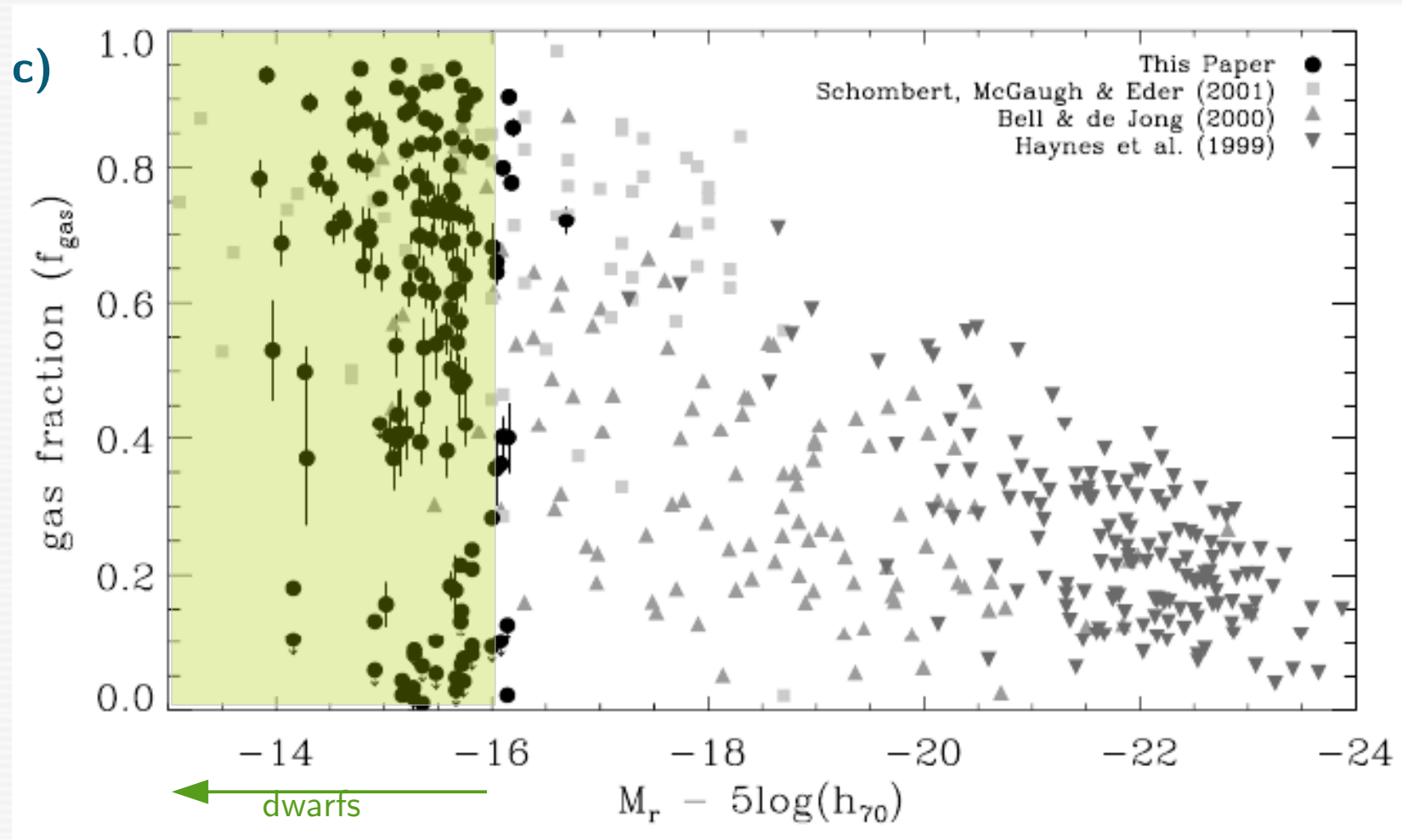
**Low-surface brightness (LSB)** galaxies are probably numerous but difficult to detect (*consequently, their statistics are strongly biased*).

Typical central surface brightness:  $\mu_0 \geq 23.5-25.0 \text{ mag arcsec}^{-2}$  i.e.  $\times 10$  fainter than the night sky (!)

Dwarf Galaxies:  
some empirical relations

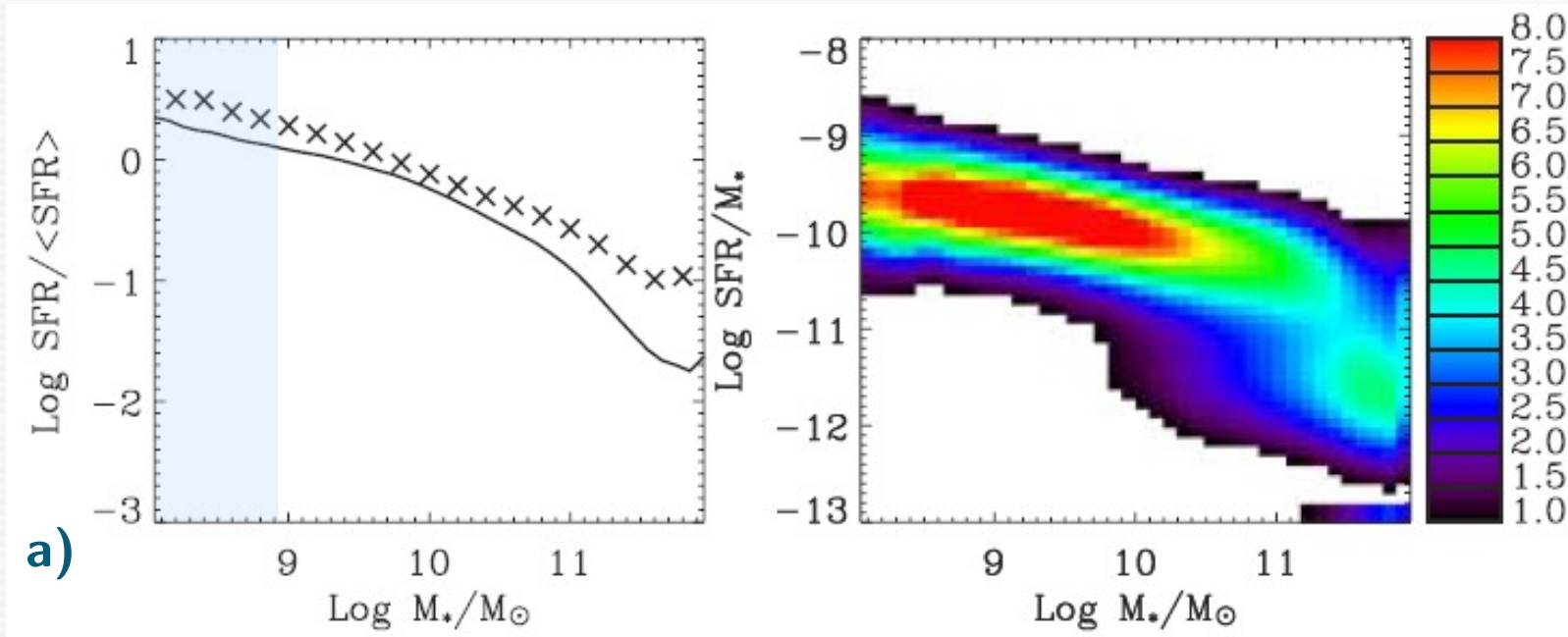


# Gas mass fraction



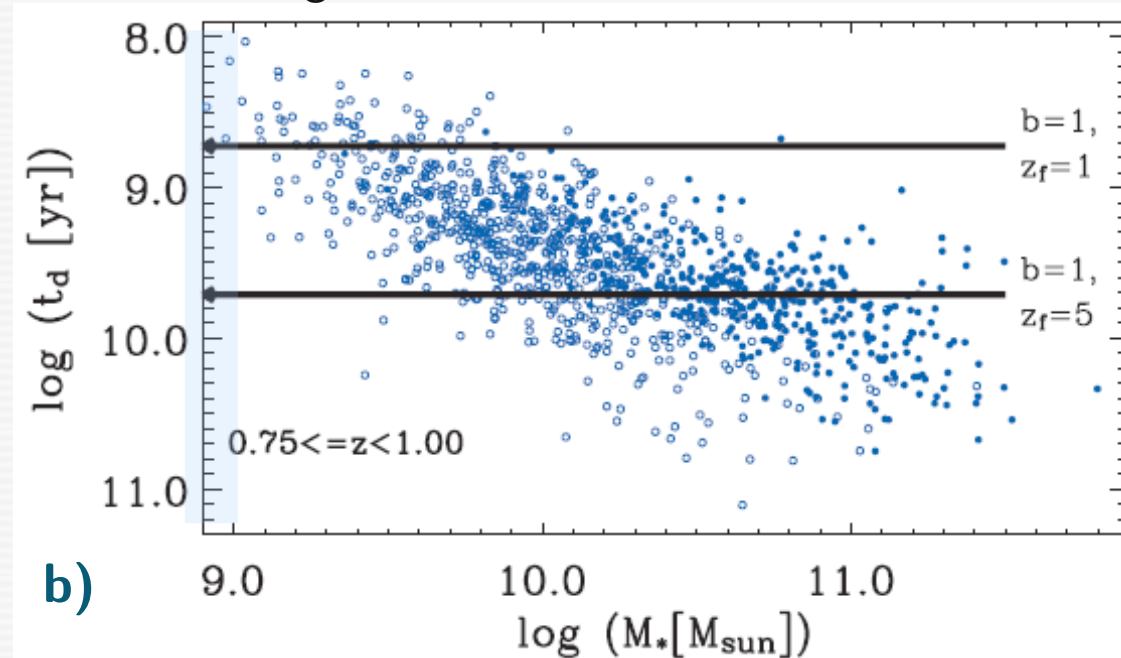
Geha et al. (2006)

# Assembly history of the stellar component galaxies & galaxy downsizing



← dwarf galaxies

Brinchmann et al. (2004)



$t_d$ : stellar mass doubling time

Noeske et al. (2007)

# L(H $\beta$ ) - $\sigma$ Relation

Melnick et al. (1987, MNRAS 226, 849)

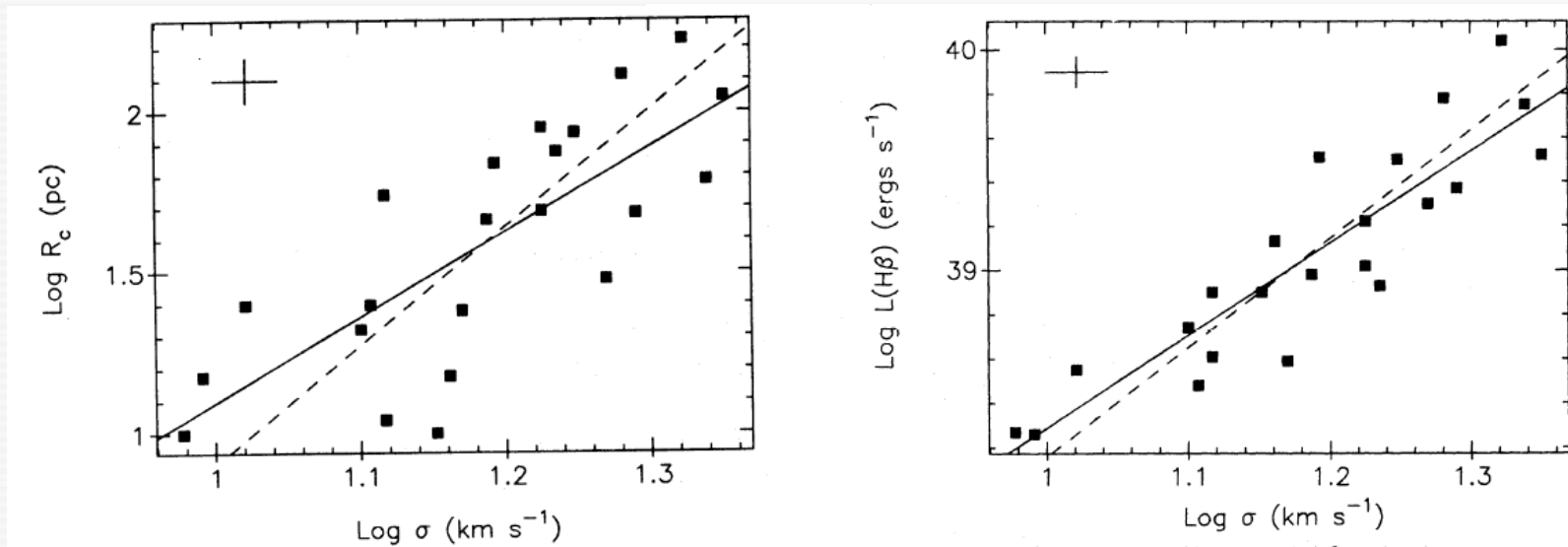


**Figure 2.** Logarithmic plot of the extinction corrected integrated H $\beta$  luminosity of giant H II regions [ $L(\text{H}\beta)$ ] as a function of velocity dispersion ( $\sigma$ ). The two lines show fits to the data obtained ignoring observational errors (solid) and using the error bar shown in the plot (dashes).

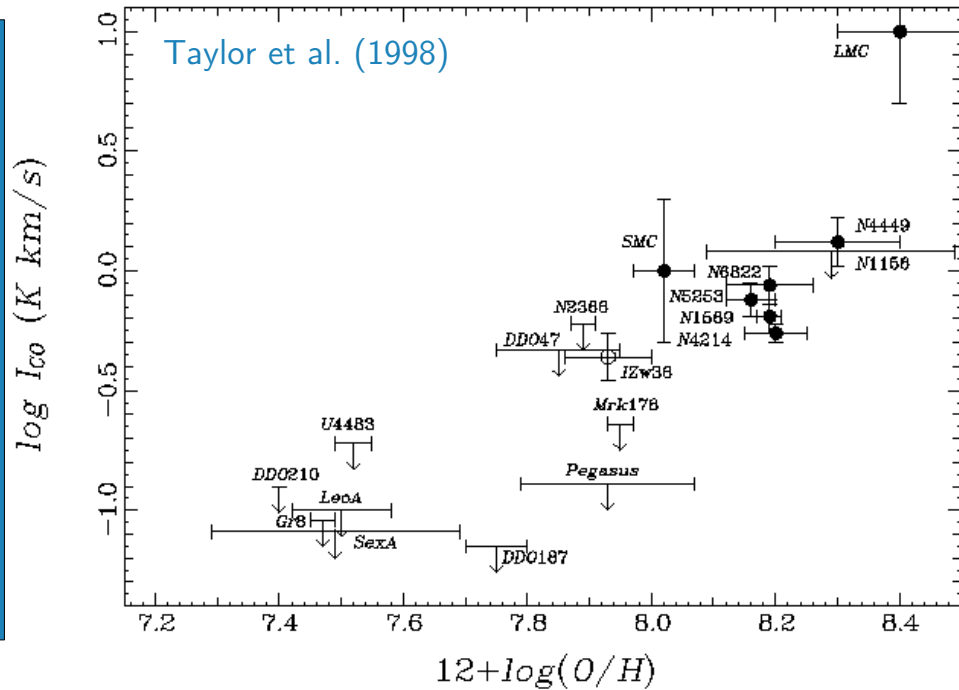
$$\log L(\text{H}\beta) = (4.17 \pm 0.47) \log \sigma + 34.12 \pm 0.56$$

- Correlation between the luminosity and velocity dispersion of the H $\beta$  emission line
- Possible distance indicator (calibration is uncertain though)



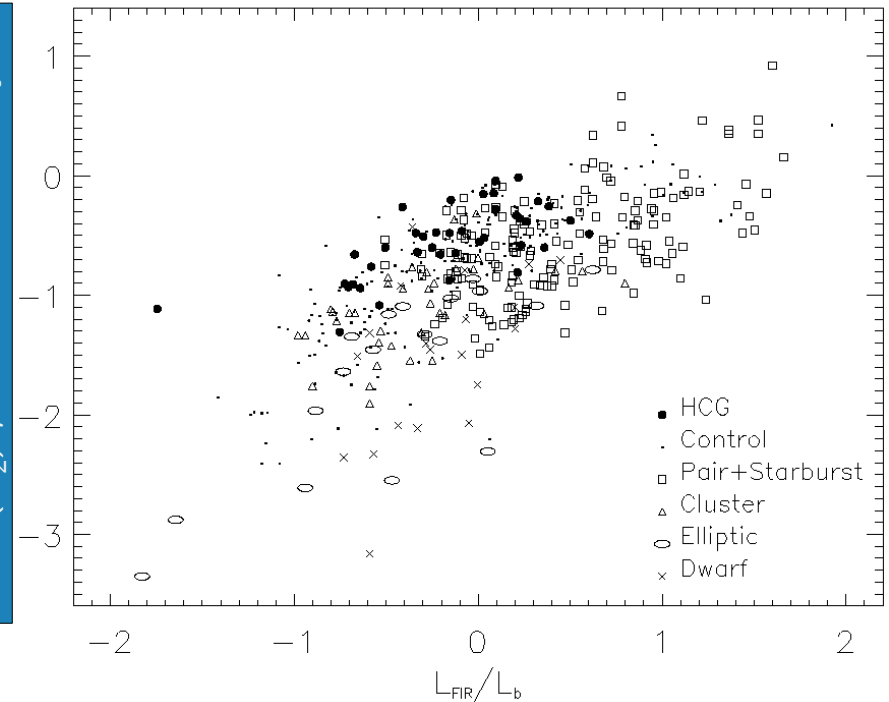
# Molecular H<sub>2</sub> gas in late-type dwarf galaxies

CO emission-line intensity



Gas-phase metallicity

M(H<sub>2</sub>) / B band luminosity

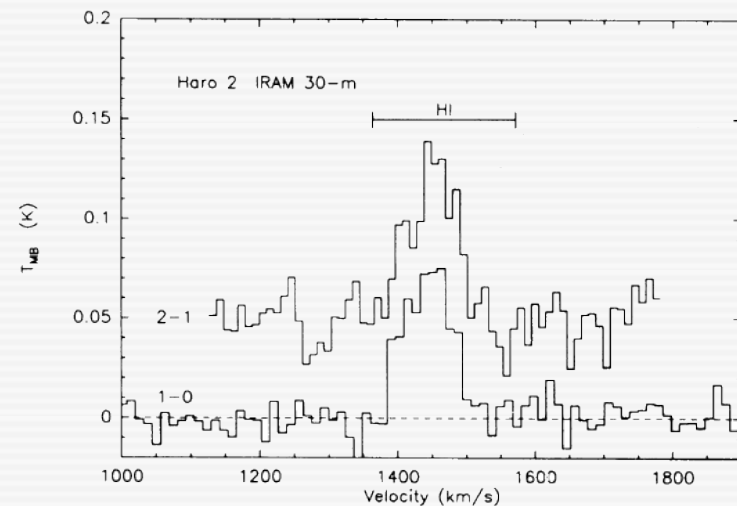


Far infrared / B band luminosity

$$a = M(\text{H}_2)/L_{\text{CO}} \quad (\text{M}_\odot/\text{K km s}^{-1} \text{pc}^2)$$

$$M(\text{H}_2)/L_{\text{CO}} = 2.1 n (\text{H}_2)^{1/2} / T_b(1 \rightarrow 0)$$

L(CO) → H<sub>2</sub> mass conversion via the α factor  
(depends on the assumed kinetic temperature T<sub>b</sub>  
and particle density n)

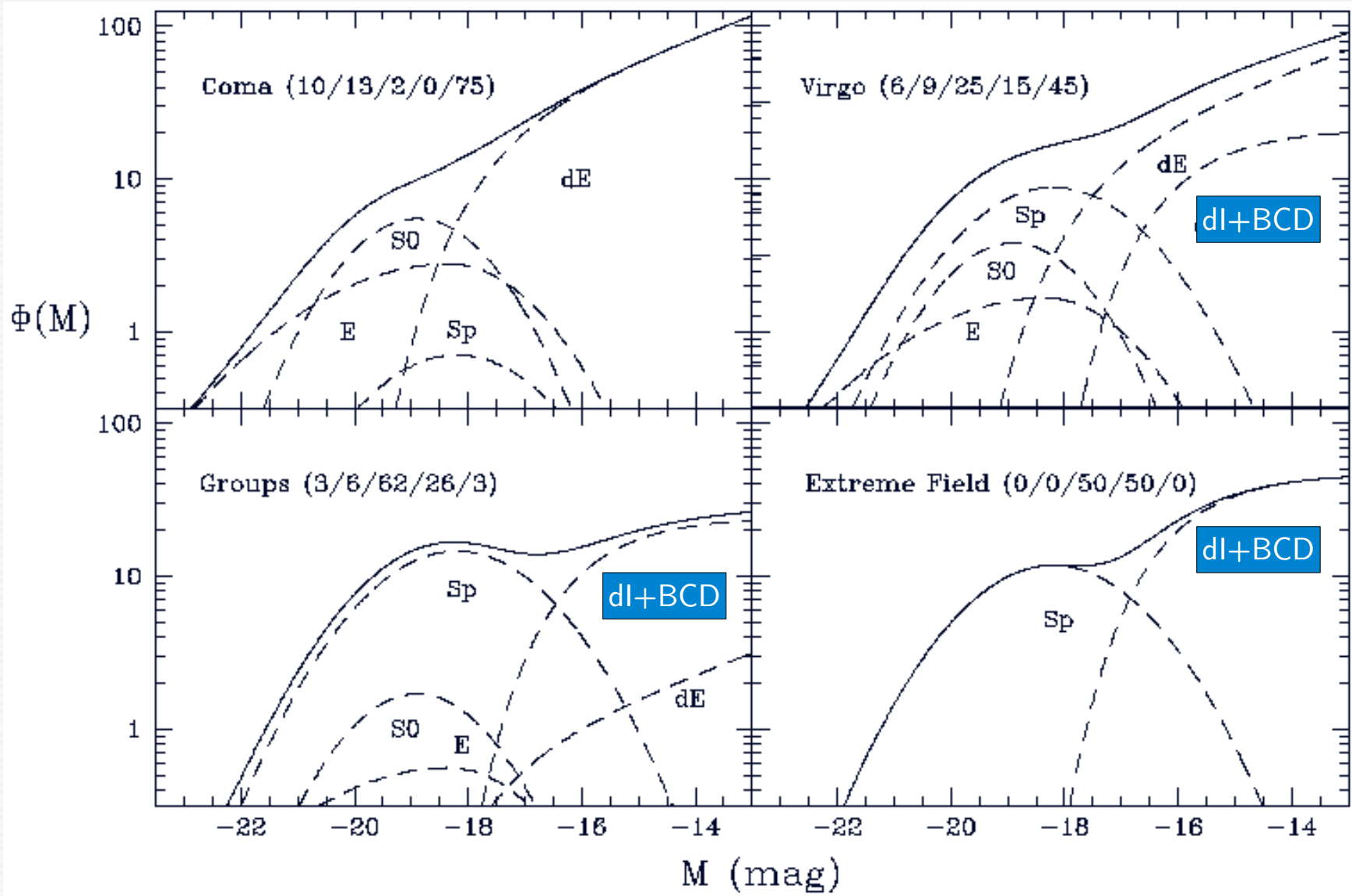


Sage et al. (1992)

# The role of the environment on the evolution of SFDGs



# Early-to-late type dwarf galaxy distribution as a function of the environment



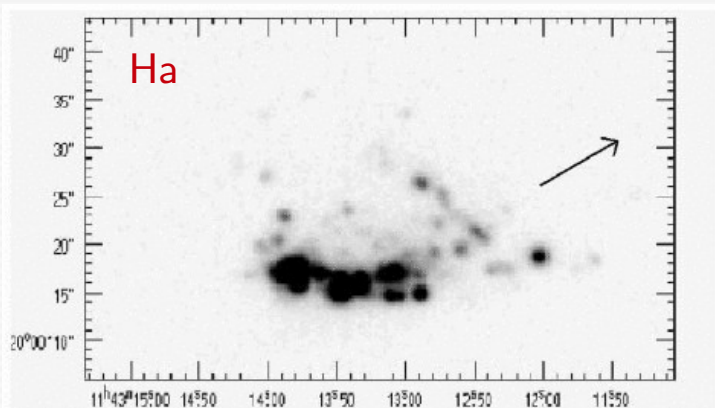
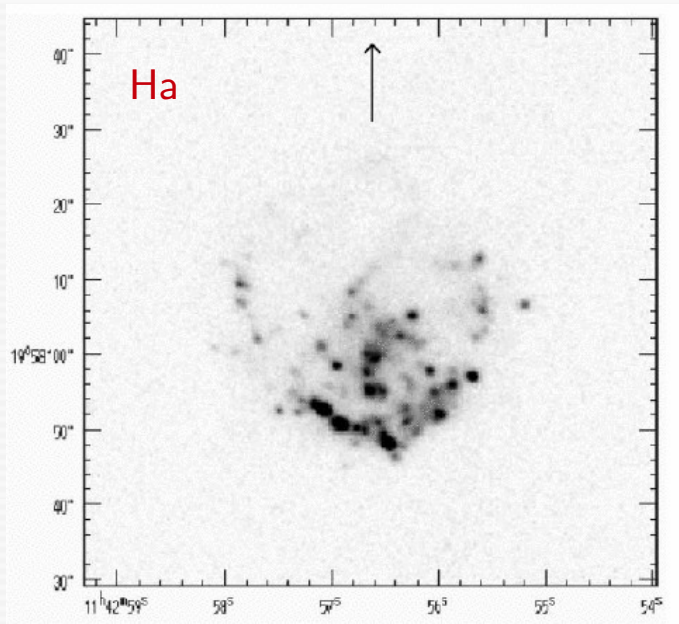
Jerjen et al. (1998)

The morphological distribution of dwarf galaxies depends on their environment.

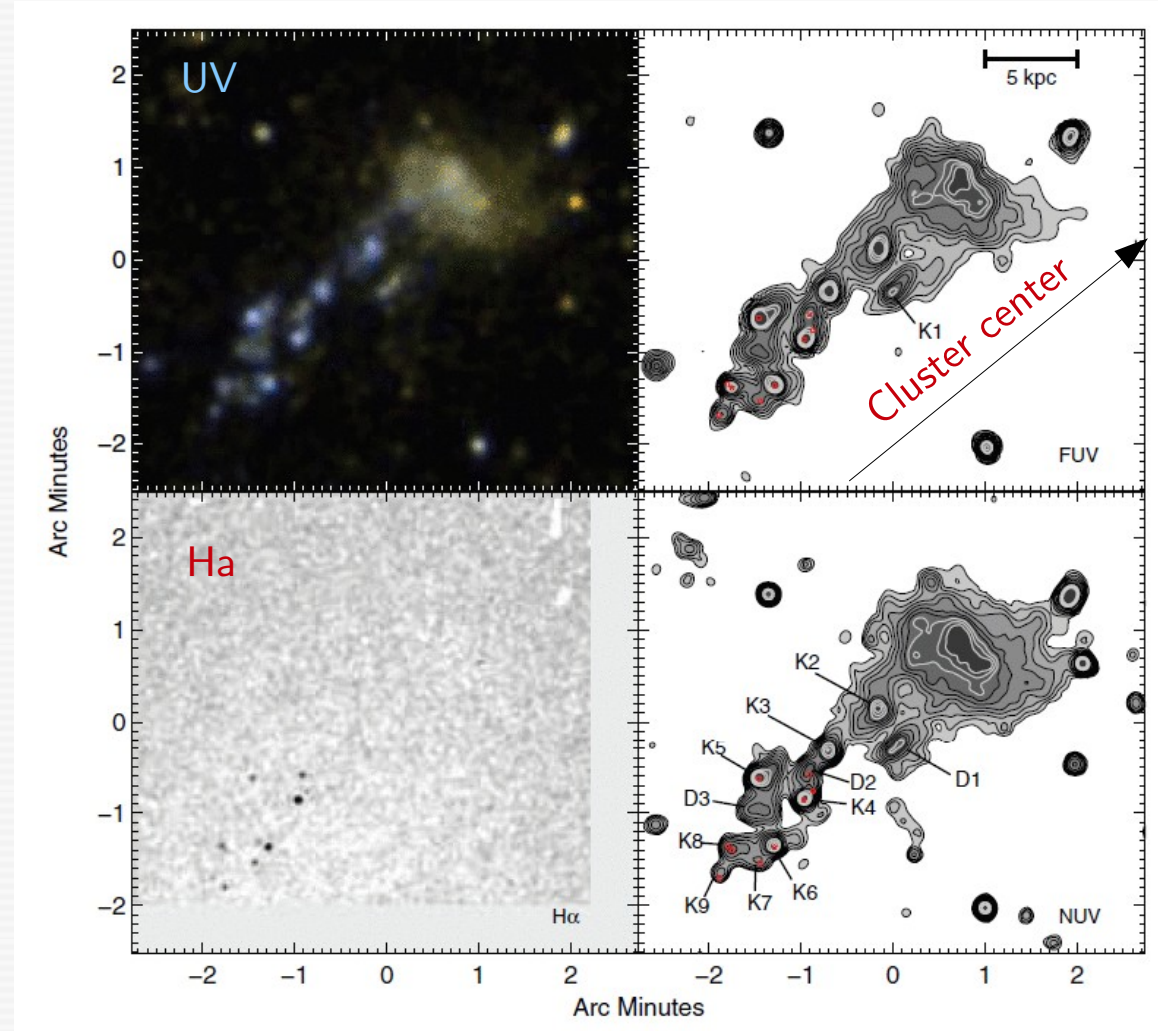


**“strong” interactions within a galaxy cluster environment**

Infalling (normal and dwarf) late-type galaxies in galaxy clusters:  
Initial star formation episode induced by the contact with the ICM and subsequent loss of gas through ram pressure stripping



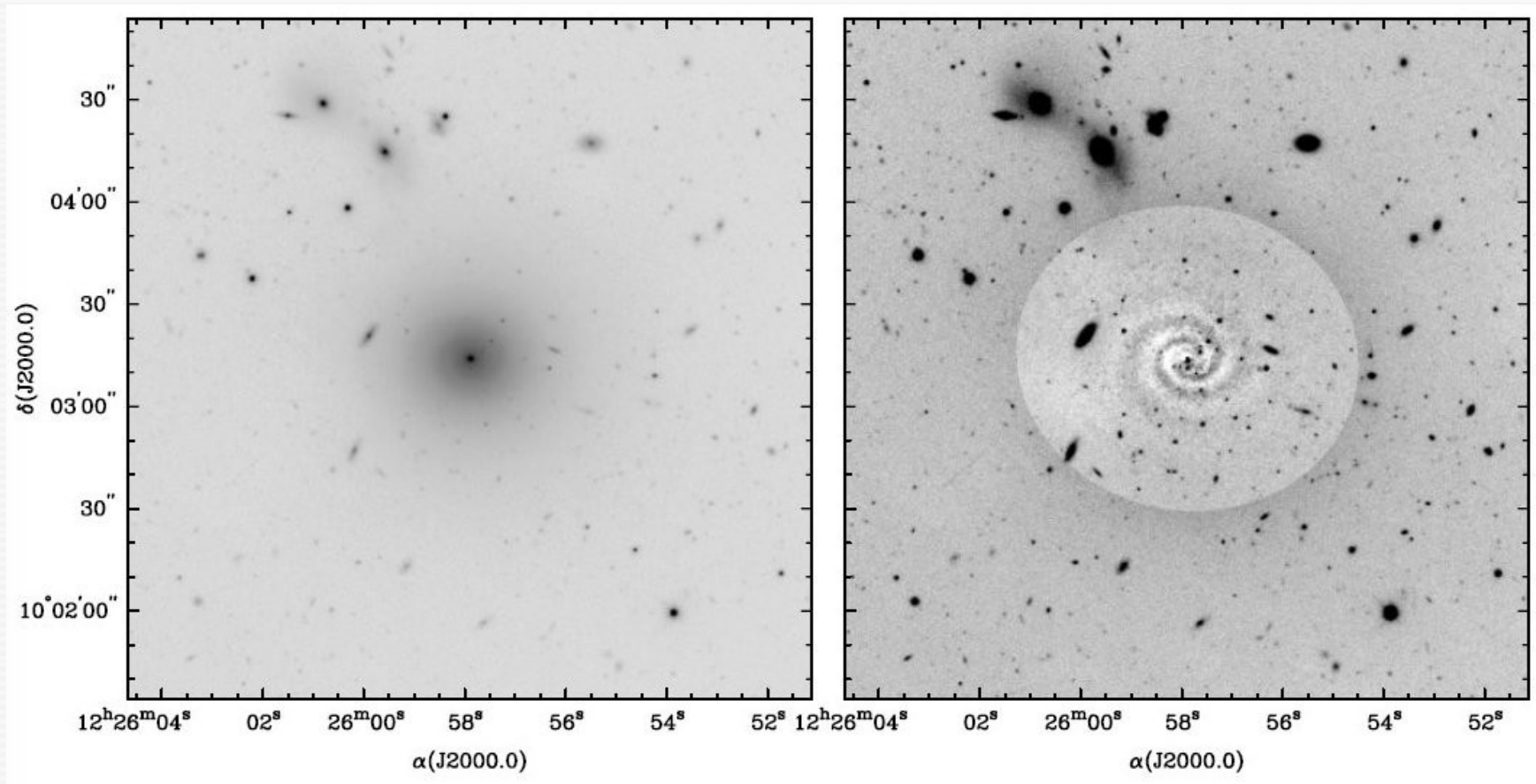
Gavazzi et al. (2009)



The late-type dwarf galaxy  
IC 3418 in the Virgo Cluster

Hester et al. (2010)

# Galaxy transformations in clusters: combined effect of photometric fading after ram pressure stripping and galaxy harassment

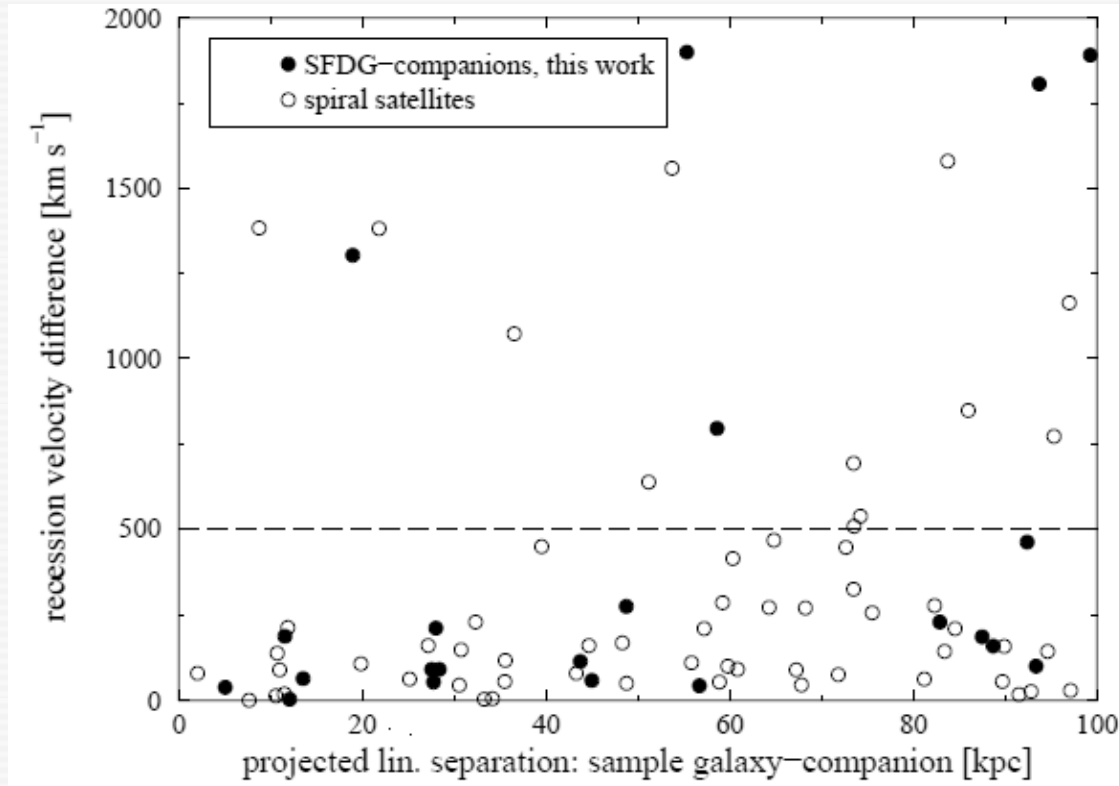


Jerjen et al. (2000)

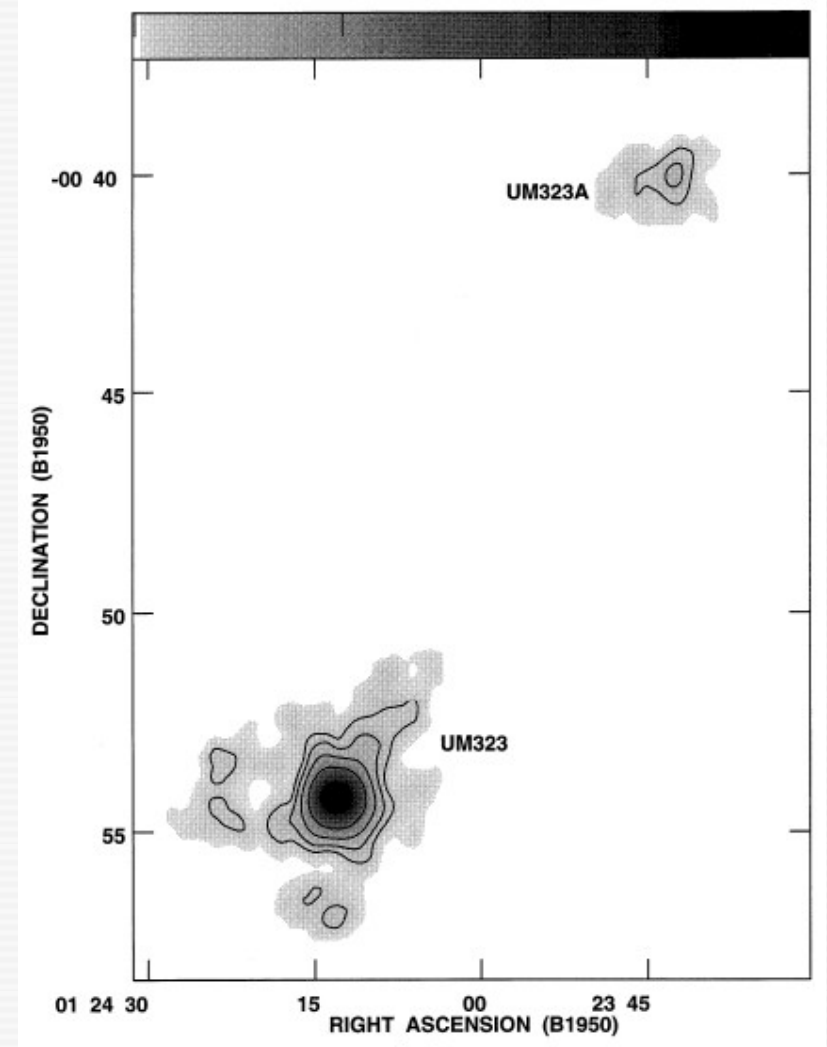
Signatures of faint embedded disks in several dEs (signatures of galaxy transformations in clusters). First detected by [Jerjen et al. \(2000\)](#) and [Barazza et al. \(2002\)](#) in small number of Virgo Cluster dEs.

Detections also in other galaxy clusters, e.g. [Graham et al. \(2003\)](#) for Coma and [De Rijcke et al. \(2003\)](#) for Fornax. See also [Lisker et al. \(2006,2007\)](#) for studies of the complete sample of galaxies in Virgo.

## “weak” interactions in the field or in loose DG galaxy pairs & groups



Noeske et al. (2001)

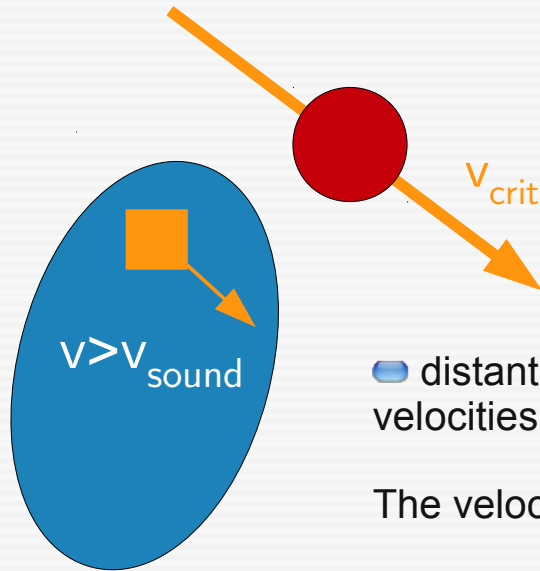


Taylor et al. (1993,1995)

SFDGs galaxies are rarely truly isolated: they have low-mass (stellar and/or gaseous) companions with a typical velocity and linear separation of  $<500$  km/s and  $<100$  kpc, respectively.



# “weak” interactions in the field or in loose DG galaxy pairs & groups



## Icke (1985) mechanism

- distant collision between galaxies: acceleration of clouds in the “victim” galaxy to velocities exceeding the local sound velocity → shocks → dissipation → star formation

The velocity increase is

$$\delta u \approx 4GM R \cdot r^{-3} \cdot 2\pi \frac{R}{u} = 8\pi \cdot u \left( \frac{R}{r} \right)^3$$

with M: mass of the galaxies, R: radius of the “victim” galaxy, r: distance between the galaxy nuclei, u: relative velocity at radius R (  $(GM/R)^{1/2}$  ).

- condition:  $\delta u \geq$  sound speed  $s_0$

$$s_0 = (k_B T / m_p)^{1/2} = 9 \text{ km/sec} \times \sqrt{T / 10^4 \text{ K}}$$

$k_B$ : Boltzman constant =  $1.381 \times 10^{-16}$  erg  $K^{-1}$   
 $m_p$ : proton mass,  $1.673 \times 10^{-24}$  g.

- estimate: minimum pericenter distance for triggering of a shock

- for a mass ratio  $\mu = M(\text{intruder}) / M(\text{victim})$

$$p_0 \approx R \cdot \left( \frac{8\pi \cdot u}{s_0} \right)^{1/3}$$

- example:  $M(\text{victim}) = 10^{10} M_\odot$ ,  $u/s_0 = 7$ ,  $\mu = 1$ ,  $R_{\text{victim}} = 10$  kpc → critical pericenter distance of 60 ... 80 kpc.

$$p_0 \approx R \cdot \left( \frac{8\pi \cdot \mu u}{s_0} \right)^{1/3}$$

- spatially extended starburst**

## The dwarf galaxy population in the Local Group (LG)



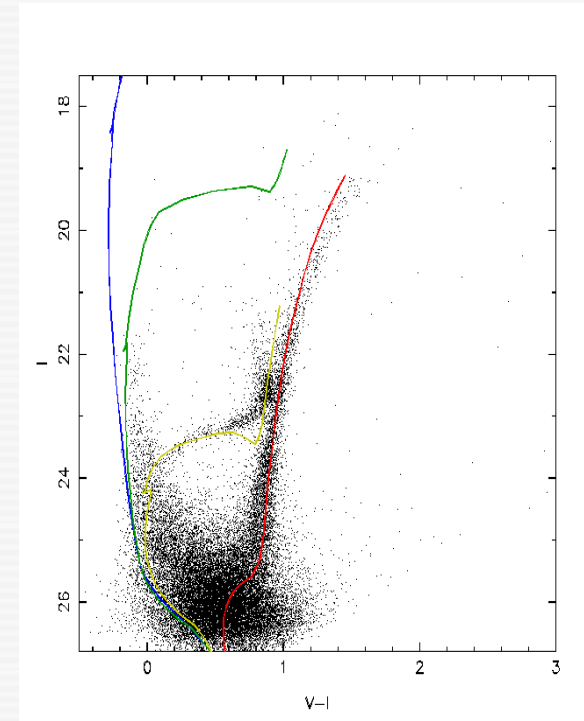
- $M \sim 3 \times 10^{12} M_{\odot}$  with  $\geq 35$  members (only two, the Milky Way and M31, are „normal“ Hubble-type galaxies)
- Dwarf galaxies in the LG show a wide variety in their SFH

# Studies of the star formation history (SFH) of dwarf galaxies in the LG with CMDs

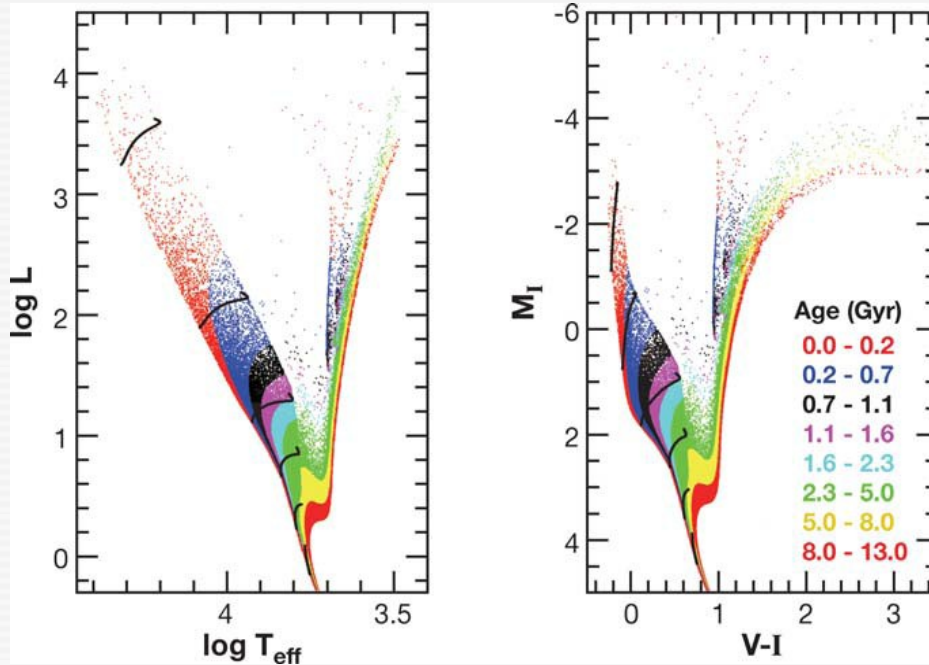
Star Formation History  
 $SFH := SFR(x,y,t)$   
 +  
 $Z(t), IMF(t)$



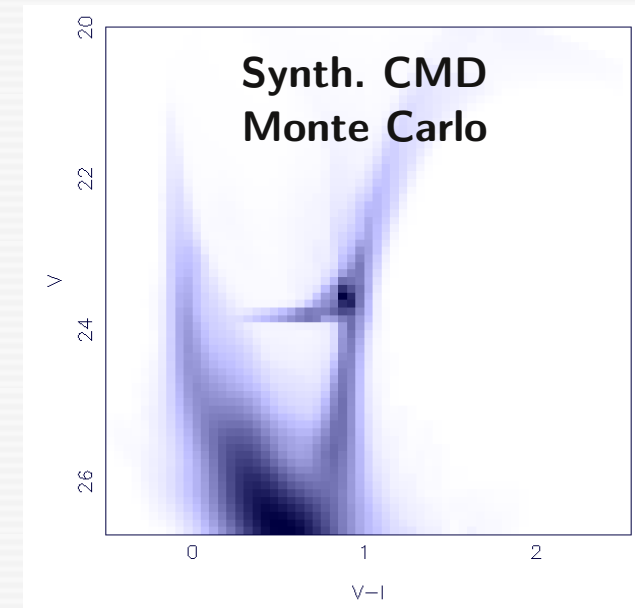
Obs. Effects  
 (photon noise,  
 completeness,  
 confusion, telescope)



Gallart et al. (2006, AR&AA 43, 387)



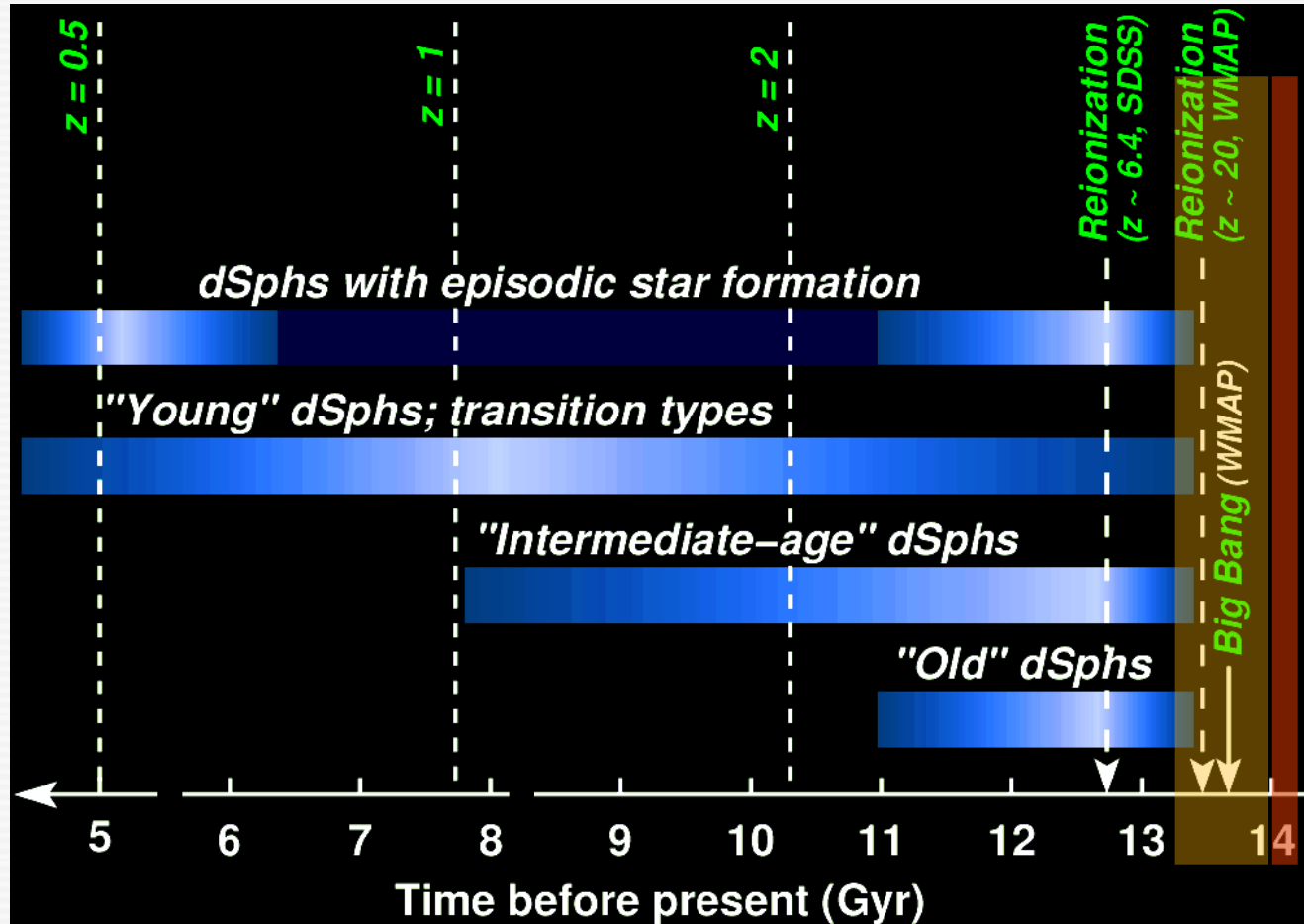
SFH  
 $Z(t)$



Synthetic CMD for continuous, constant SF over 13 Gyr

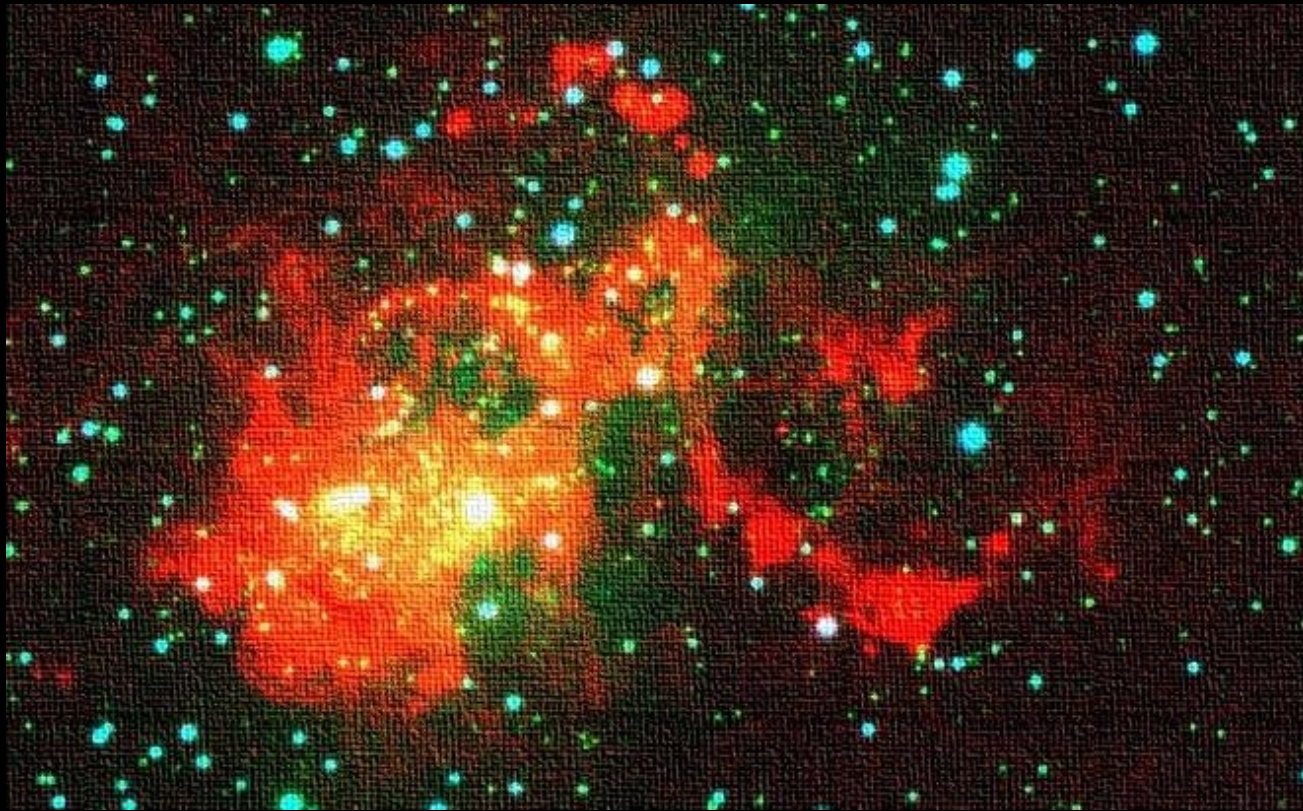


# The SFH of Local Group dSphs



Grebel & Gallagher 2004, ApJ, 610, L89

see reviews by, e.g., Mateo (1998) and McConnachie (2012) ...

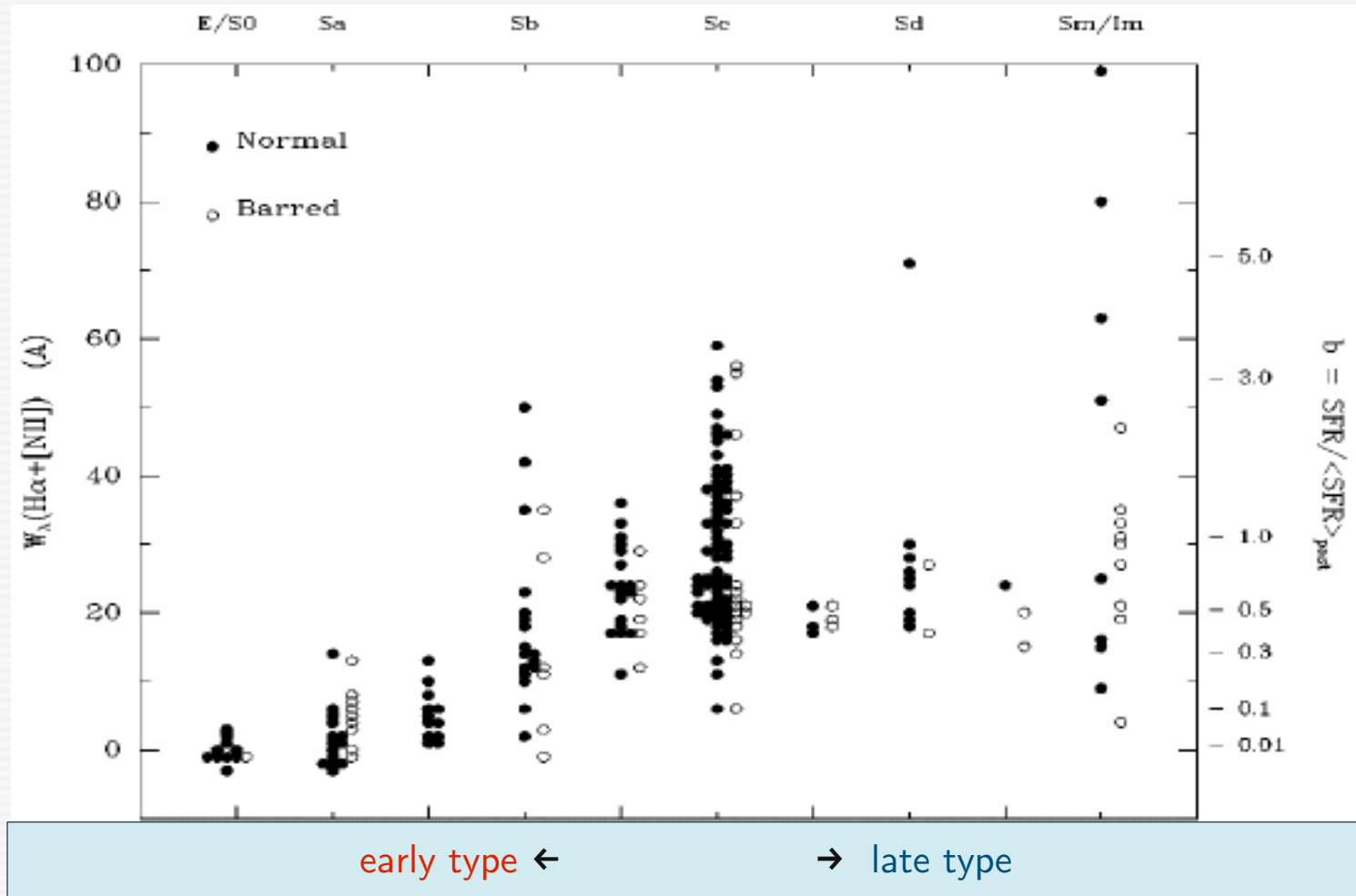


IC 10

Star Formation in late-type dwarf galaxies

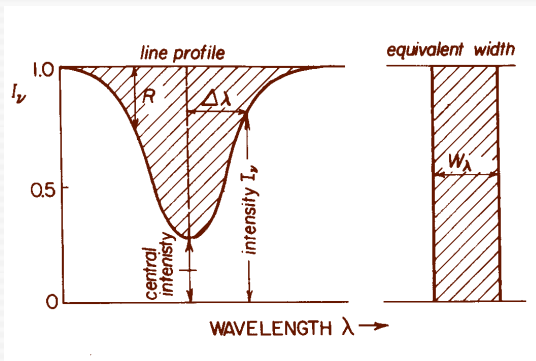
# Star Formation along the Hubble Sequence

equivalent width of  $H\alpha + [NII]$



**b**: current-to-past star formation rate (SFR)

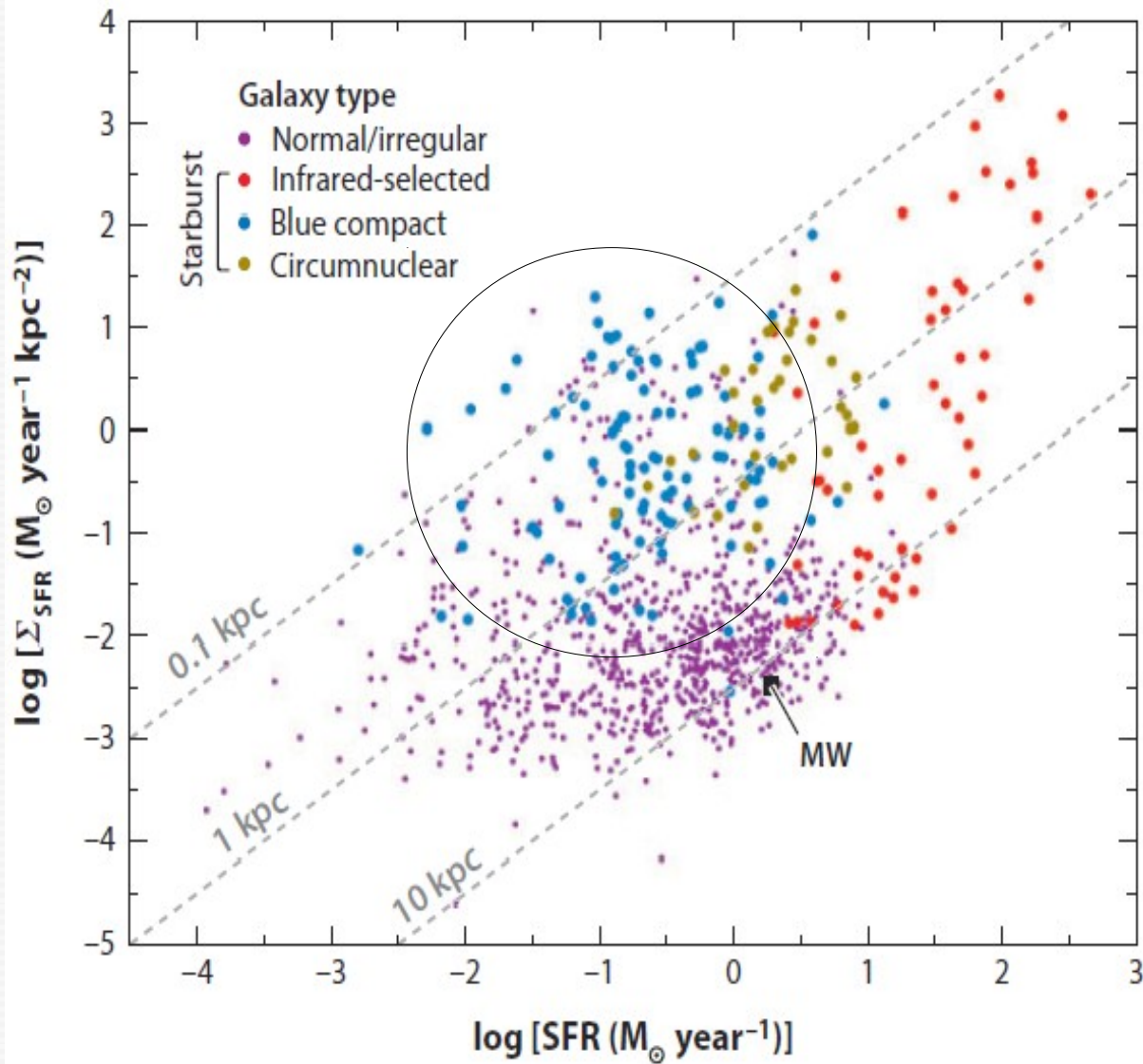
Kennicutt (1989)



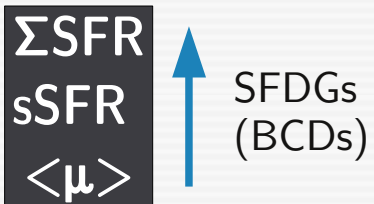
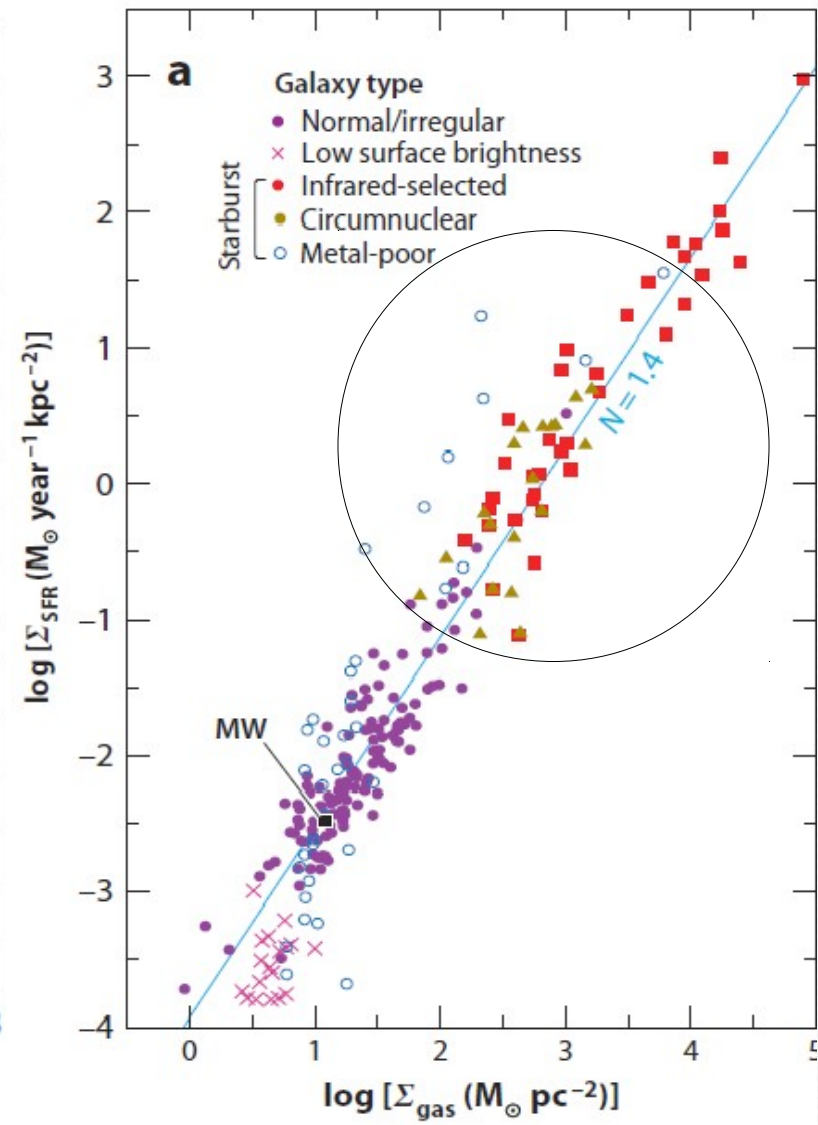
The current star formation rate (SFR) and the burst parameter  $b$  correlate with the Hubble type. Some of the highest- $b$  parameter galaxies are late-type dwarfs.



# Integral SFR vs SFR surface density



# Gas- vs SFR surface density



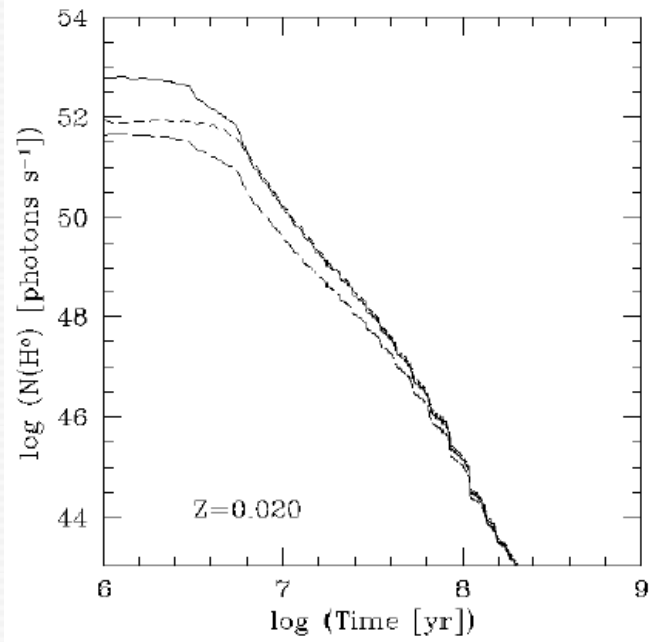
Kennicutt & Evans (2012)

## Remarks on uncertainties in the determination of star formation rates in SFDGs

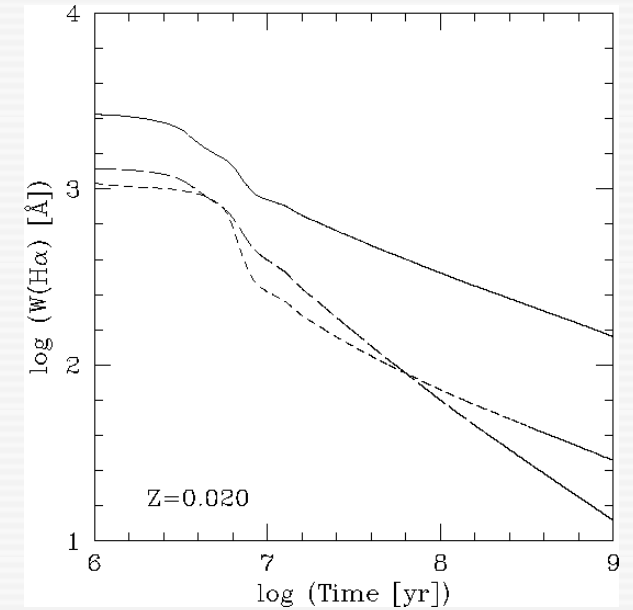
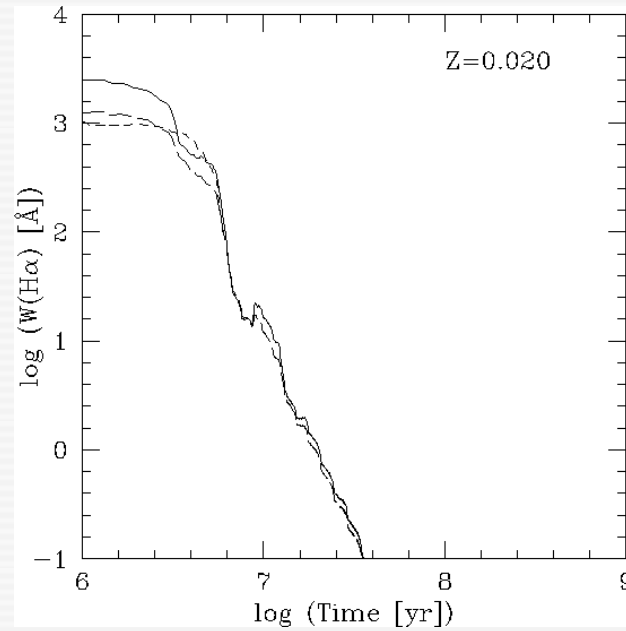
- poorly constrained star formation history
- unknown Lyman continuum photon leakage fraction

# Time evolution of the equivalent width of Balmer emission lines

Lyman con. Rate (1/s)



Equivalent width ( $\text{\AA}$ )



instantaneous star formation ( $10^6 M_{\odot}$ ),  
Salpeter IMF (solid line), solar metallicity

continuous star formation ( $1 M_{\odot}/\text{yr}$ ),  
Salpeter IMF (solid line), solar metallicity

Starburst99 (Leitherer et al.)

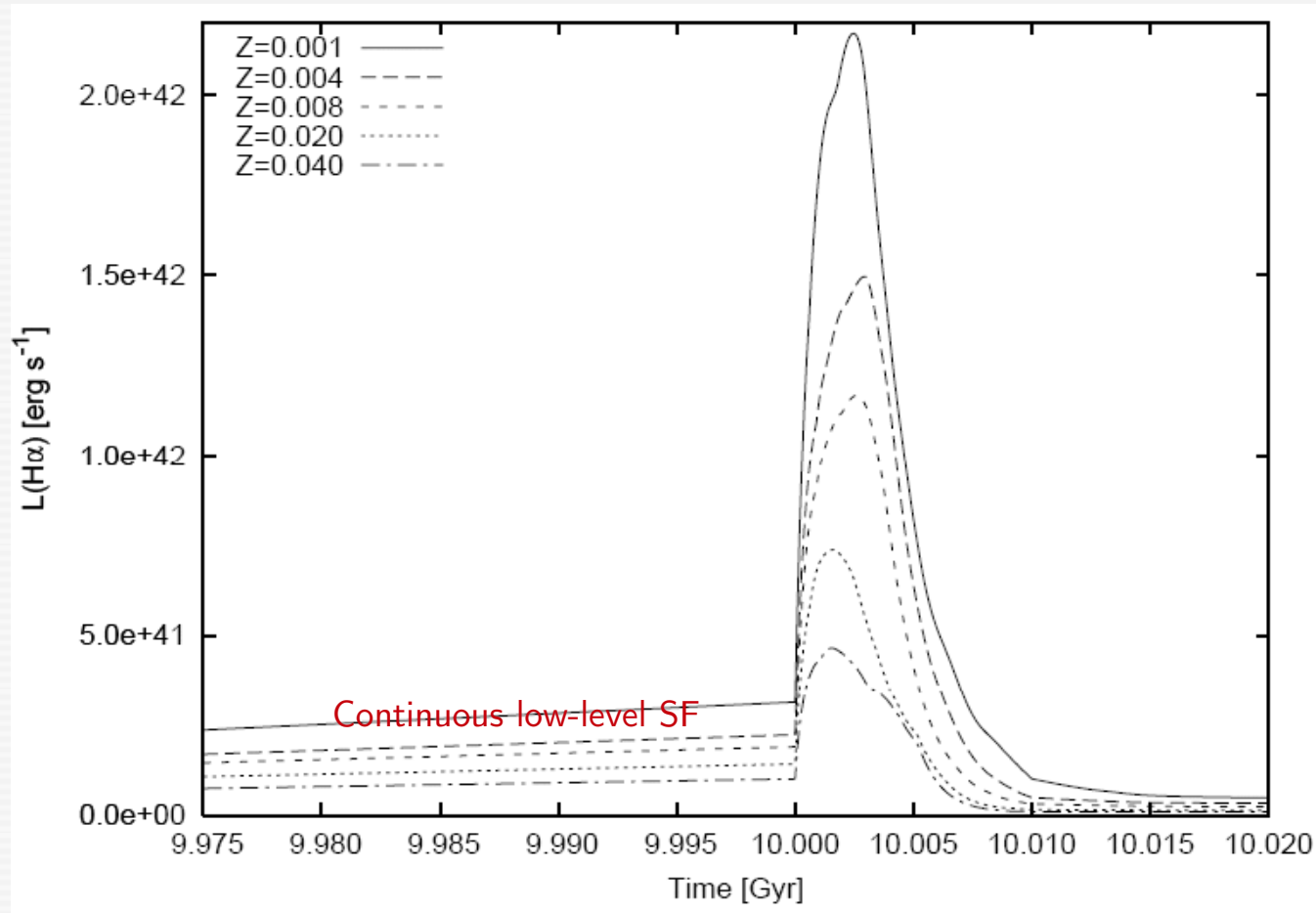


# Evolution of $L(\text{H}\alpha)$ and its dependence on **metallicity**

Caveat: **i)**  $L(\text{H}\alpha)$  is a reliable SFR indicator only in the case of continuous star formation at nearly constant SFR over  $>10^8$  yr, and when photon leakage is negligible

**ii)** The **metallicity** of the ionizing stars has also a significant impact on  $L(\text{H}\alpha)$

Weilbacher & Fritze von Alvensleben (2001)



The observed  $L(\text{H}\alpha)$  depends on

- **starburst age**
- **metallicity**
- **(and the IMF)**

Evolutionary synthesis model: Starburst superimposed on a stellar component forming over 10 Gyr continuously at constant SFR.

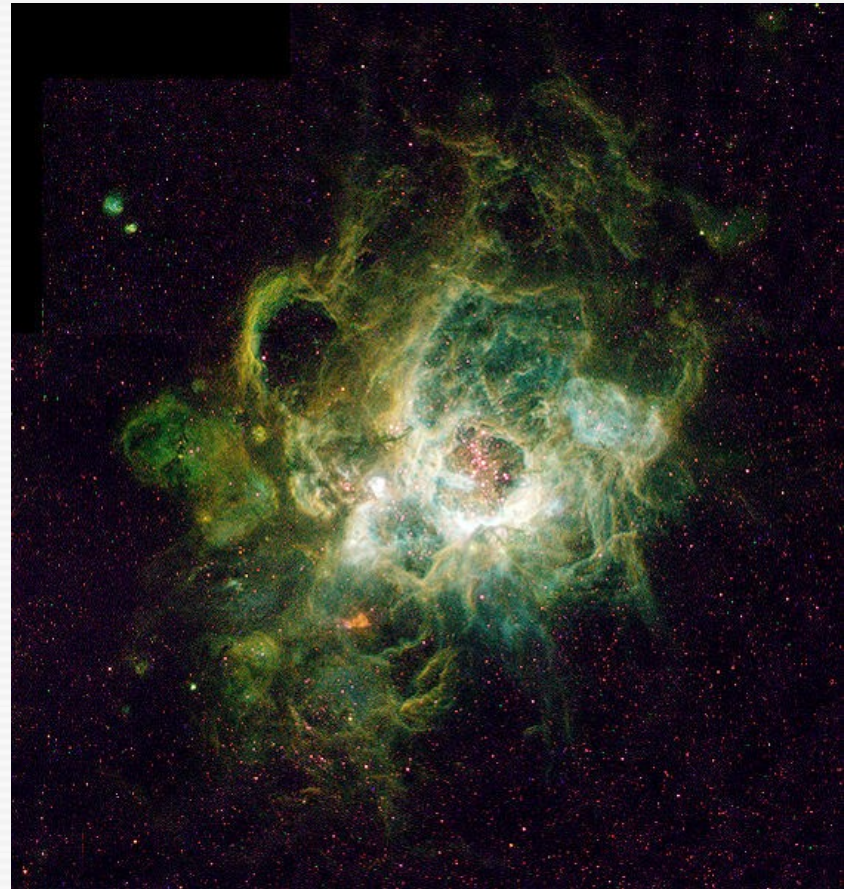
# Evolution of $L(\text{H}\alpha)$ and its dependence on photon leakage

Caveat 1:  $L(\text{H}\alpha)$  is a reliable SFR indicator only when photon leakage is negligible

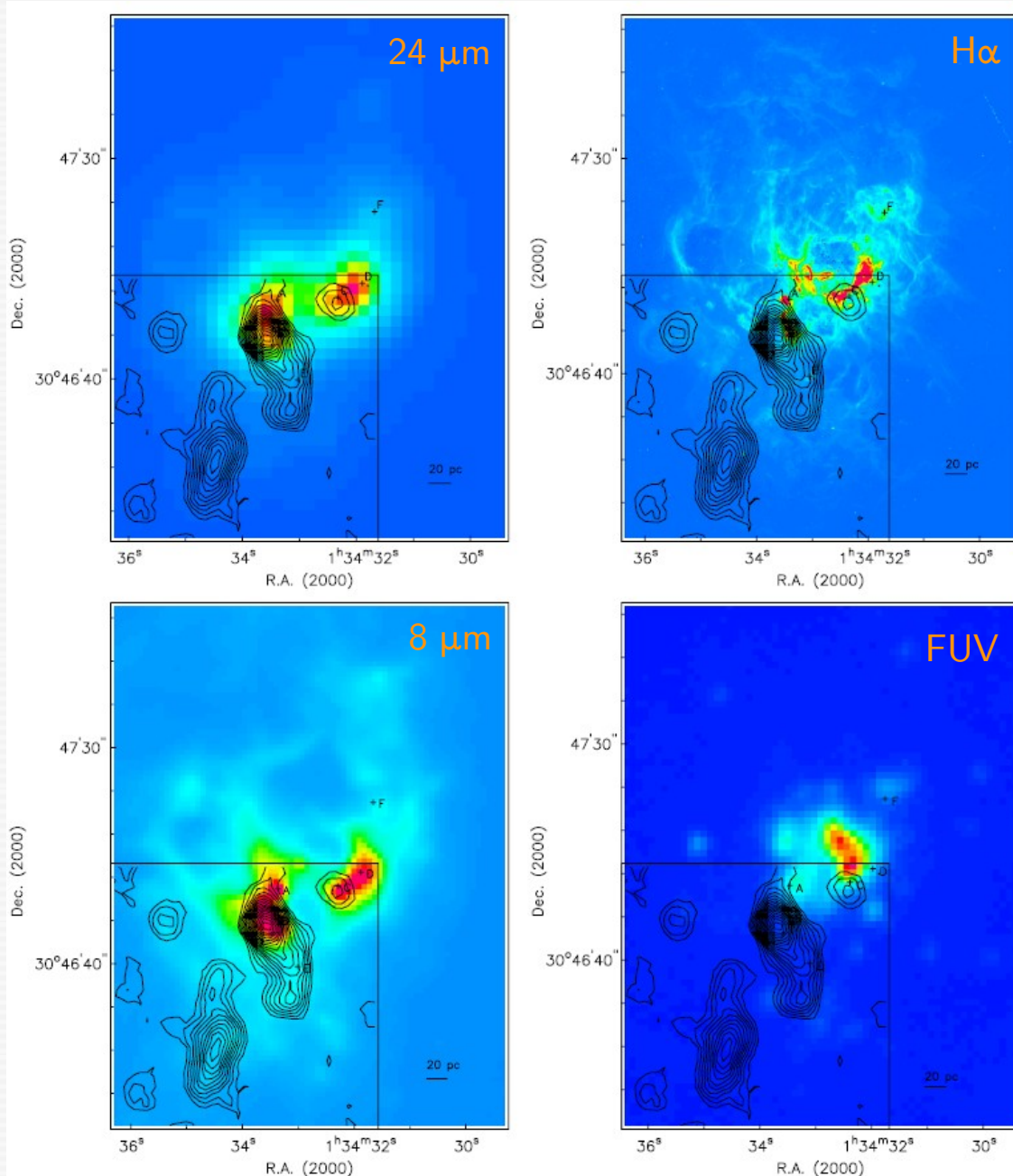
But detailed studies of individual HII regions indicate that 10%-73% of the Lyman continuum photons with energies between 13.6 and 24.4 eV escape (e.g., Castellanos et al. 2002, Eldridge & Relano 2011)

Example: NGC 604 (the most luminous HII region in M33 with a stellar mass of  $5 \times 10^5 M_{\odot}$ , containing a number of young Wolf-Rayet stars) shows a large discrepancy between the  $\text{H}\alpha$  flux expected from its massive young stellar cluster and the one observed about → 50% of the ionizing photons produced by massive stars have to leak out of the HII region

$\log(\text{Age/yr})$	$\log[F(\text{H}\alpha_{\text{Single}})]$ ( $\text{erg s}^{-1} M_{\odot}^{-1}$ )
6.0	34.34
6.1	34.35
6.2	34.35
6.3	34.35
6.4	34.25
6.5	34.16
6.6	33.96
6.7	33.67
6.8	33.27
6.9	32.75
7.0	32.27



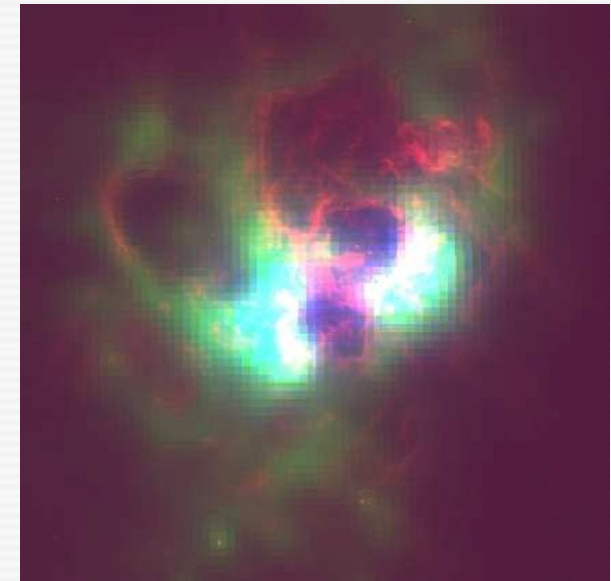
# Evolution of $L(H\alpha)$ and its dependence on photon leakage and metallicity



IR at 24  $\mu\text{m}$  and 8  $\mu\text{m}$  show the dust emission from Spitzer satellite data.

FUV (1344-1786  $\text{\AA}$ ) emission from the GALEX satellite reflects the massive stellar content.

The contours show the CO molecular gas distribution.



$H\alpha$  (red), 8  $\mu\text{m}$  (green) 24  $\mu\text{m}$  (blue)



# Extended H $\alpha$ emission in SFDGs shows an exponential decrease

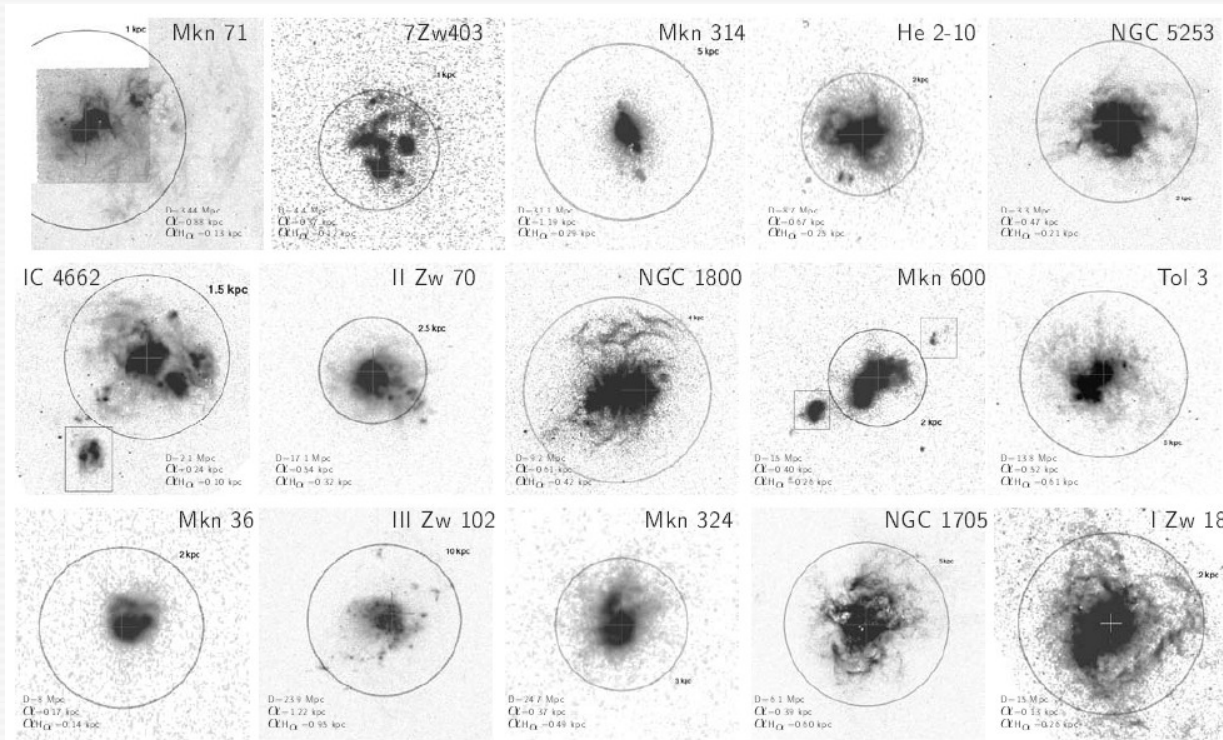
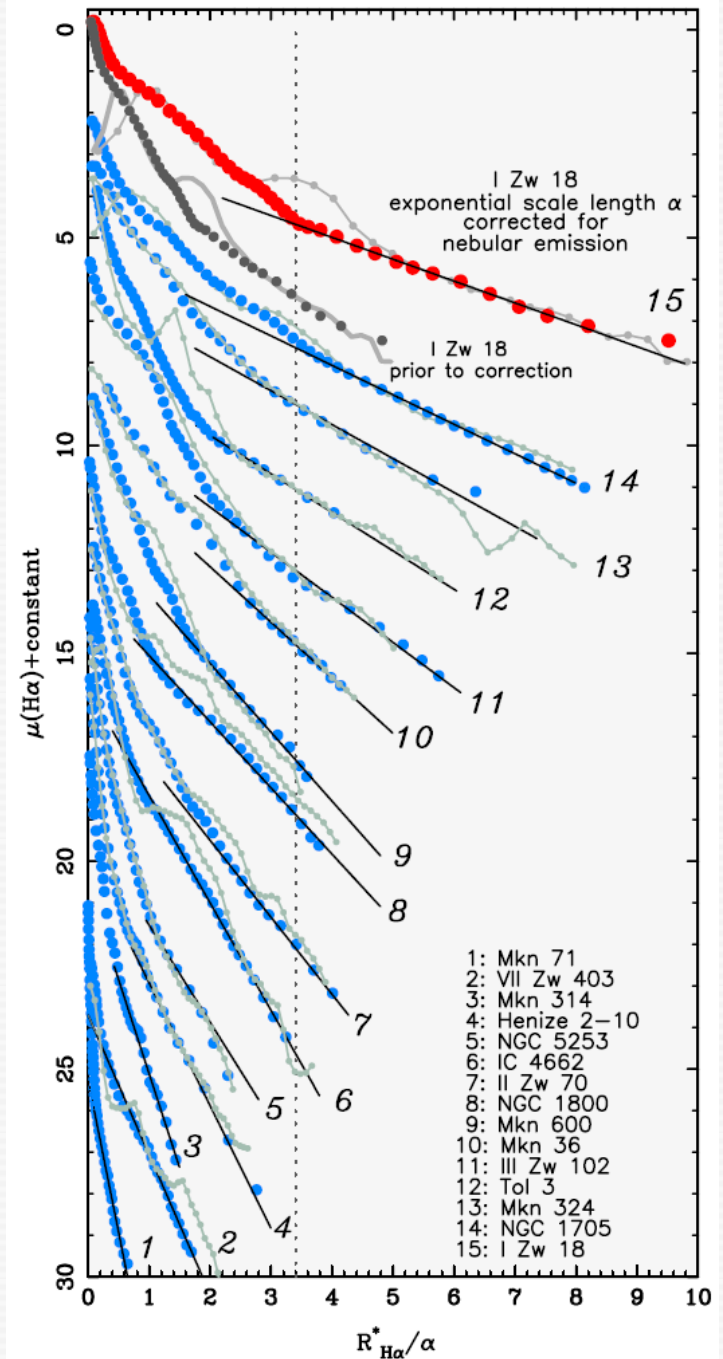


Fig. 14. Continuum-subtracted H $\alpha$  images of a sample of nearby BCDs, the H $\alpha$  surface brightness profiles of which are shown in Fig. 15. Each sample galaxy is labelled with the adopted distance and the  $B$  exponential scale length  $\alpha$  of its stellar LSB host.  $\alpha_{H\alpha}$  is the scale length of the outer exponential part of the corresponding H $\alpha$  profile. Each circle is labelled with its diameter in kpc.

- The radial H $\alpha$  distribution of starburst dwarf galaxies shows an outer exponential decrease with an average scale length of  $\sim 1/2$  of that of the stellar component (typically 1-3 kpc).
- Deep narrowband imaging is necessary for an accurate determination of the total H $\alpha$  luminosity of SFDGs (and other starburst galaxies)

Papaderos et al. (2002)

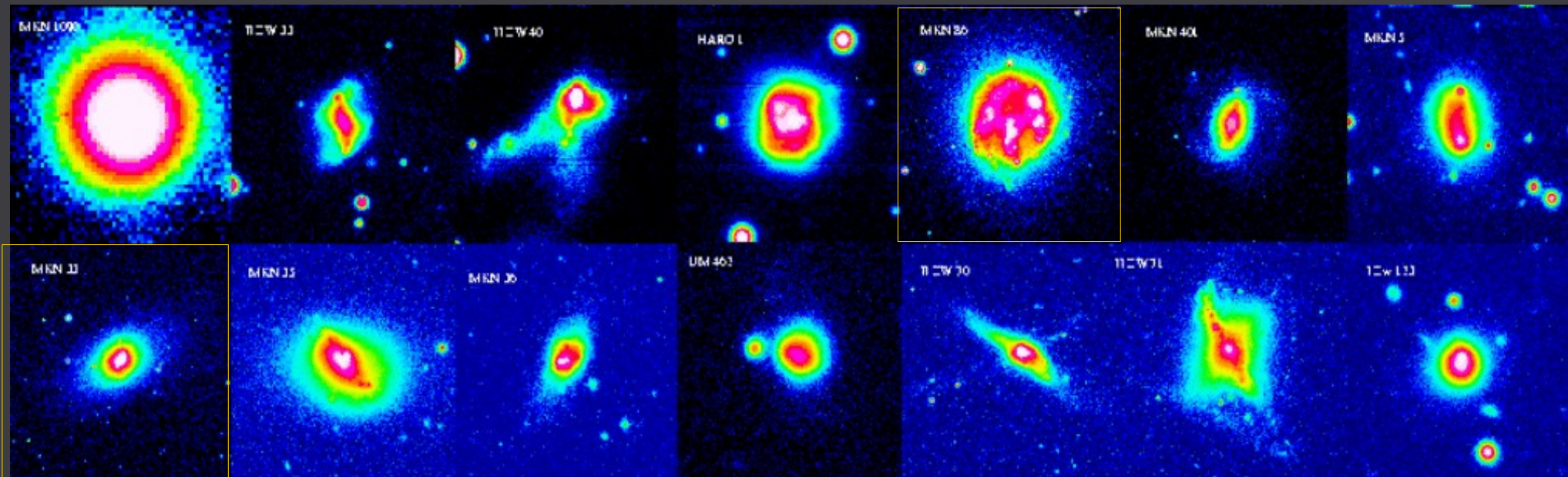
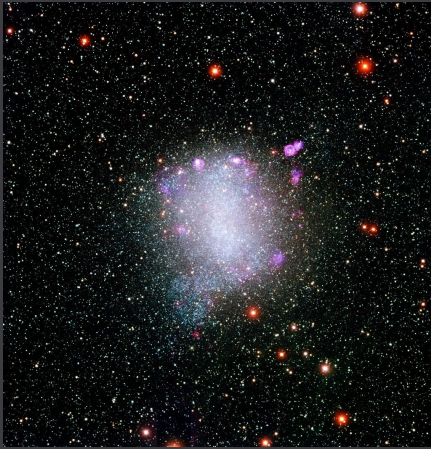


- 1: Mkn 71
- 2: VII Zw 403
- 3: Mkn 314
- 4: Henize 2-10
- 5: NGC 5253
- 6: IC 4662
- 7: II Zw 70
- 8: NGC 1800
- 9: Mkn 600
- 10: Mkn 36
- 11: III Zw 102
- 12: Tol 3
- 13: Mkn 324
- 14: NGC 1705
- 15: I Zw 18

# Star-Forming Dwarf Galaxies: dIs & BCD/HII galaxies

Dwarf irregulars (**dIs**): gas-rich, metal-poor, **low-level star formation**

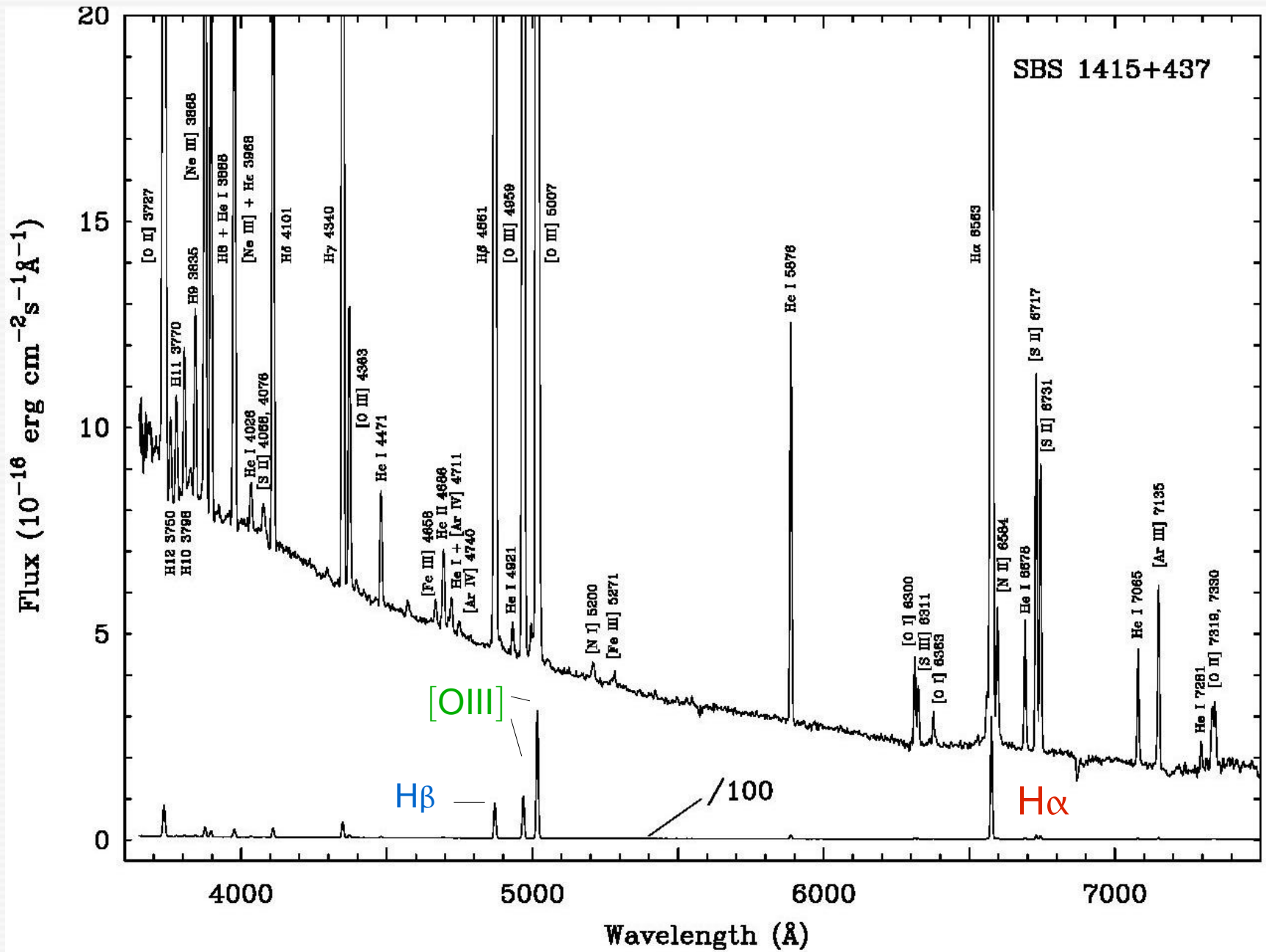
( $10^7 \leq L/L_{\odot} \leq 10^{9.6}$ ,  $M_B > -18$  mag;  $M_T \sim 10^8 \dots$  a few  $10^9 M_{\odot}$ )



Cairós et al. (2001)

Blue Compact Dwarf (**BCD/HII**) galaxies: gas-rich, metal-poor, strong **starburst activity** that is typically confined to the central part of an underlying evolved stellar host

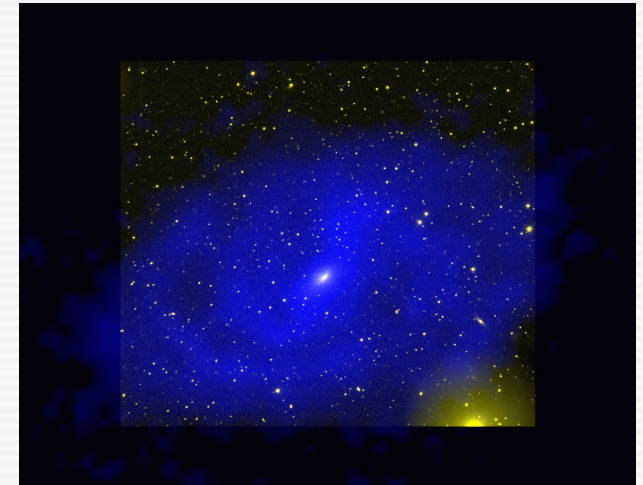
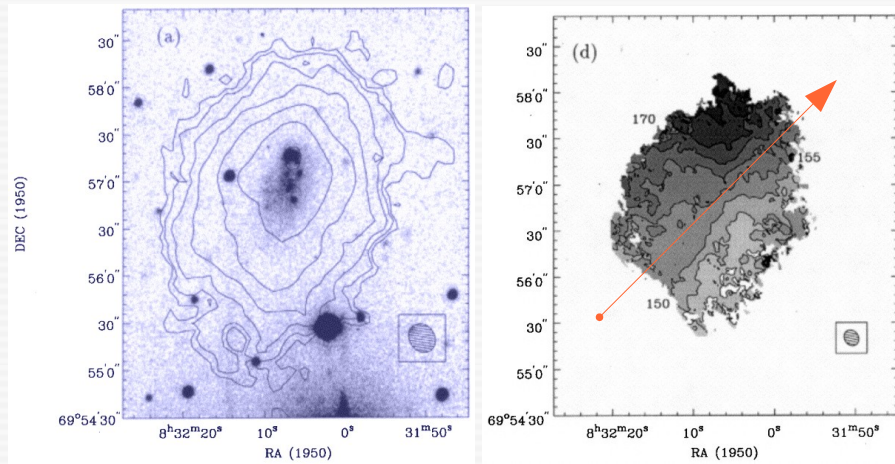






# Properties of the HI component in BCDs

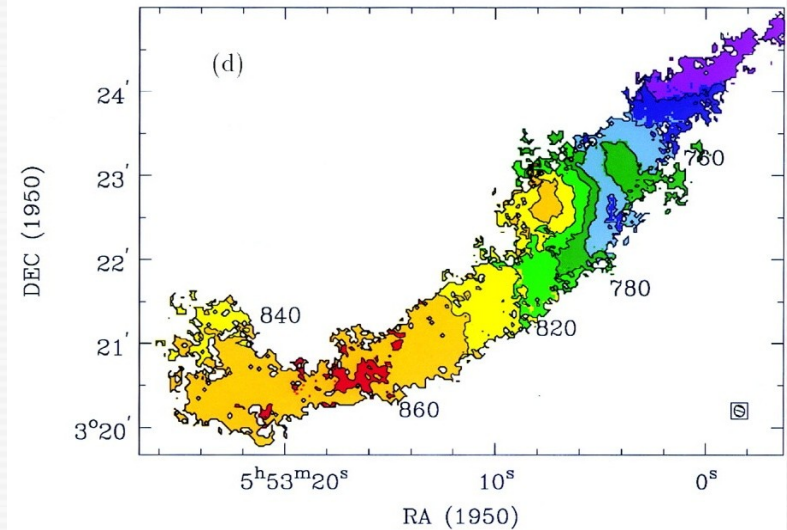
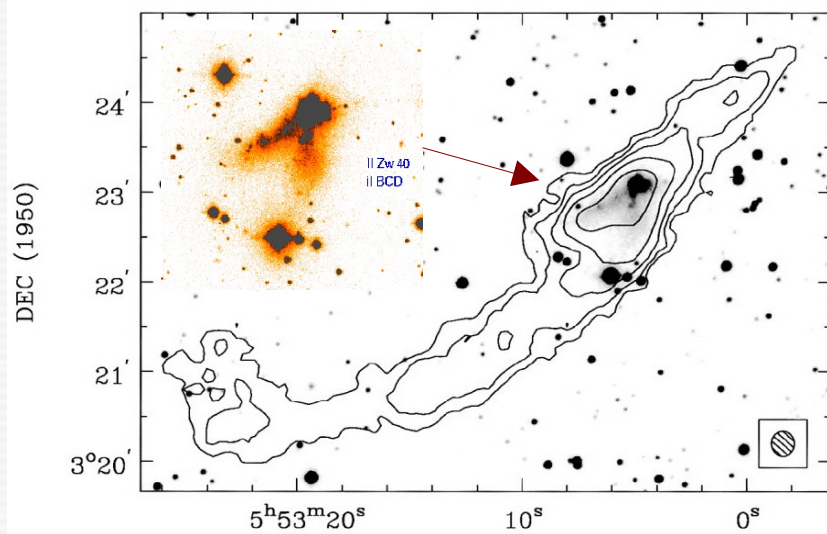
UGC 4483



NGC 2915

van Zee et al. (1998)

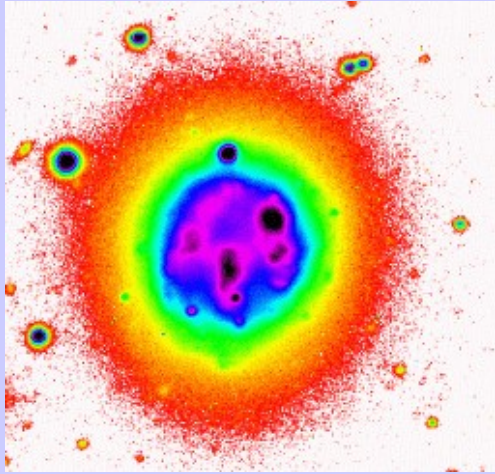
II Zw 40



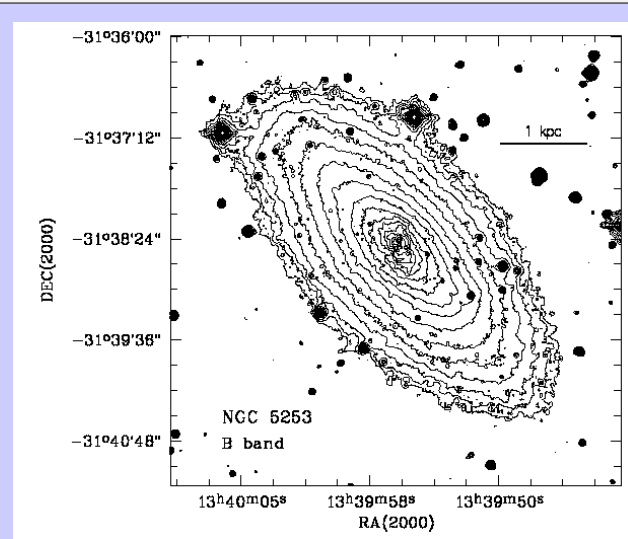
mass ratio: typically  $M_{\text{HI}} = (0.1-1) \times 10^9 M_{\odot}$ ,  $M_{\text{Gas}}/M_{\text{T}} = 0.3-0.9$ ,  $M_{\text{T}}/L_{\text{B}} = 2-6$

$$\frac{\text{HI radius}}{\text{optical radius}} \sim 3 \dots 10$$

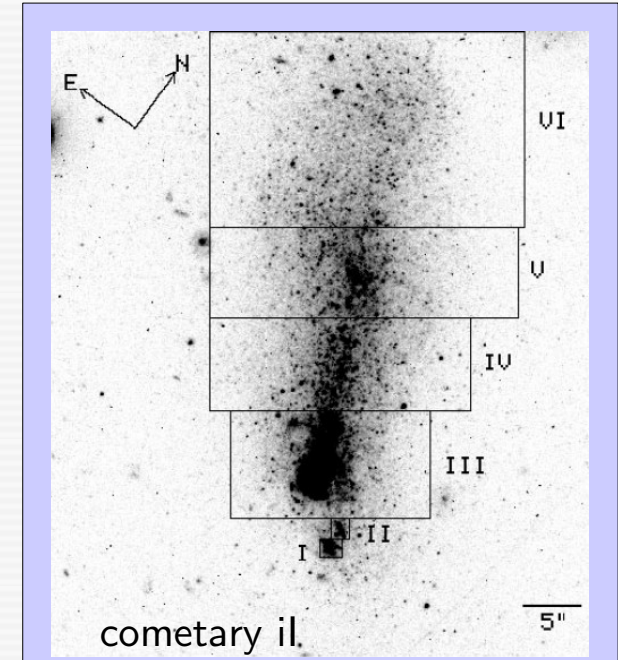
# The BCD classification scheme by Loose & Thuan (1986)



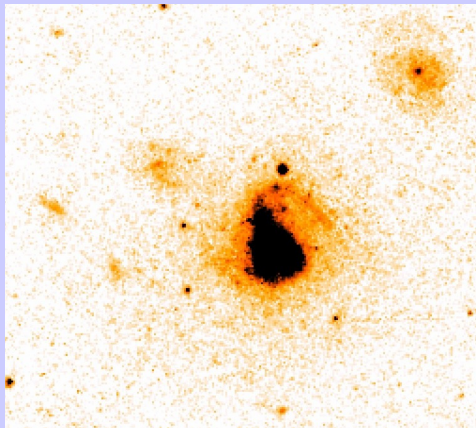
irregular elliptical (iE)  
70%



nuclear elliptical (nE)  
20%

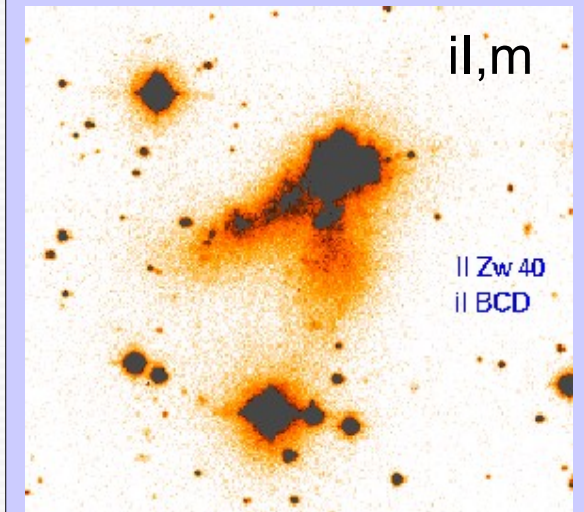


cometary il.



Irregular 0 (i0)  
≤5%

- Discovery of a host galaxy underlying the star-forming component
- Definition of four main morphological classes (iE, nE, il and i0 + il,Cometary)



irregular irregular (il) or il,m  
for possible mergers: ~10%



# The (spectroscopic) classification scheme for HII (BCD) galaxies (Salzer et al. 1989)

TABLE 3  
AVERAGE PHYSICAL PARAMETERS

ELG Type	$B - V_{\text{corr}}$	$V_0$ ( $\text{km s}^{-1}$ )	$M_B$	$D$ (kpc)	$W(\text{O III})$ ( $\text{\AA}$ )
Seyfert 1 .....	0.71	24778	-21.43	34.7	36.2
Seyfert 2 .....	0.77	10966	-20.08	21.1	51.3
Starburst nucleus .....	0.63	14508	-20.07	20.1	21.3
Dwarf amorphous nuclear					
starburst .....	0.59	7005	-18.38	9.4	21.0
H II hotspot .....	0.43	10435	-18.43	9.3	193.1
Dwarf H II hotspot .....	0.43	5241	-16.56	3.8	238.8
Sargent-Searle .....	0.27	2549	-14.08	1.6	1090.5
Giant irregular .....	0.48	13425	-19.88	21.9	138.3
Magellanic irregular .....	0.40	2677	-16.48	5.9	646.8
Interacting pair .....	0.48	8344	-18.42	13.5	82.4

- Galaxies with a spectrum similar to that of an HII region
- Sample: mainly from the University of Michigan (UM) survey
- BCDs  $\in$  HII galaxies of type DANS, HIIH, DIIH and SS

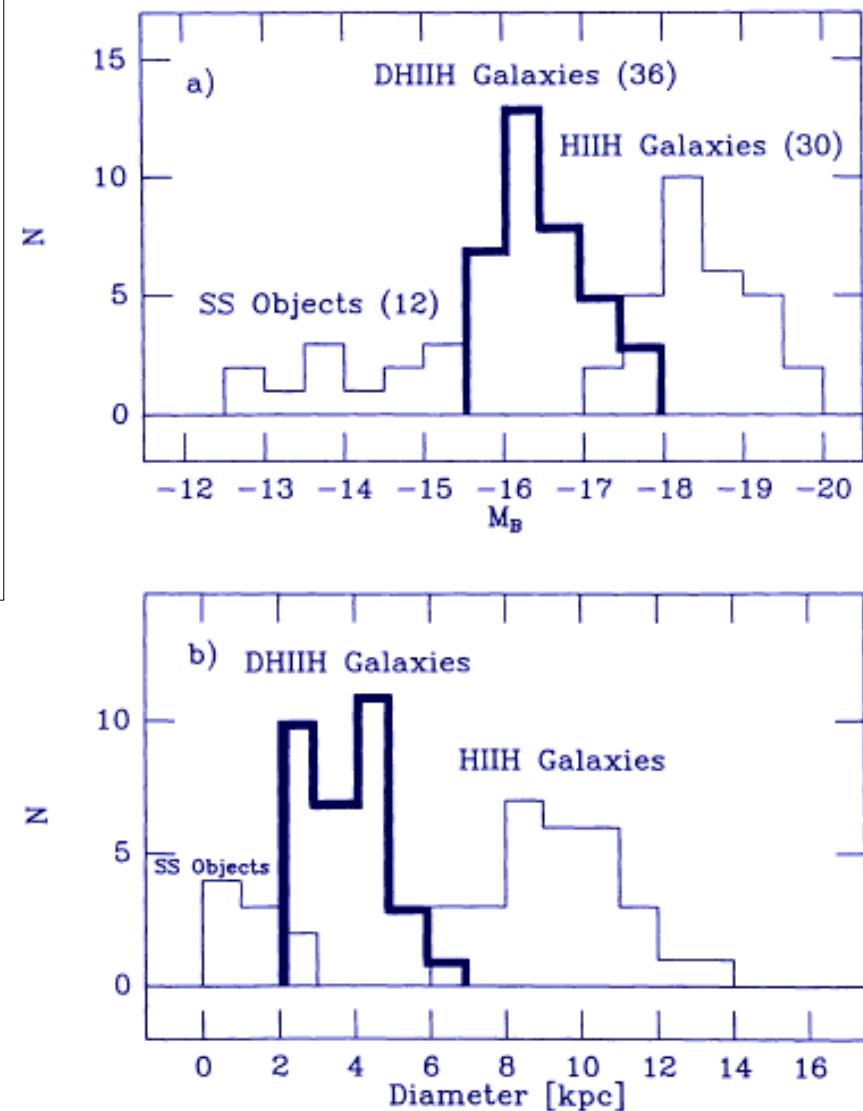


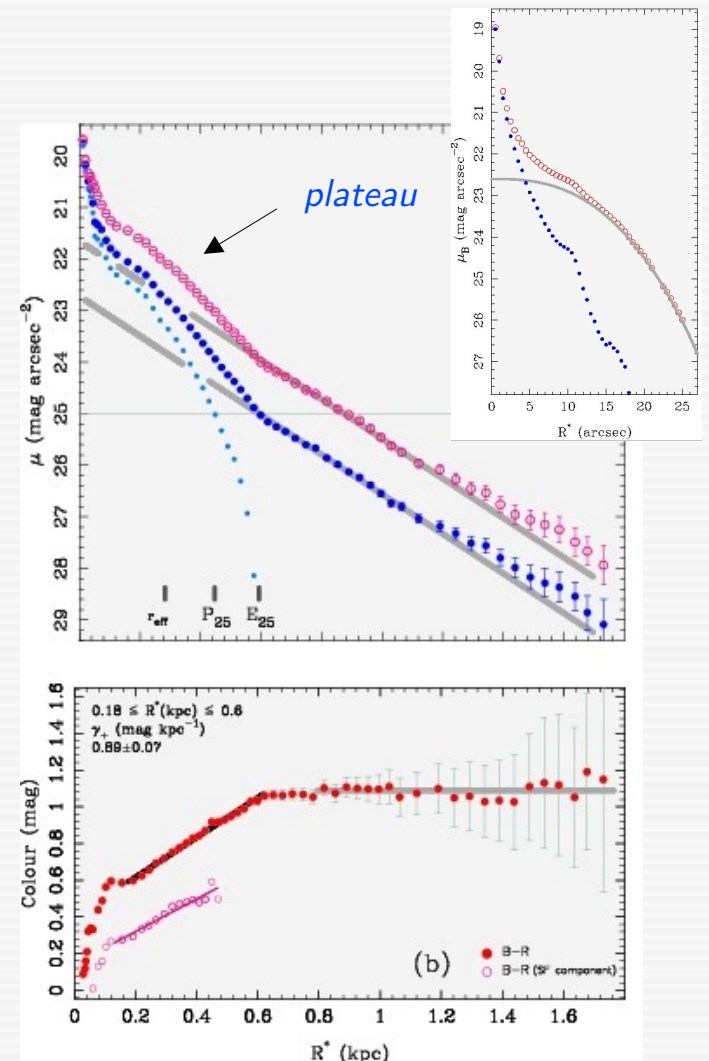
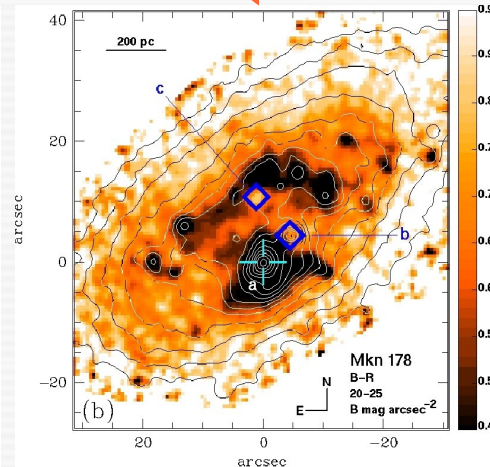
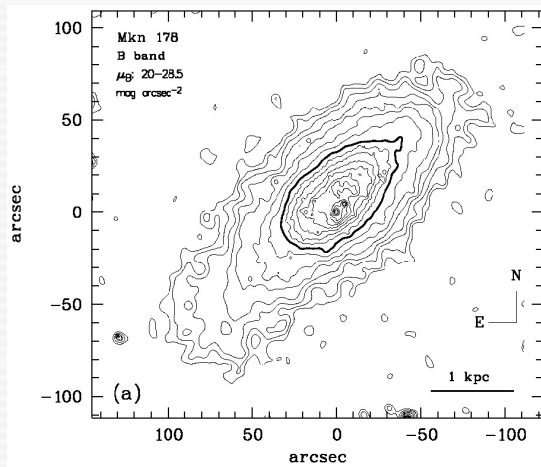
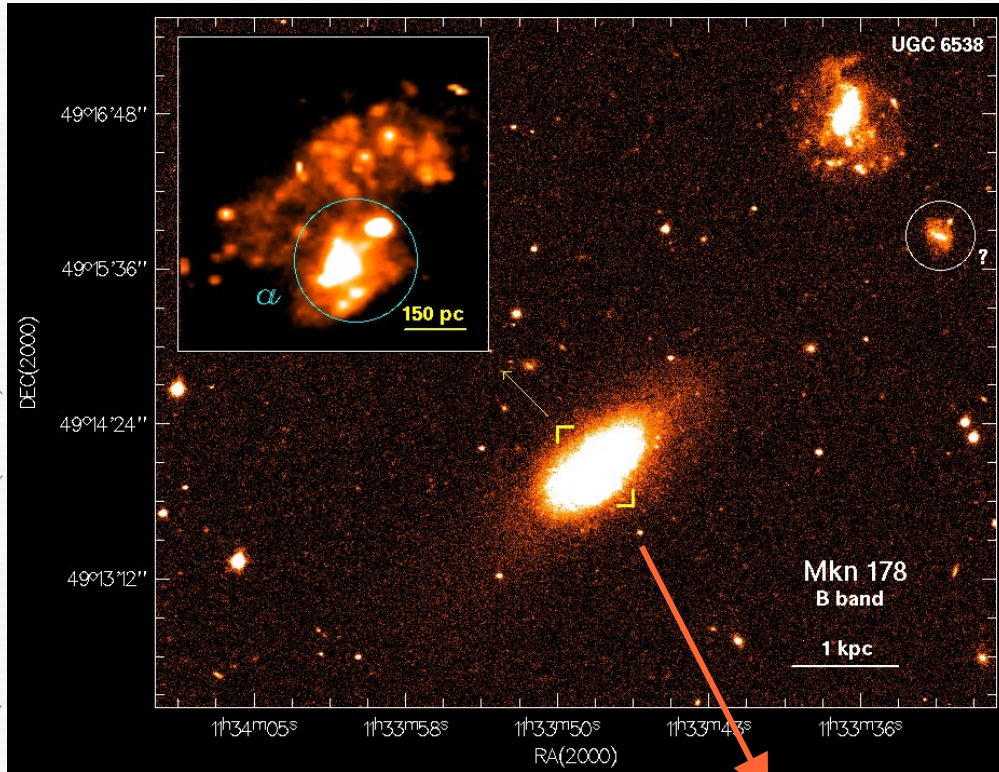
FIG. 9.—Physical parameters for the H II hotspot, dwarf H II hotspot, and Sargent-Searle galaxies. The two diagrams show the distributions of (a) absolute magnitudes and (b) diameters.

Salzer et al. (1989)



# The photometric structure of BCDs

Papaderos et al. (2002)



$P_{25}$ ,  $E_{25}$ : isophotal radius of the star-forming and LSB component

line-of-sight intensity contribution of the SF component:  $<40\%$  at  $P_{25}$ ,  $4\%$  at  $E_{25}$

$D = 4 \text{ Mpc}$   
 $M_B = -13.9 \text{ mag}$

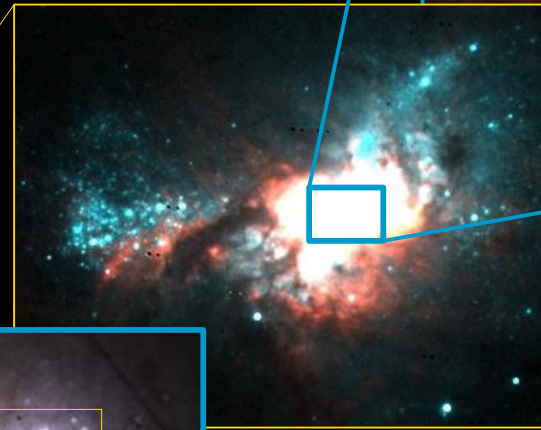
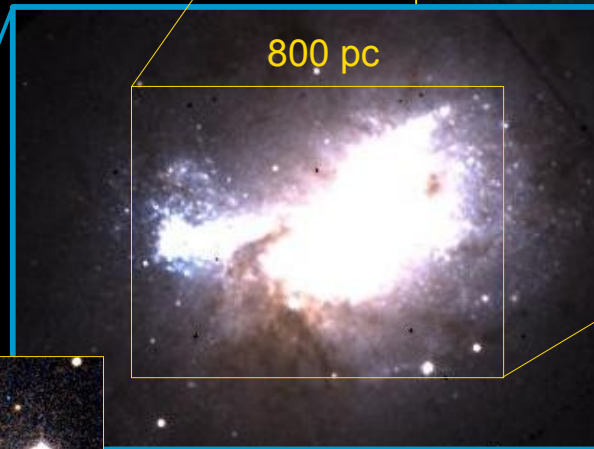
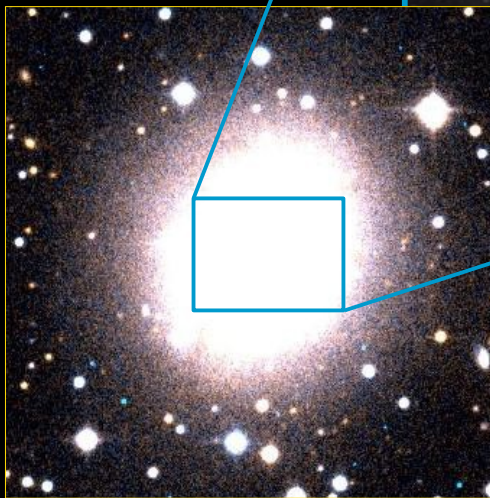
Mkn 178

# Starburst activity in BCDs

## Henize 2-10

- Nearby ( $D=8.7$  Mpc) BCD
- Starburst since  $10^7$  yr  
(Conti & Vacca 1996,  
Papaderos & Fricke 1998)
- Prominent Wolf-Rayet features

Papaderos et al. (2006)



## Star formation in BCDs

- diffuse component consisting of low-mass stellar clusters ( $\approx 10^2 - \text{a few } 10^3 M_{\odot}$ )
- luminous, very compact stellar clusters ( $\approx 10^4 M_{\odot}$ ) all through to “Super-Star Clusters” (SSCs) with mass: up to  $10^5 M_{\odot}$ !  
radius: 3-10 pc  
density: up to  $10^4 M_{\odot} \text{ pc}^{-3}$

Nearly coeval star formation on spatial scales of  $\sim 1$  kpc



# Kinematical decoupling of gas and stars in the starburst component of He 2-10

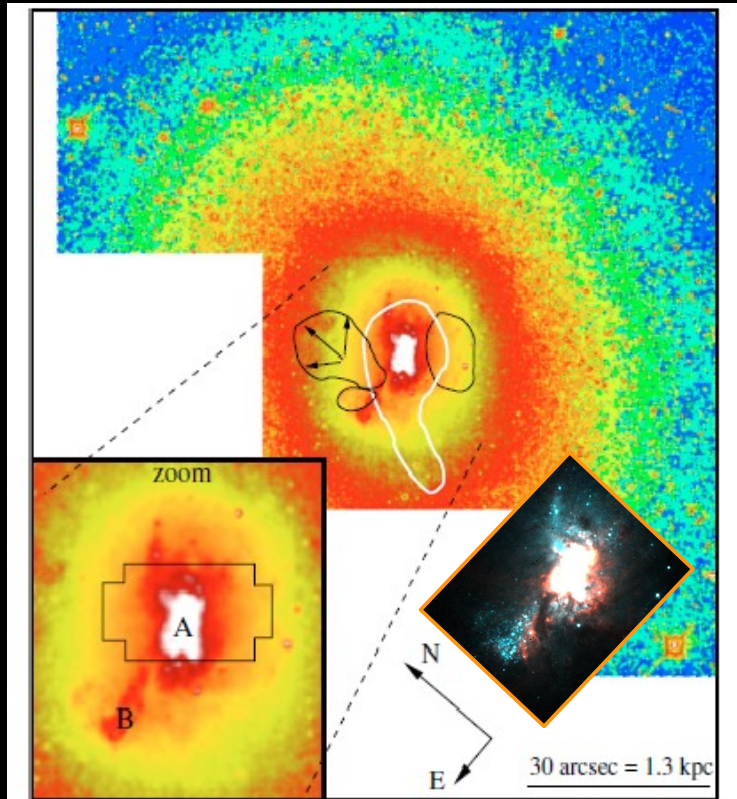


Fig. 1. HST/WFPC2 F814W archival image of He 2-10 with an overlaid CO (thick white) contour from Kobulnicky et al. (1995). The thin black lines outline the positions of bubbles observed in H $\alpha$  emission (Méndez et al. 1999). The inset shows the central region at larger scale together with the footprint of our ARGUS observations and regions A and B, as discussed in the text.

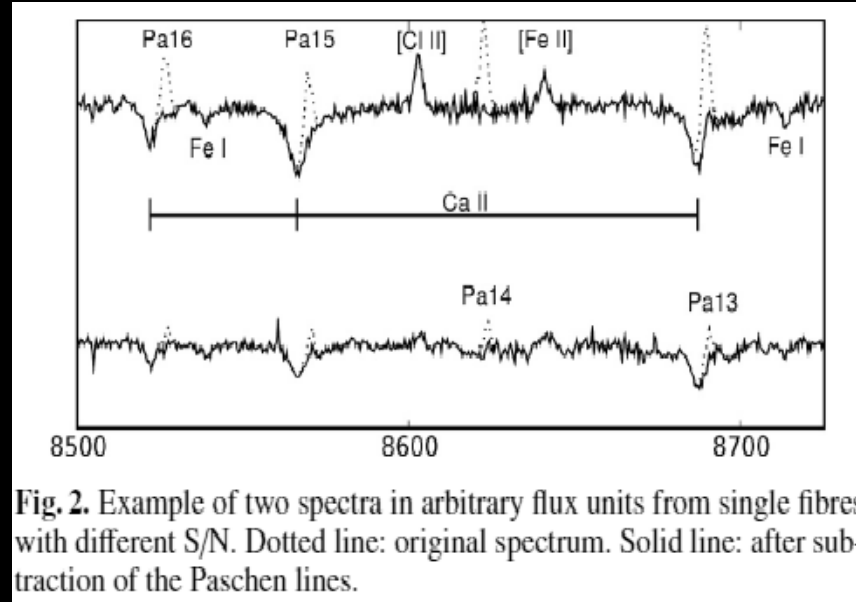
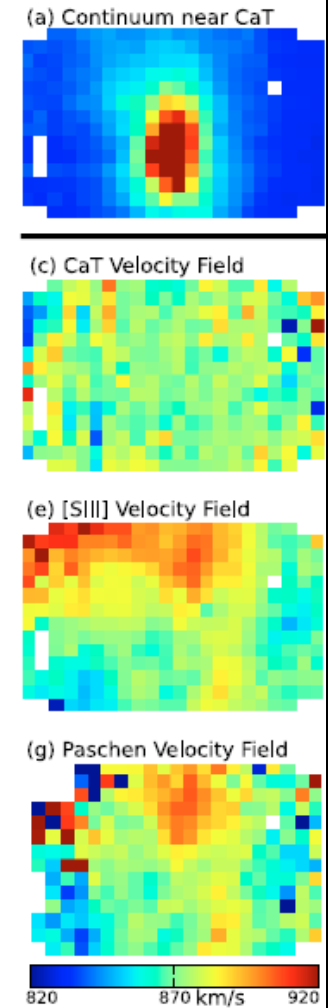


Fig. 2. Example of two spectra in arbitrary flux units from single fibres with different S/N. Dotted line: original spectrum. Solid line: after subtraction of the Paschen lines.



ARGUS/FLAMES IFS data at  
Ca II  $\lambda\lambda$ 8498, 8542, 8662 Å triplet

Marquart et al. (2007)

- stellar kinematics are governed by random motions  $\sigma \sim 45$  km/s
- dynamical mass of the nuclear starburst region  $M\sigma = 1.1 \times 10^6 \cdot r_{\text{eff}} \cdot \sigma^2 = 4 \times 10^7 M_{\odot}$
- velocity difference between gas and stars  $\sim 50$  km/s

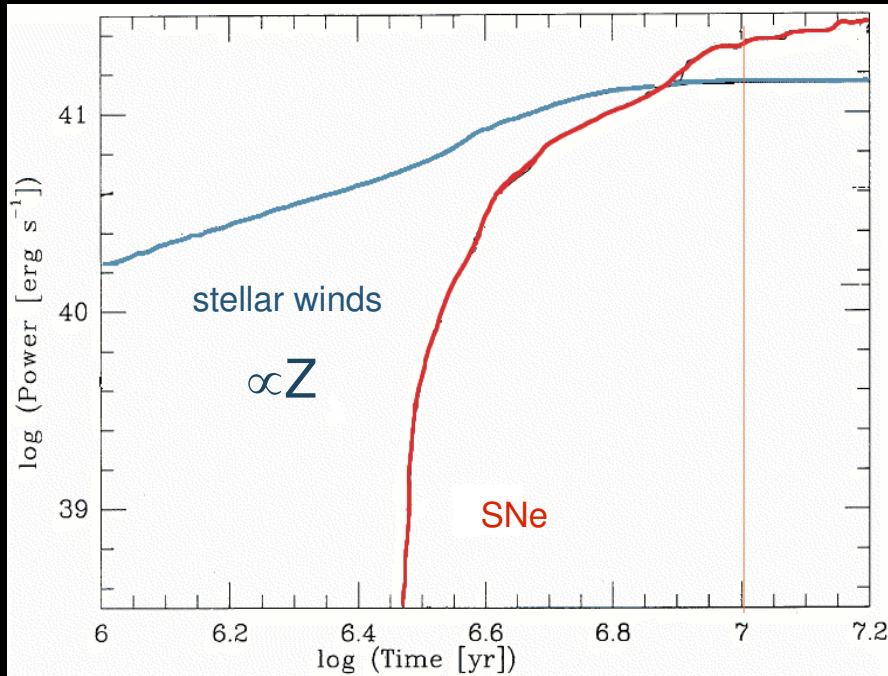


# Henize 2-10: H<sup>-</sup> supershells and large-scale gas outflows

a)

Log (mechanical luminosity)

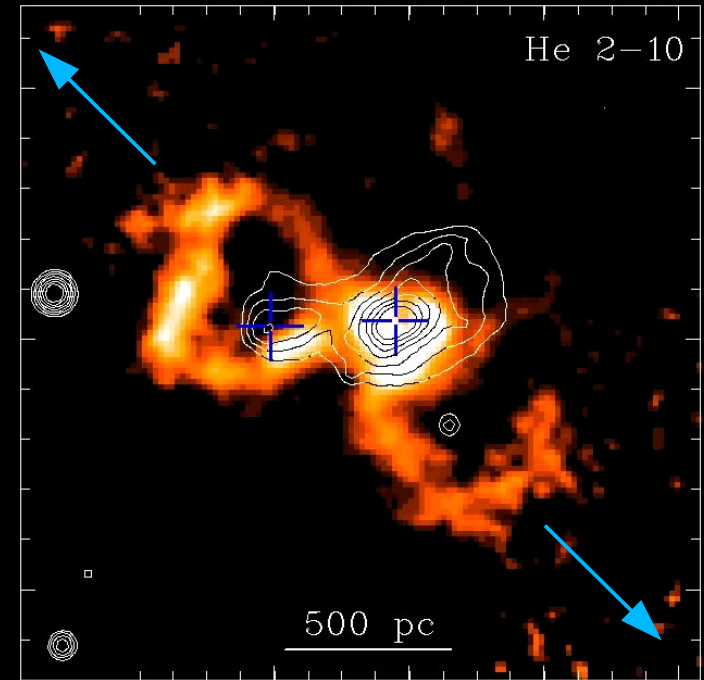
Leitherer et al. (1992)



Log (time)

b)

Papaderos & Fricke (1998)

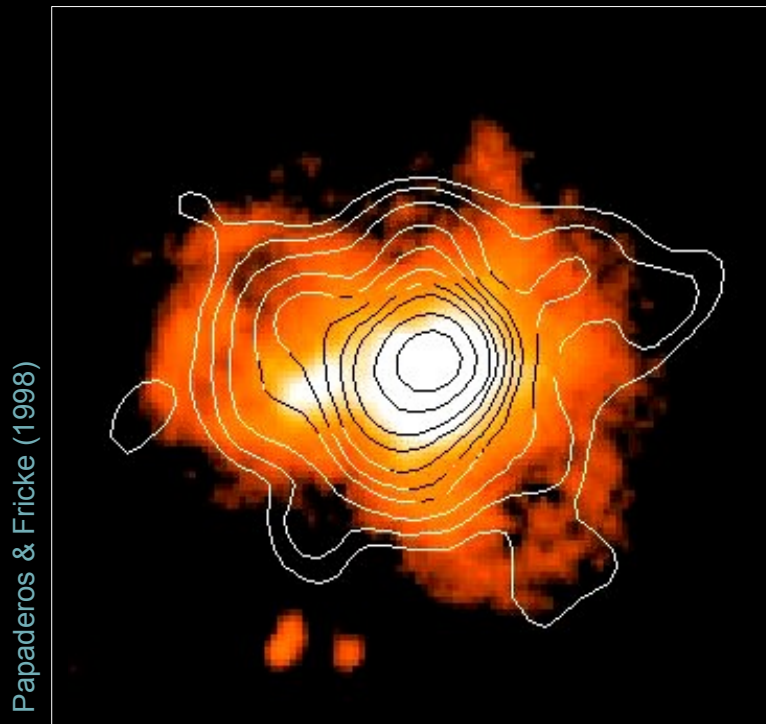


H $\alpha$  equivalent width map

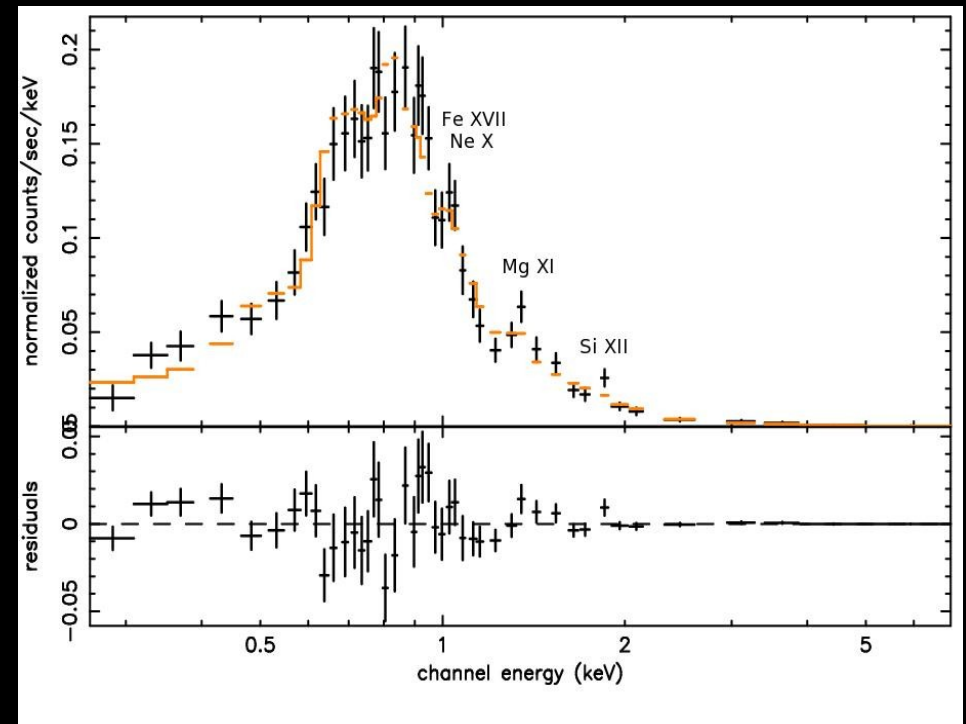
a) mechanical luminosity for a Star Formation Rate of  $1 M_{\odot} \text{ yr}^{-1}$  as a function of time  
Luminosity Power at  $t=10^7 \text{ yr}$  :  $4 \times 10^{41} \text{ erg s}^{-1}$   
(total energy injected into the ISM:  $4.5 \times 10^{55} \text{ erg}$ )

b) observations: gigantic bipolar outflow of hot and metal-enriched gas from the starburst component, expanding with velocities of  $\geq 200 \text{ km s}^{-1}$  into the ambient interstellar medium.

# Henize 2-10: H<sup>-</sup> supershells and large-scale gas outflows



X-ray contours (ROSAT HRI) overlaid with a continuum-subtracted H $\alpha$  map.



XMM-Newton X-ray spectrum (0.25-6 keV)

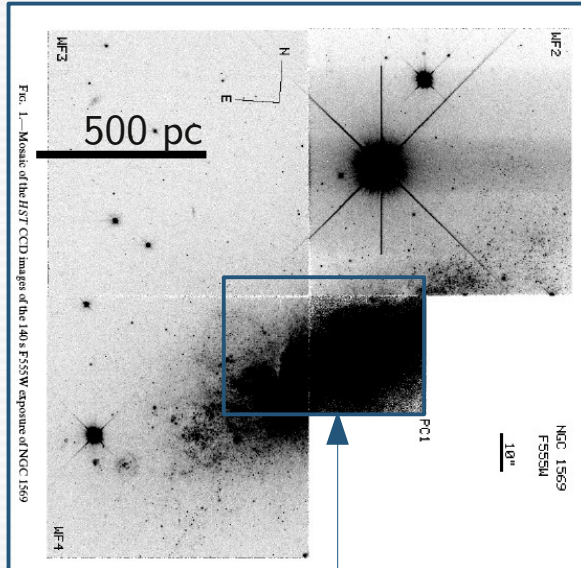
- Thermalization of the ISM (hot ( $10^7$  K) X-ray emitting gas)
- Expansion into the ambient ISM and ejection into the halo (and possibly beyond): **galactic winds**
- Chemical enrichment of the interstellar and intergalactic medium.
- **Lyman continuum photon escape and ionization of the intergalactic space**





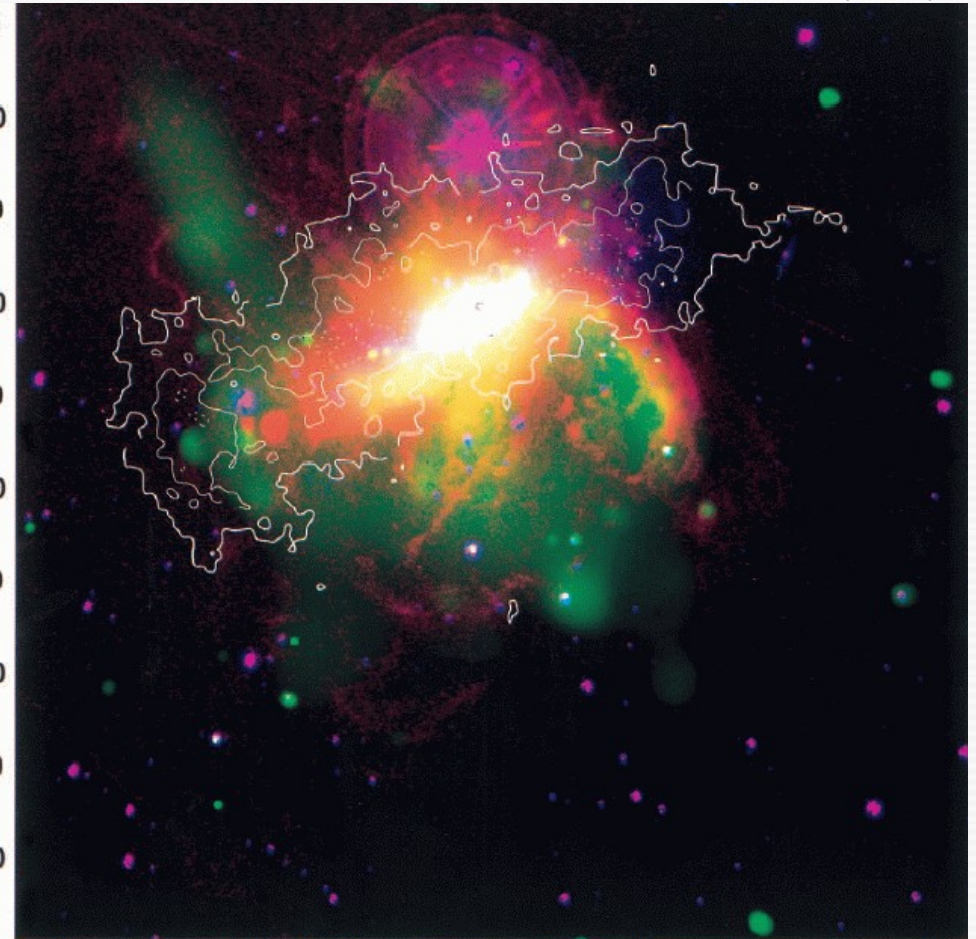
# BCDs: starburst-driven mass ejection into halo

NGC 1569



Super-Star Clusters

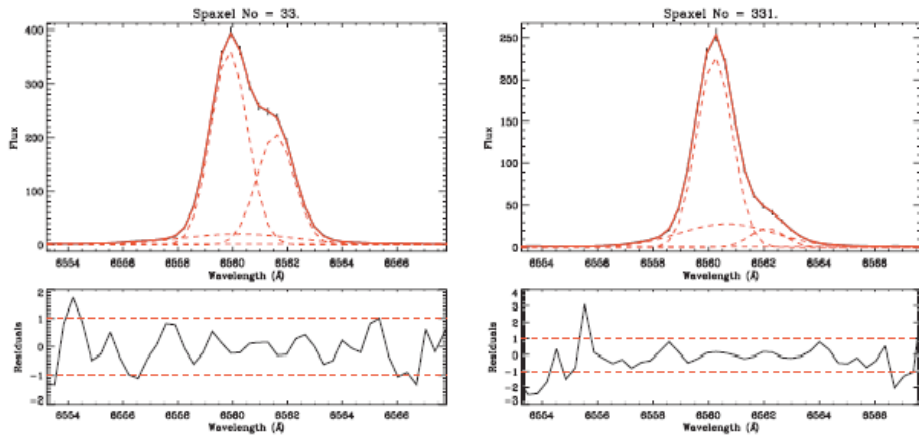
Martin et al. (2001)



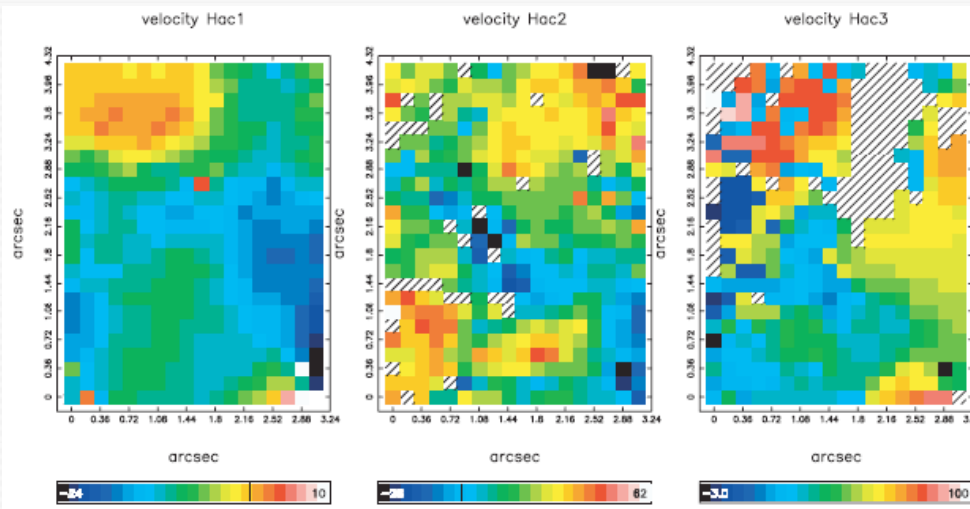
— HI    — H $\alpha$     — X-ray



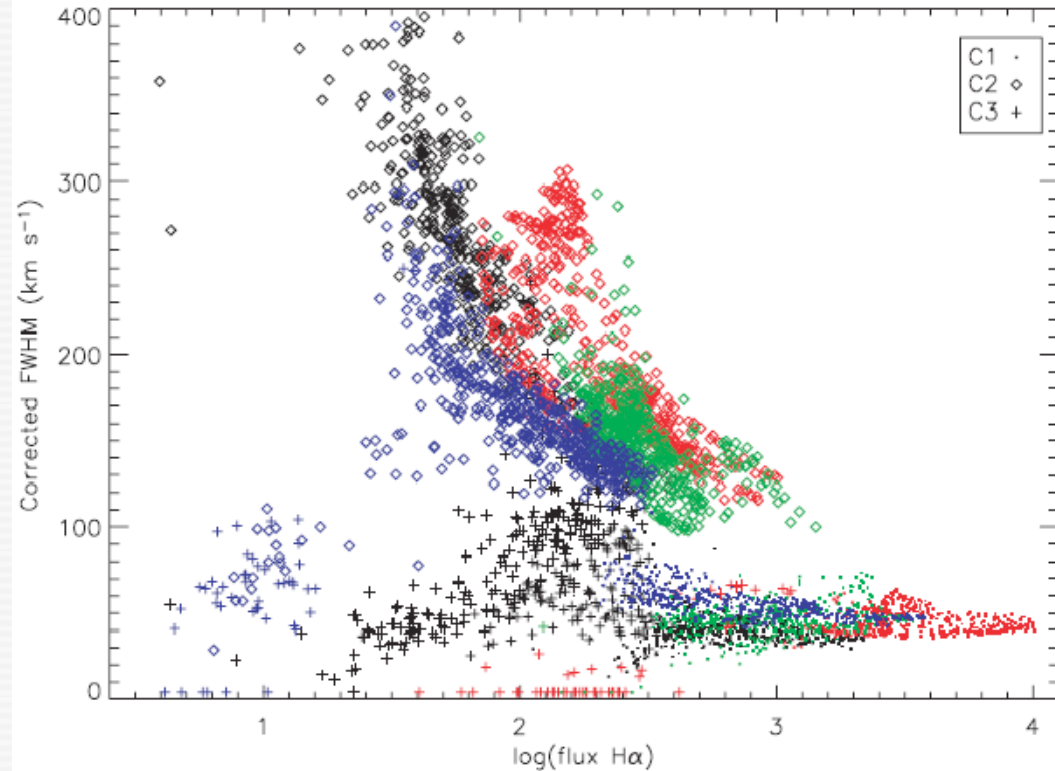
# High-velocity ionized gas in NGC 1569



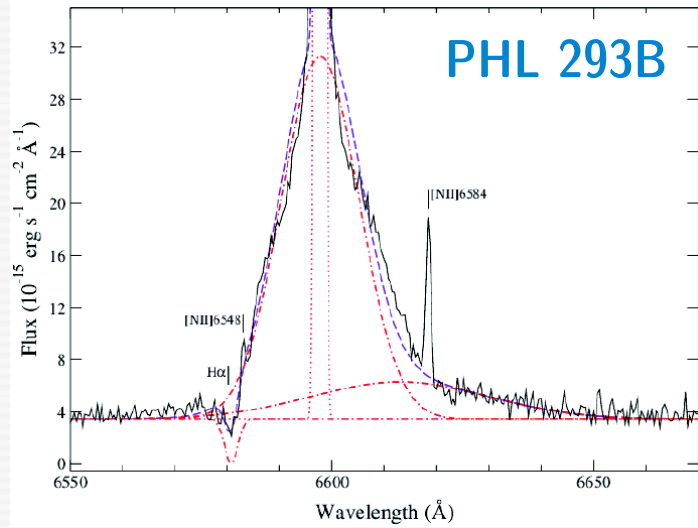
- highly-complex gas kinematics on spatial scales of 20-100 pc
- High-velocity (350-400 km/s) ionized gas component underlying the bright nebular emission lines that is produced in a turbulent mixing layer on the surface of cool gas knots



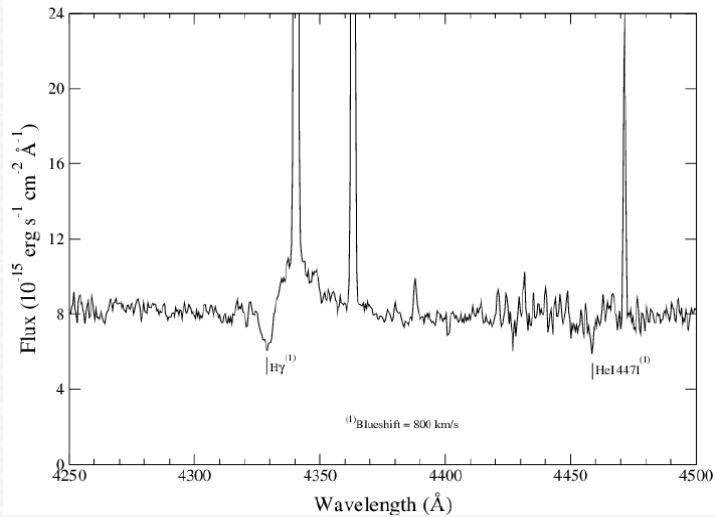
Westmoquette et al. (2007)



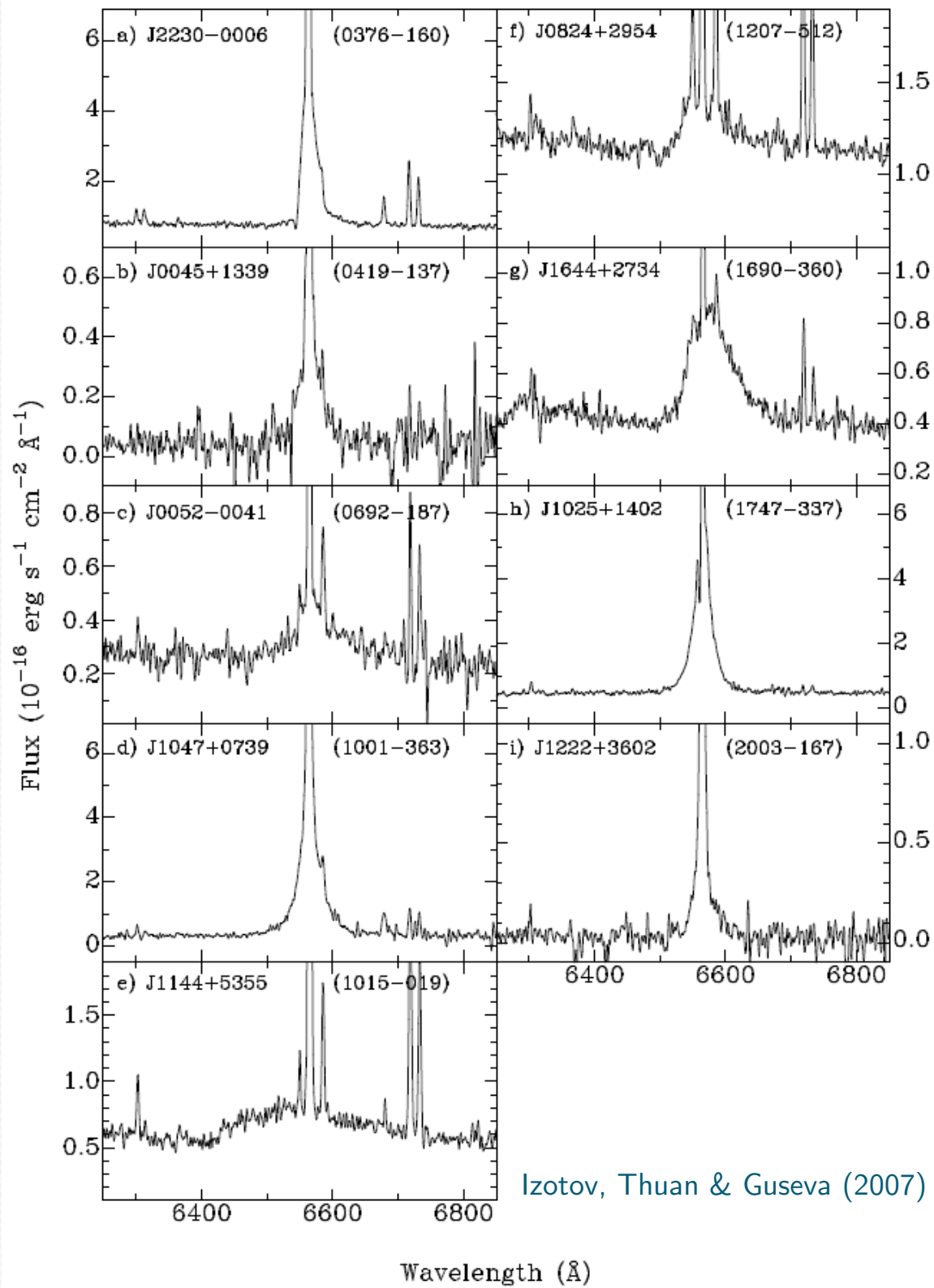
# High-velocity ionized gas in SFDGs



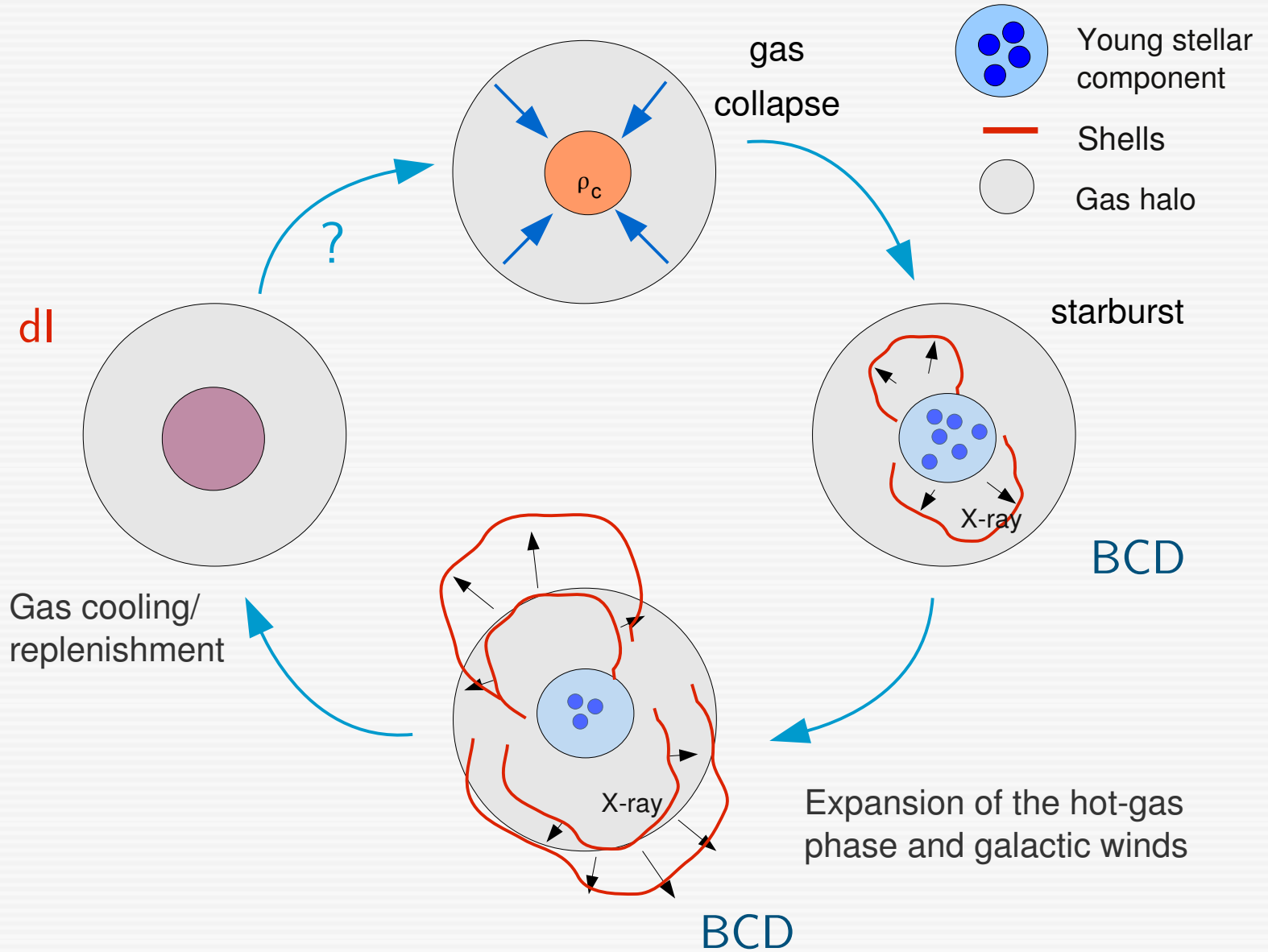
Terlevich et al. (2014)



- broad (FWHM =  $10^3$  km/s) and very broad (FWZI =  $4 \times 10^3$  km/s) Balmer emission lines
- narrow absorption components in the Balmer series blueshifted by  $\sim 800$  km/s

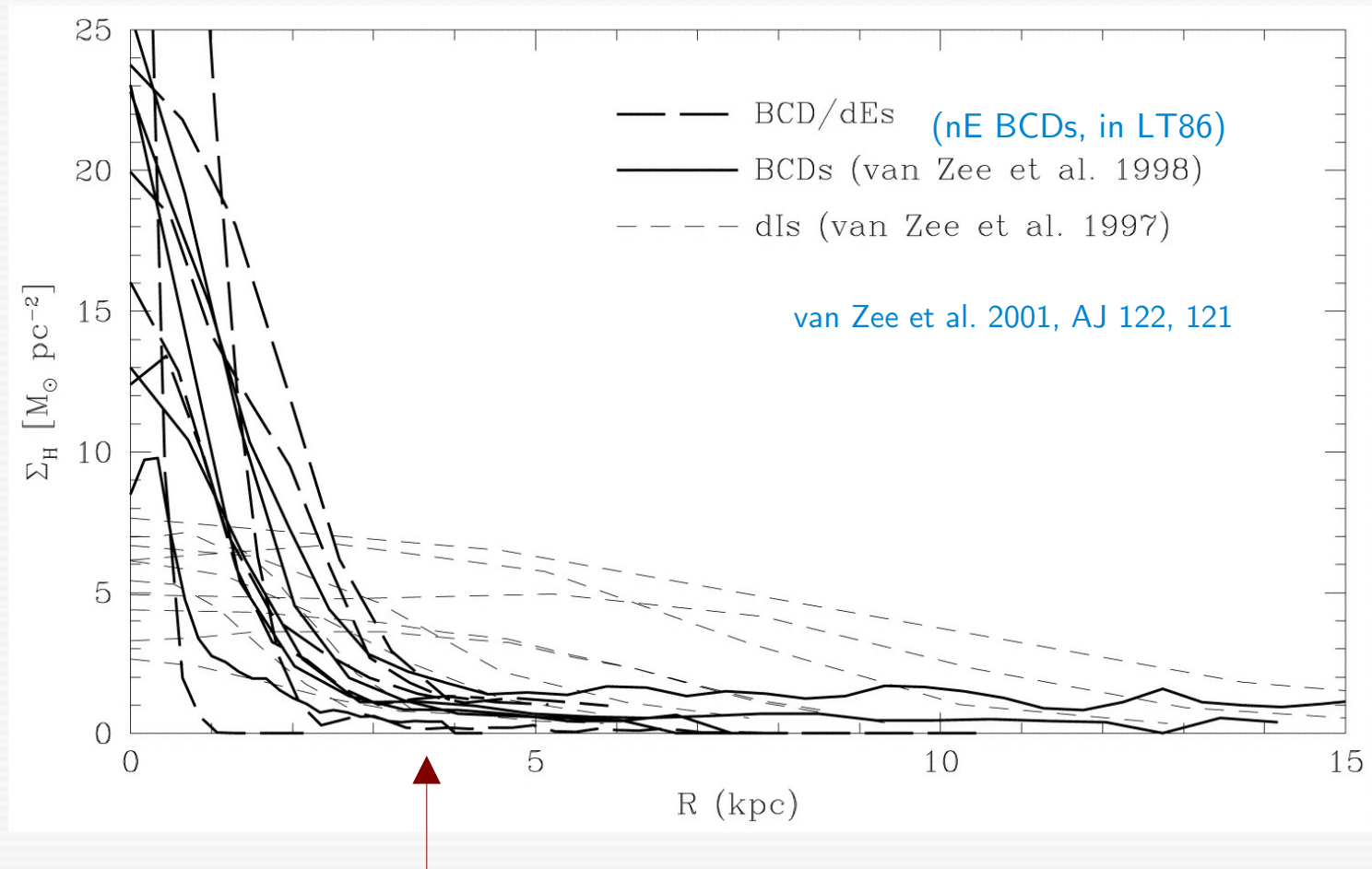


# Chronology of a starburst in a dl/BCD





# Comparison of the radial HI surface density distribution in BCDs and dIs



Optical Radius

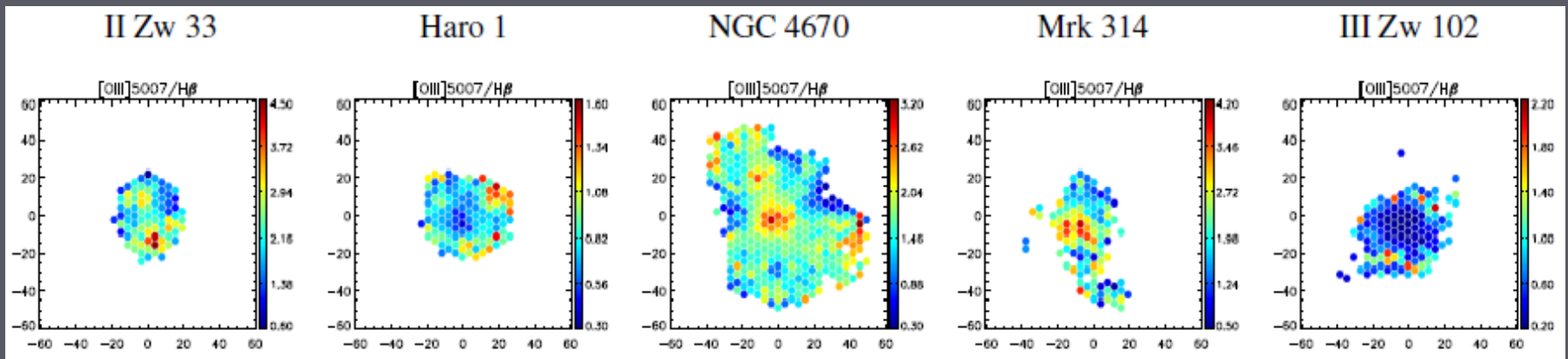
BCDs are more compact than dIs with respect to their HI distribution

$$\Sigma_{\text{HI}}(\text{BCDs}) \sim 5 \times \Sigma_{\text{HI}}(\text{dIs})$$

See also Taylor et al. (1995), Simpson & Gottesmann (2003)

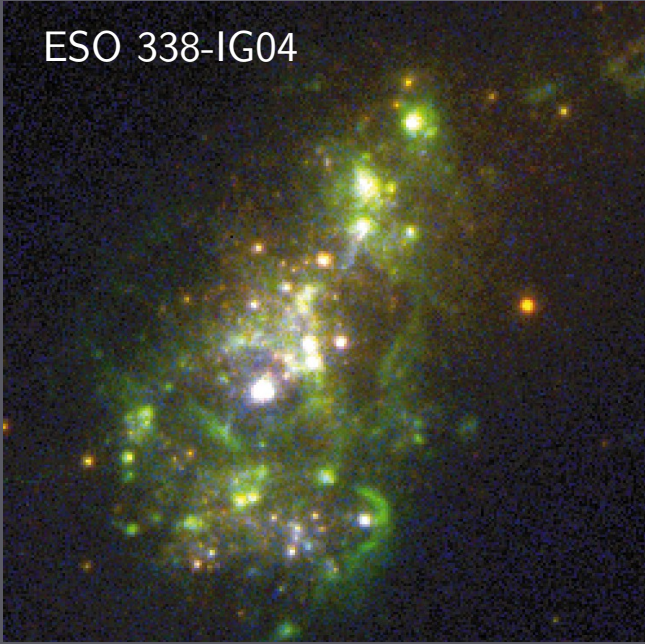
## Some open questions

- Origin of starburst activity in BCDs
- IFS studies of BCD samples (see, e.g., Cairos et al. 2012)
- Origin of the hard ionizing field in low-metallicity SFDGs (see, e.g., Izotov et al. 2004)
- **Synchronization of star-forming activities in BCD/HII galaxies**
- Chemical abundance patterns and homogeneity of BCD/HII galaxies (see Lagos & Papaderos 2014, for a recent review)
- Mechanisms regulating the Ly $\alpha$  escape fraction in starburst galaxies (see Tenorio-Tagle et al. 1999)
- **Evolutionary links between dIs and BCD/HII galaxies**

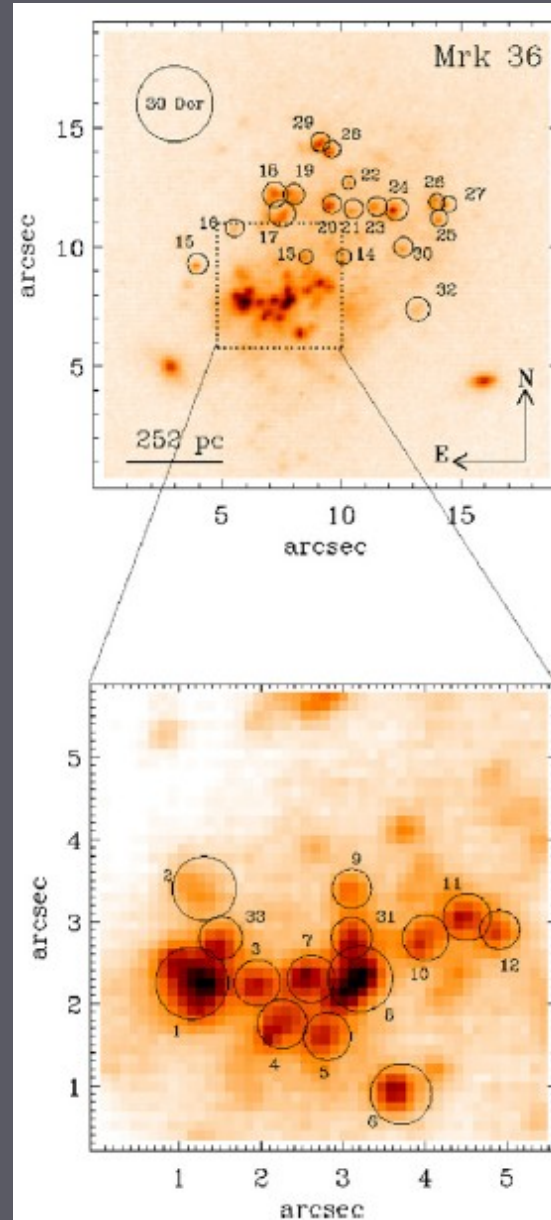
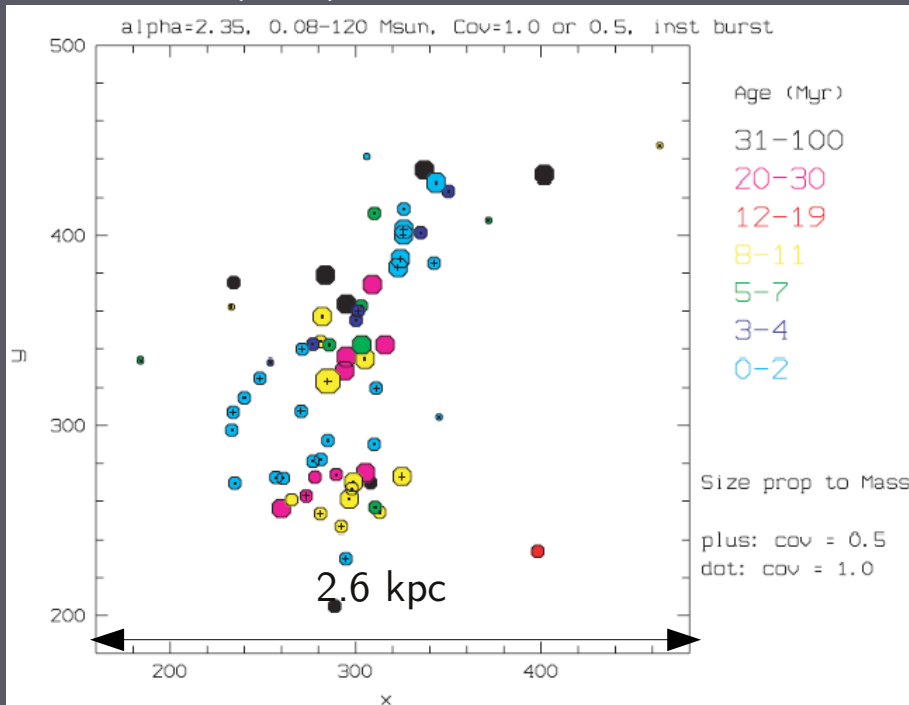


# Synchronization of star-forming activities in BCDs/HII galaxies

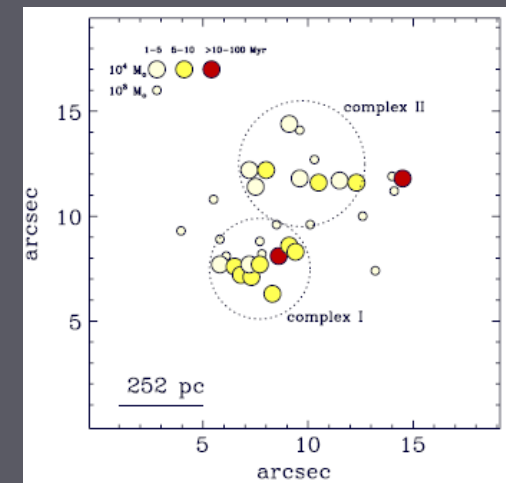
ESO 338-IG04



Östlin et al. (2003)



Lagos et al. (2011)

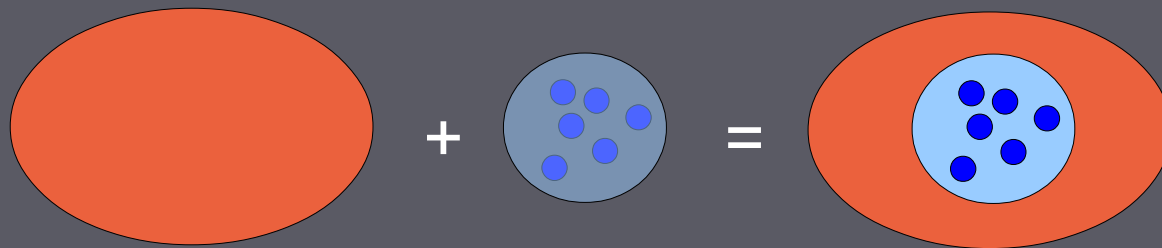
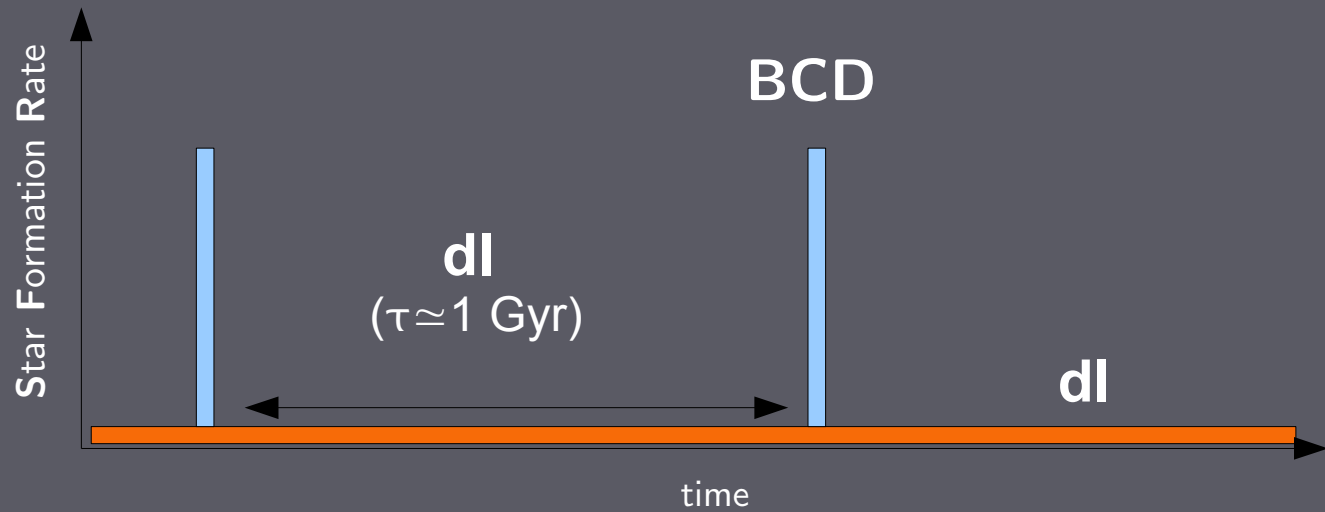


Nearly coeval star formation on spatial scales of 0.2-1 kpc



# Evolutionary links between active (BCD/HII) and quiescent (dl) star-forming dwarf galaxies

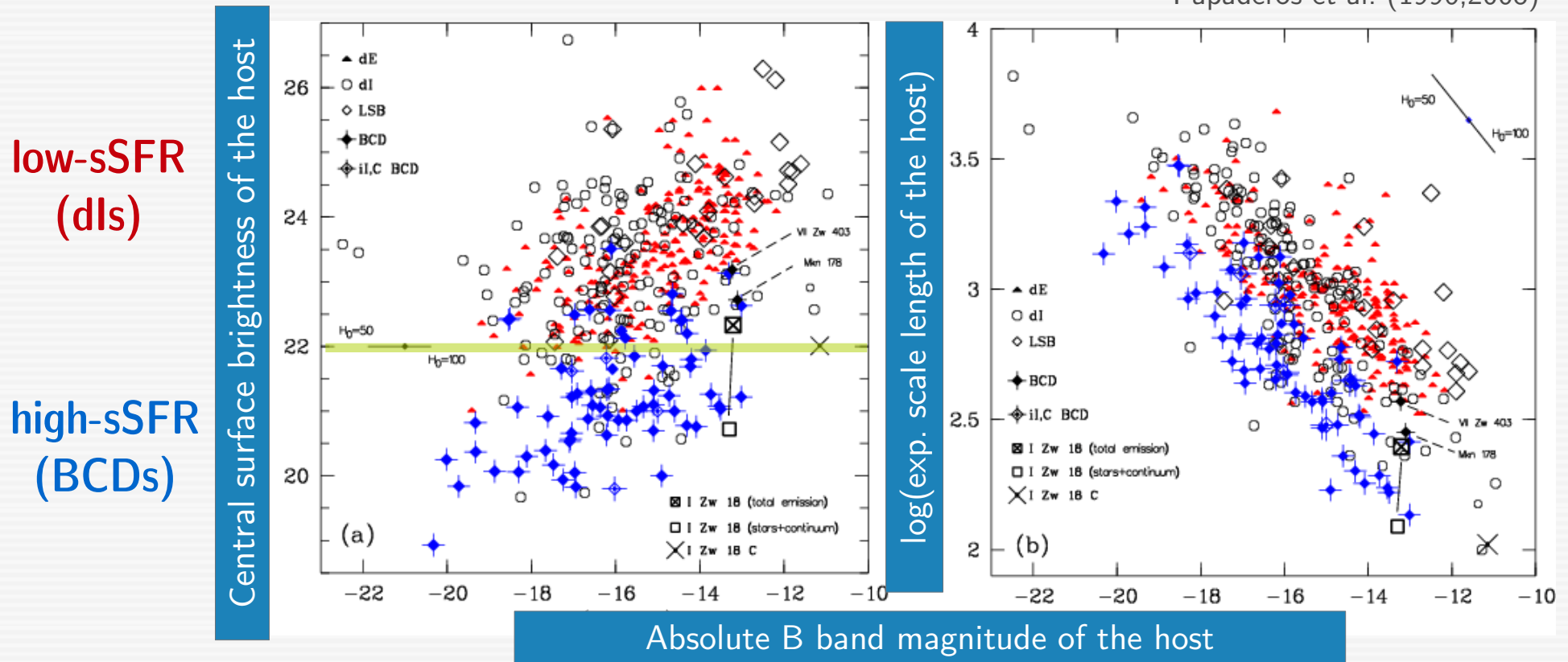
The "standard" dl↔BCD evolutionary scenario



Dwarf irregular + Starburst = Blue Compact Dwarf

# Starburst activity in low-mass galaxies occurs preferentially in compact, high-stellar density ( $\rho_*$ ) hosts

Papaderos et al. (1996,2008)



- Central  $\rho_*$  of in the **BCD host** galaxy is  $\sim 10 \times$  higher than in **(low-sSFR) dIs**
- The density of the local stellar background (and the form of the gravitational potential it produces) is one of the parameters regulating star-forming activity (i.e. the Schmidt-Kennicutt law provides an incomplete parametrization of the SFR in triaxial, low-mass galaxies)

# Evolutionary links between BCDs and dIs: Possible interpretations

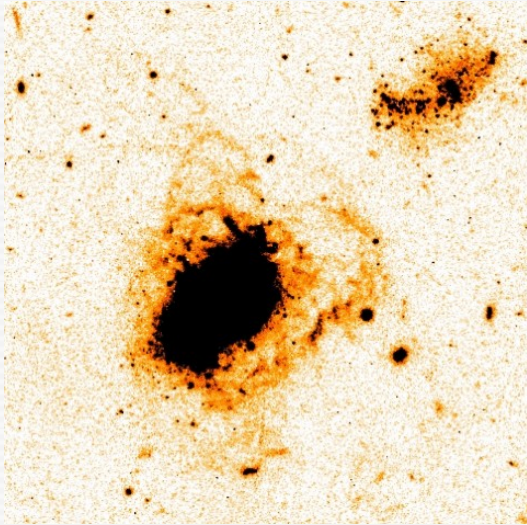
- a) **bimodality** with regard to certain intrinsic properties (e.g. **spin**): why?
- b) dynamical/evolutionary effect: **adiabatic contraction & expansion** of the dI/BCD host in response to gas infall *prior to* the starburst and subsequent gas ejection *during/after* the starburst.

Possible only if Dark Matter **does not** dominate the mass within the Holmberg radius (P96).

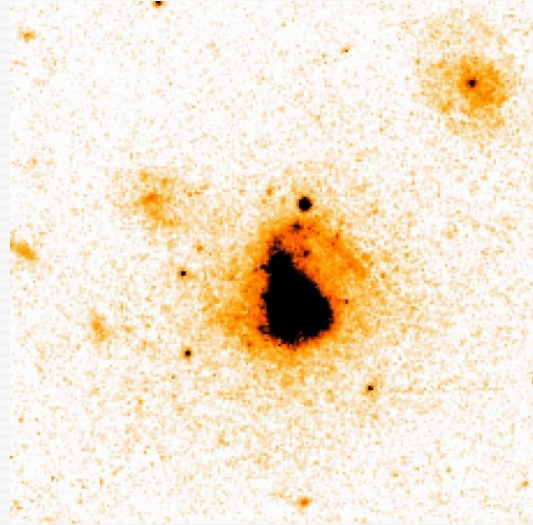


# Extremely metal-poor (XMP) BCDs: XBCDs

## Young galaxy candidates in the nearby universe?

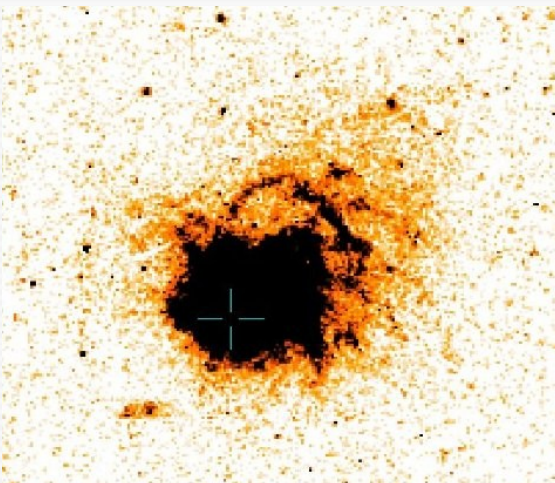


Papaderos et al. (2002)

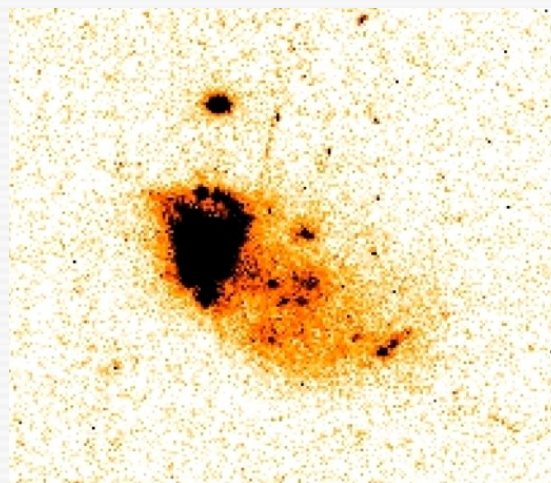


Guseva, Papaderos, Izotov et al. (2004)

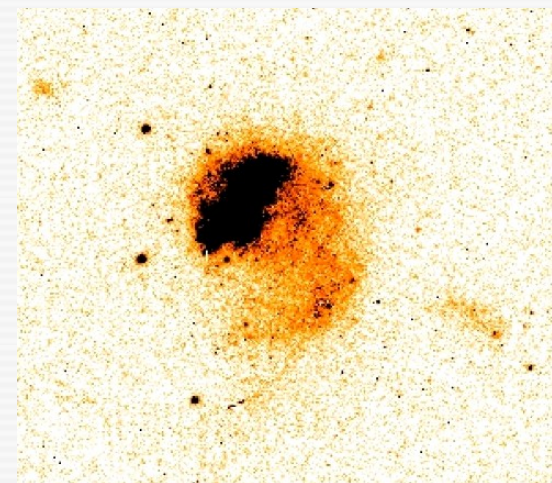
- Gas-phase metallicity:  
 $6.9 \lesssim 12 + \log(O/H) \lesssim 7.6$
- No evidence for a dominant old stellar population (>50% of  $M_*$  formed in the past 1-3 Gyr)
- Irregular morphology, with a remarkably large fraction of **cometary** systems



Thuan et al. (1997), Papaderos et al. (1998)



Fricke et al. (2001)

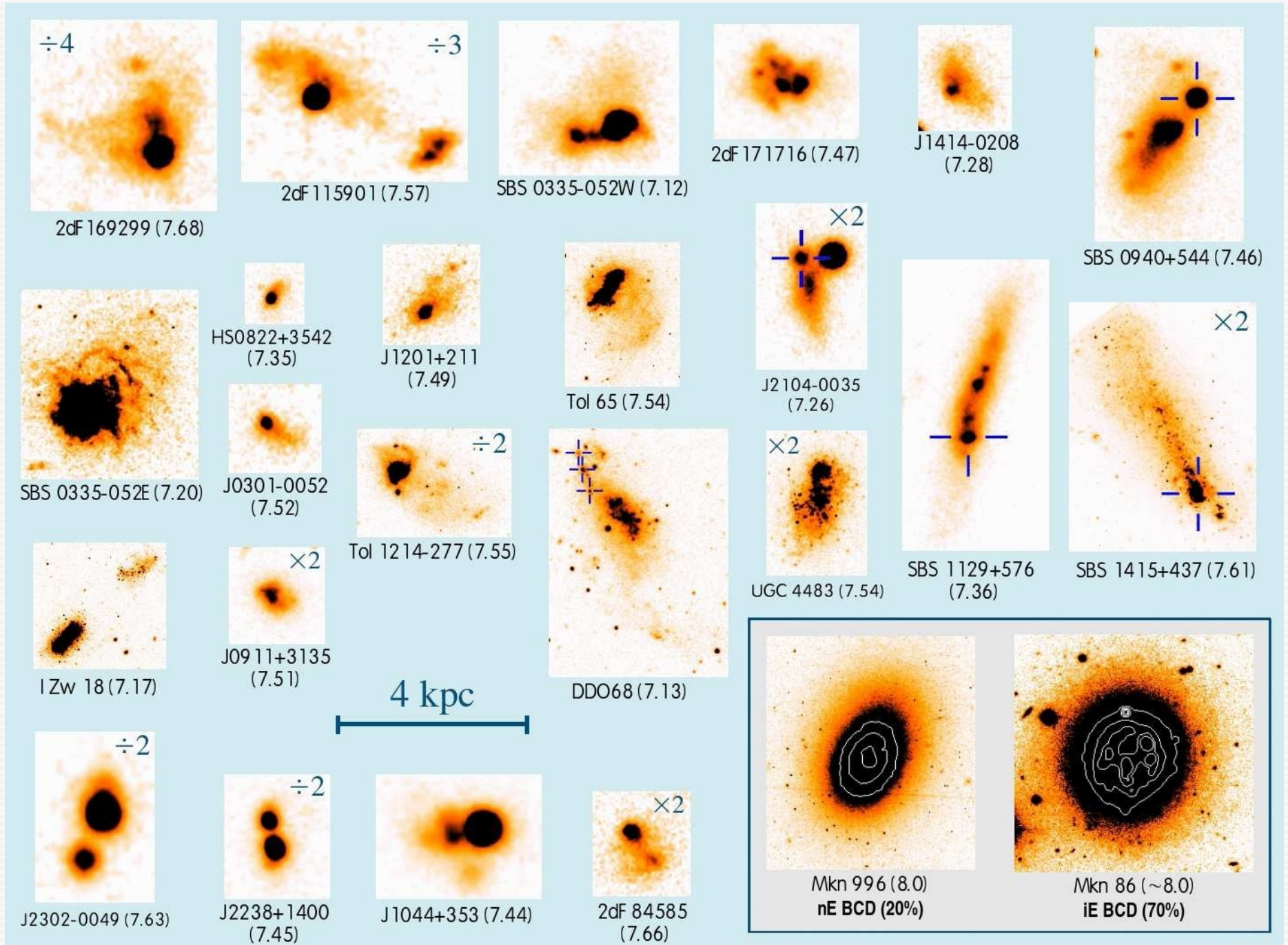


Papaderos et al. (1999,2007)



# Morphological comparison of BCDs and XBCDs

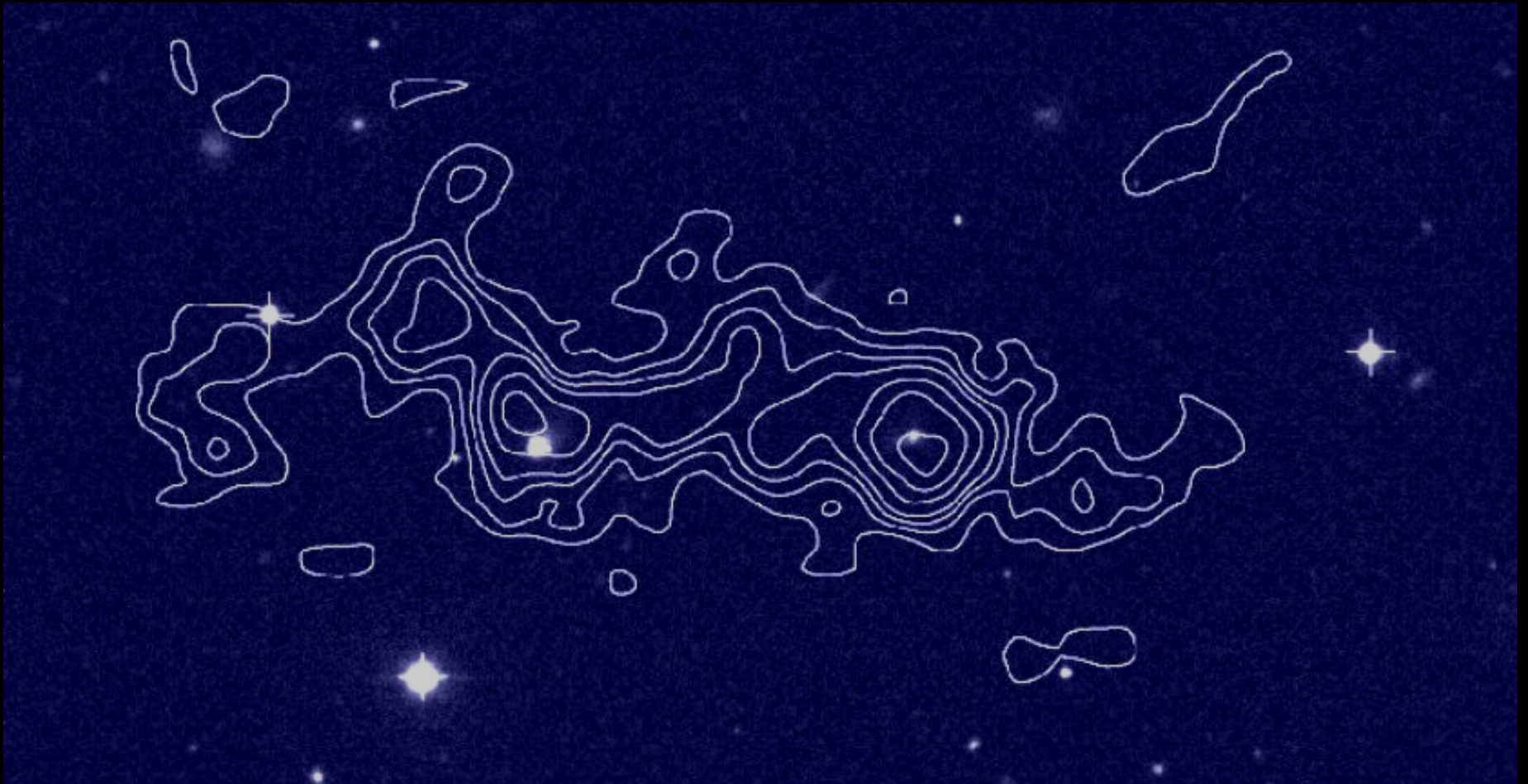
XBCDs



BCDs

# Pairwise XBCD formation

Example: the XBCD pair SBS 0335-052 E&W



Pustilnik et al. (2001)

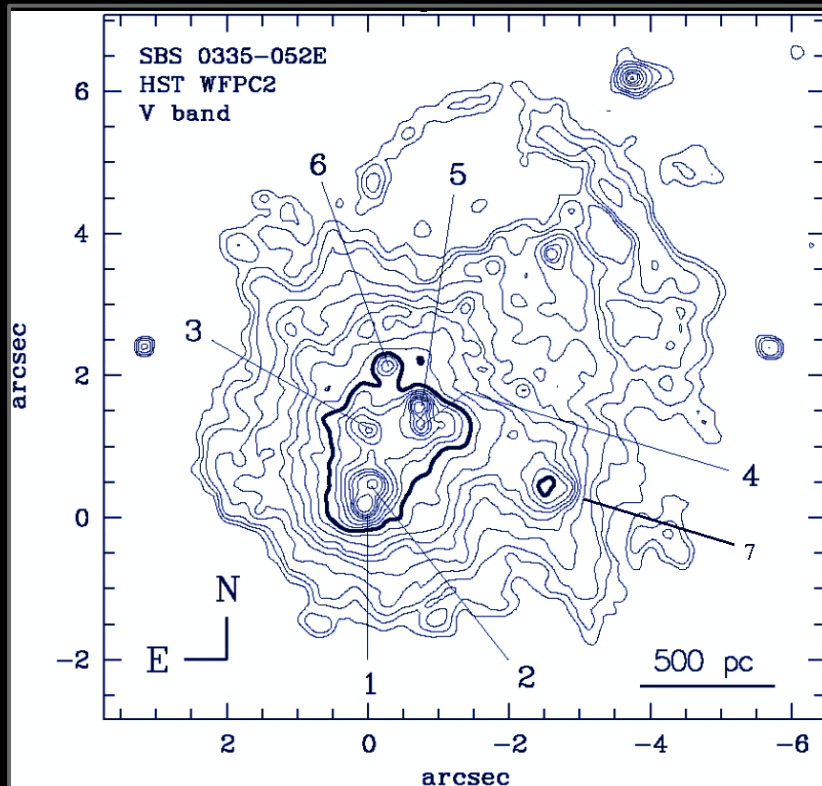
SBS 0335-052: HI cloud with a projected size of  $70 \times 20$  kpc; mass of  $\sim 10^9 M_{\odot}$



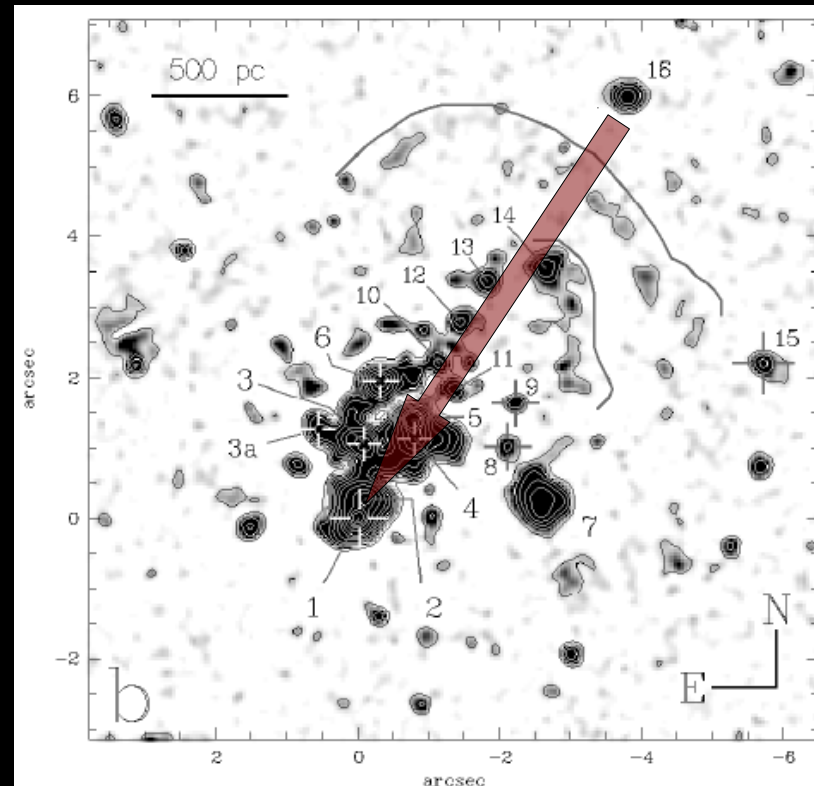
# SBS 0335-052 E: formation through propagating star formation



- Study of the V-I color and spatial distribution of stellar clusters using HST data
- 
- galaxy formation in a propagating mode from NW to SE with a mean velocity of  $\sim 20$  km/s.

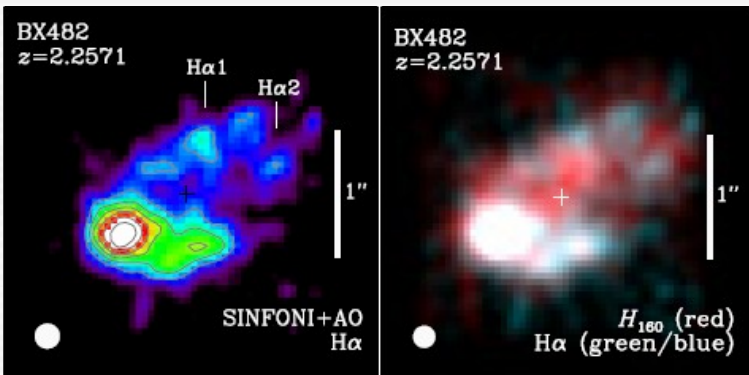
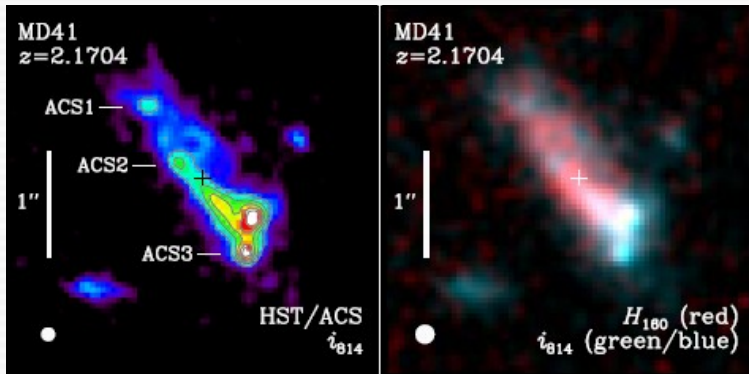


HST/WFPC2, V band



HST/WFPC2, I band, unsharp masked

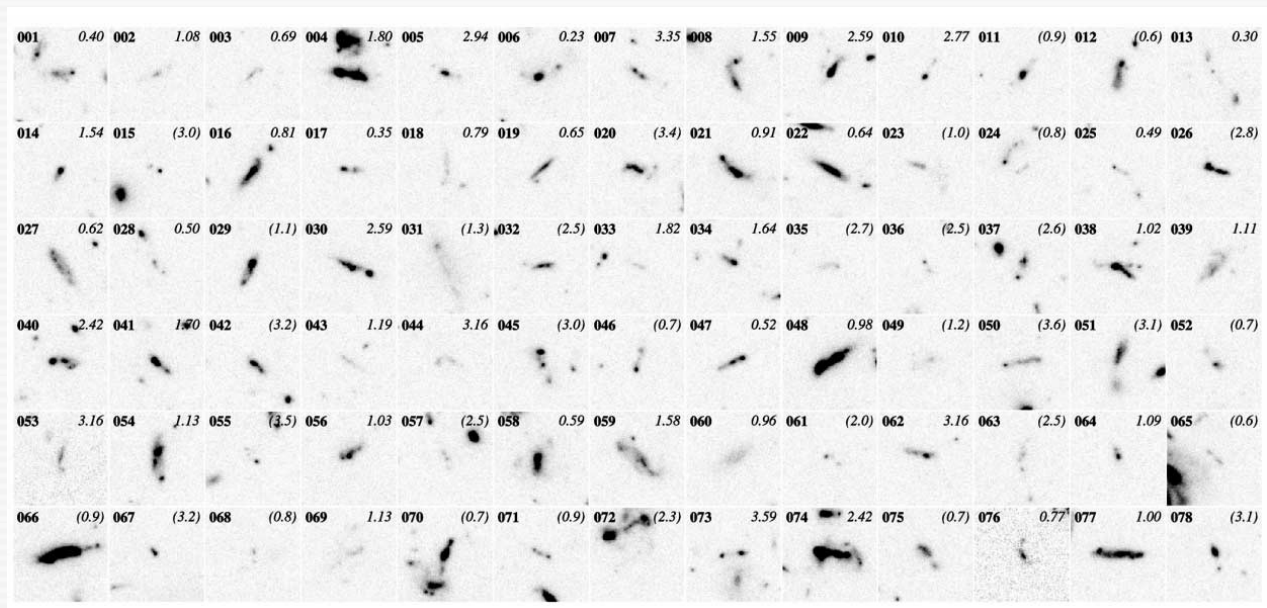
# Cometary (or tadpole) massive galaxies at high redshift



Förster-Schreiber et al. (2011)



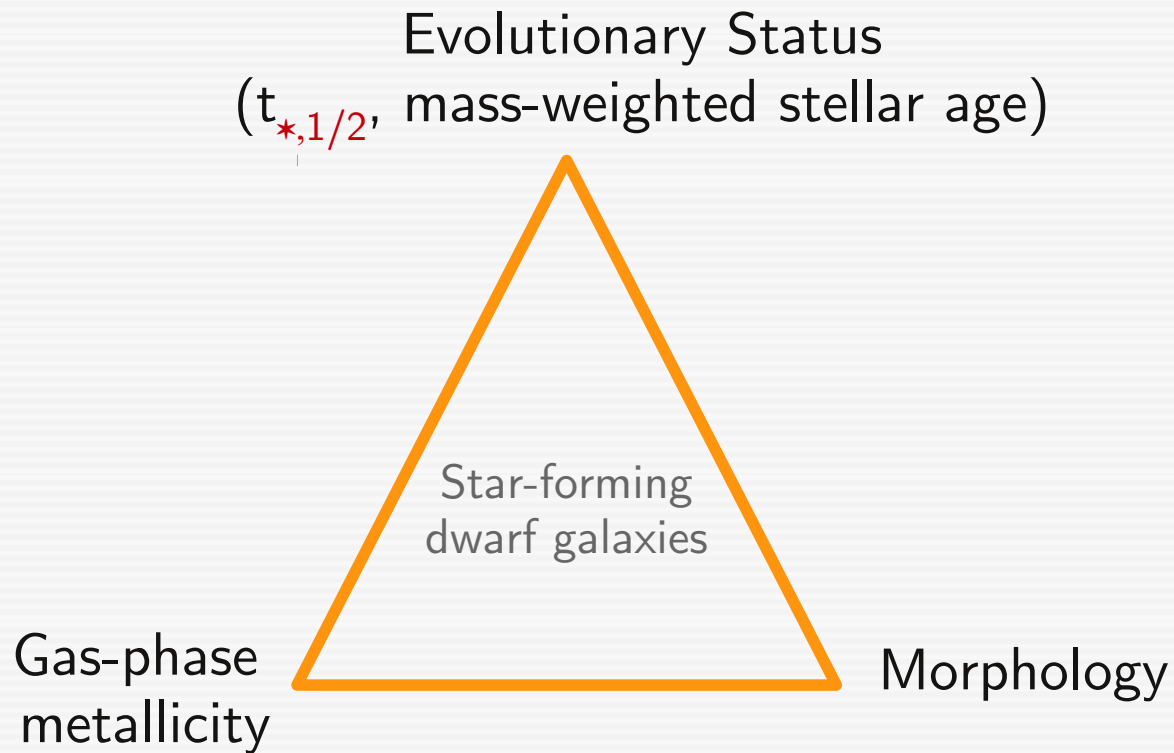
HUDF: Elmegreen et al. (2005)



Hubble Ultra Deep Field (HUDF): Straughn et al. (2006)

## Possible mechanisms

- propagating star formation (Papaderos et al. 1998)
- weak tidal interactions (Straughn et al. 2006)
- turbulent clumpy galactic disks in formation at high redshift (cf Bournaud et al. 2009)
- stream-driven accretion of metal-poor gas from the cosmic web (see Sanchez-Almeida et al. 2014 for a review; Dekel & Birnboim 2006, Dekel et al. 2009)

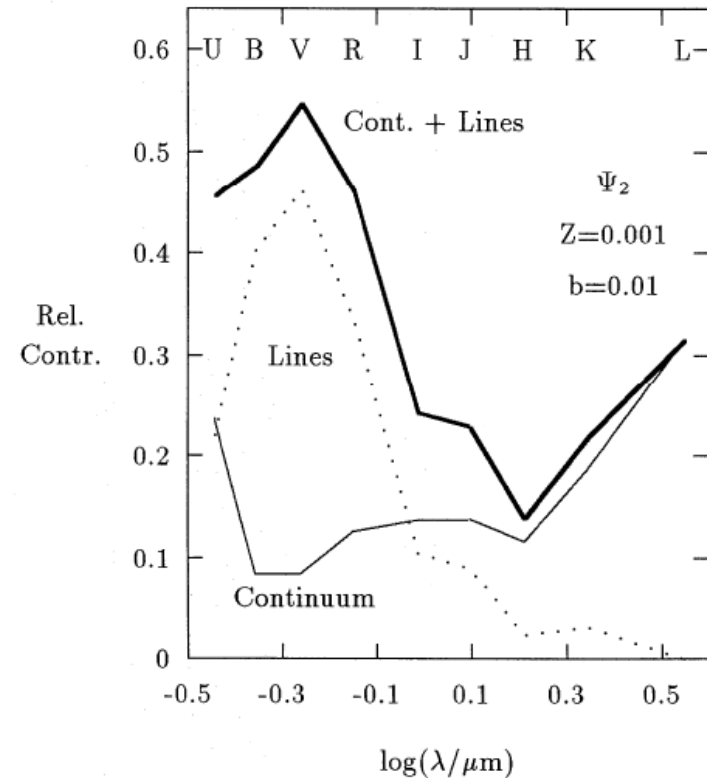
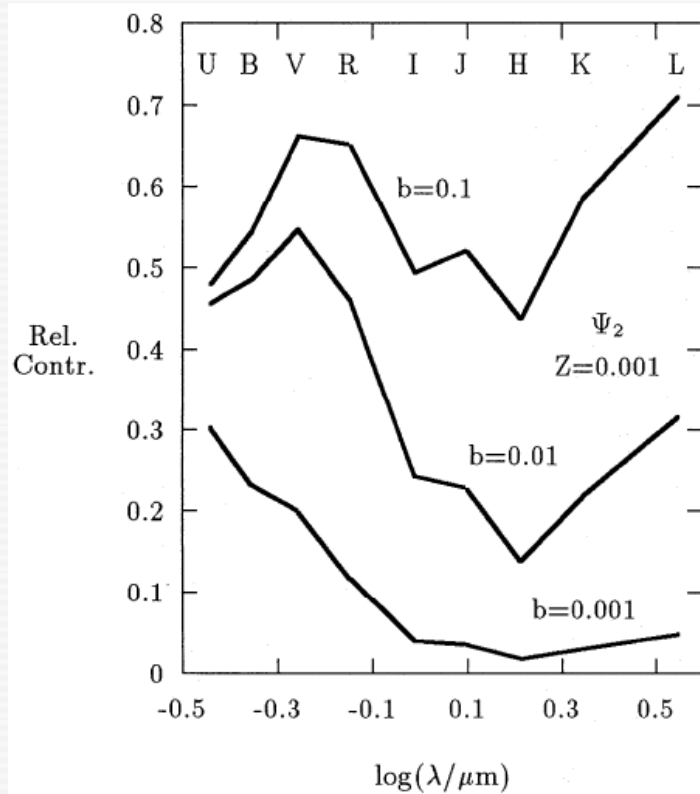


Integral Field Spectroscopy provides a powerful means for the exploration of the assembly history of low-mass galaxies, resolved in space and time



# Impact of nebular emission on photometric studies of star-forming galaxies

# Impact of nebular emission on photometric quantities



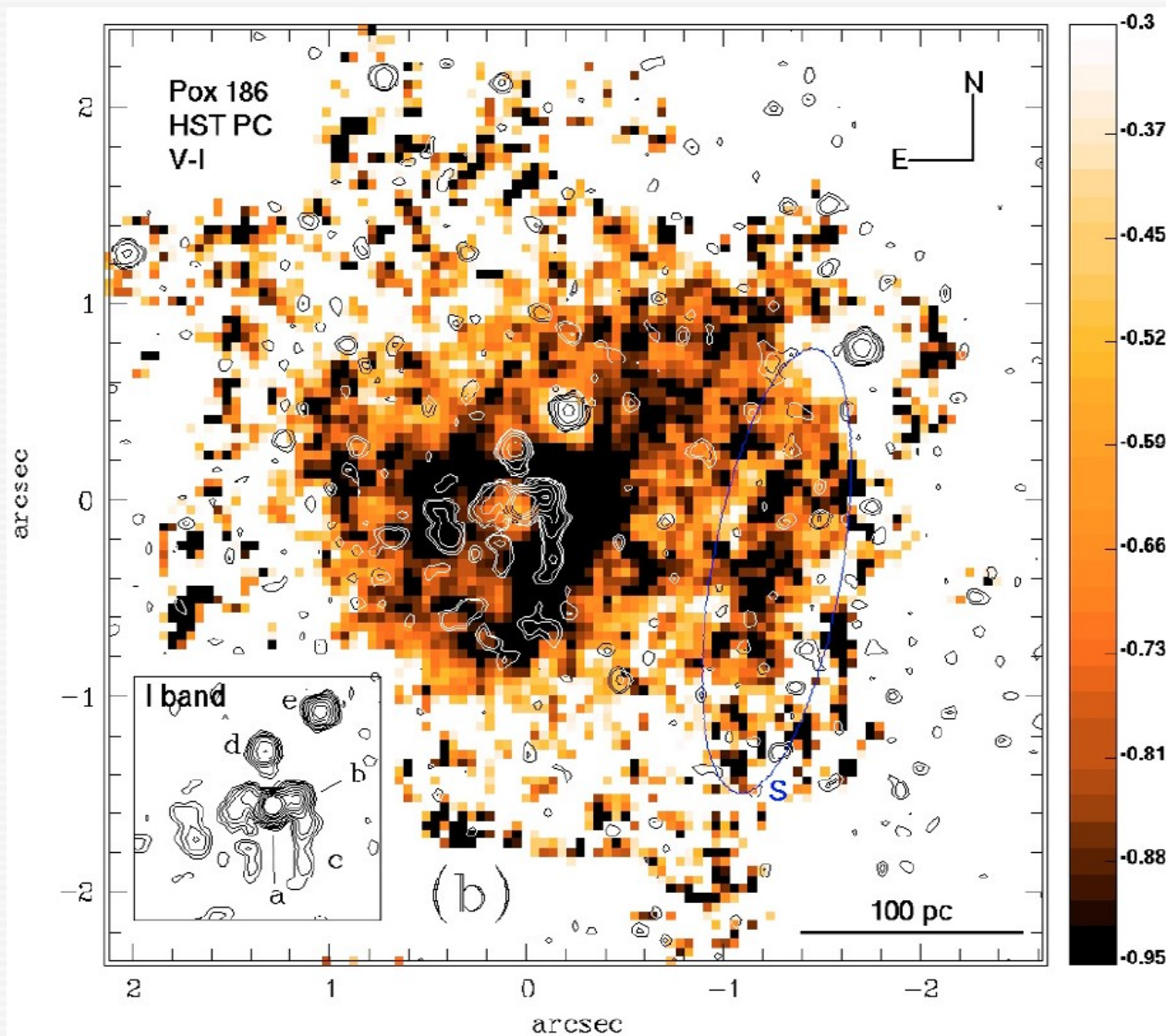
Contribution of nebular emission to broadband fluxes (Krüger et al. 1995)

Chemically consistent evolutionary synthesis model for various SFHs (continuous or exponentially decreasing SFR for the underlying **host** + **burst**)

**Table 3.** Colour indices (Johnson's system) of the total gas component (lines + continuum) for both metallicities and for the pure gas continuum

Colour index	Total gas component		Continuum
	$Z = 0.02$	$Z = 0.001$	
U - B	-1.30	-0.59	-1.79
B - V	0.40	0.45	0.34
B - R	1.10	0.48	0.97
V - R	0.70	0.02	0.64
R - I	-0.08	-0.67	0.13
V - K	0.37	0.14	2.00
J - H	-0.01	-0.01	0.29
H - K	0.69	0.69	0.72

# Impact of ionized gas emission on broadband colors



Several starburst dwarf galaxies (BCDs, and in particular extremely metal-poor BCDs) show intense nebular emission ( $EW > 1000 \text{ \AA}$ ), 0.1-1 kpc away from their SF regions

Typical signatures:  
very blue (-0.5 .. -1 mag) V-I and R-I and  
moderately red (0.4 ... 0.6) B-R and V-R colors

Corrections for ionized gas emission are necessary for age-dating of stellar populations using colors and/or color magnitude diagrams

Guseva et al. (2004)



# Age dating of starburst galaxies

## through simultaneous modeling of stellar and nebular emission

Spectral synthesis model for the extremely metal-poor BCD SBS 0335-052E

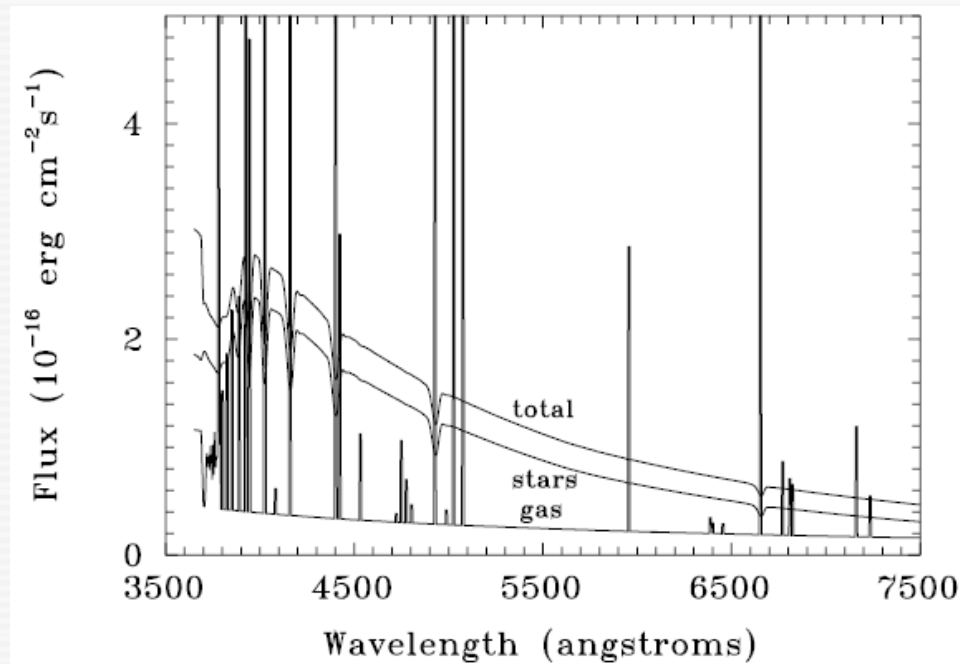


Table 3. Synthetic colours for the central part of SBS 0335-052E

$\log t$	$U - B$	$B - V$	$V - I$	$R - I$	$V - K$
a) Stellar emission					
6.3	-1.14	-0.21	-0.14	-0.12	-0.70
6.6	-0.71	-0.05	0.04	-0.04	-0.24
6.7	-0.67	0.03	0.19	0.04	0.10
7.0	-0.86	-0.10	0.02	-0.06	-0.16
b) Stellar and gaseous emission					
6.3	-0.96	0.20	-0.44	-0.43	0.12
6.6	-0.64	0.29	-0.32	-0.35	0.23
6.7	-0.61	0.34	-0.21	-0.28	0.34
7.0	-0.75	0.26	-0.33	-0.37	0.25
obs	...	...	-0.6 $\div$ 0.2	...	...

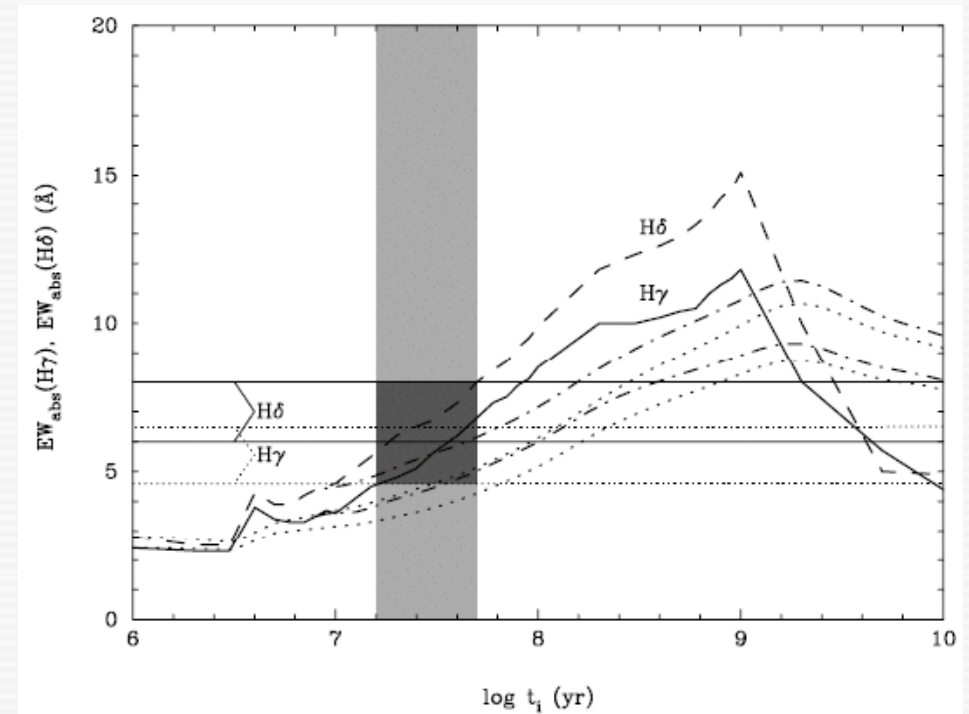
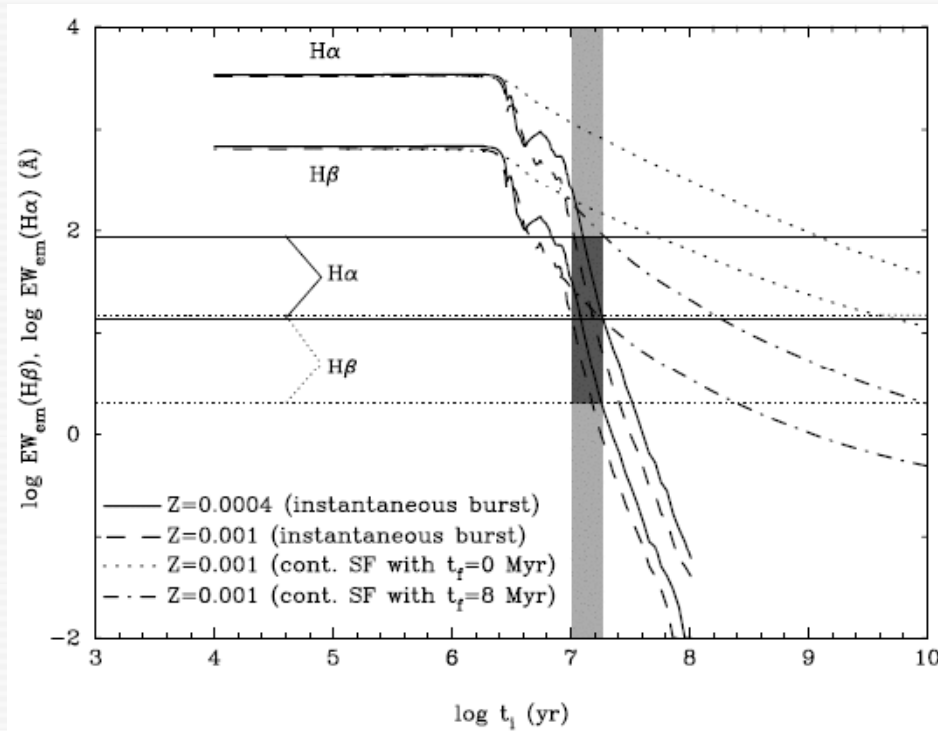
Papaderos et al. (1998)

**Option 1:** Computation of the contribution of ionized gas emission from the expected Lyman continuum rate and subtraction from the observed spectrum in order to isolate (and age date) the pure stellar spectral energy distribution (SED) from the total SED.

### Option 2:

- Superposition of different synthetic stellar SEDs to the observed nebular SED to match the observed total emission.
- Scaling of the contribution of the nebular emission to the stellar emission by the ratio of the observed equivalent (EW) width of the H $\beta$  line to the EW of H $\beta$  expected for pure gaseous emission.
- Computation of the nebular continuum SED (incl. bound-free, free-free, two-photon continuum emission; cf Aller 1984; Ferland 1980).

# Steps towards self-consistent evolutionary synthesis involving both stellar and nebular emission in SFDGs



Guseva et al. (2001)

## Goal

Identification of the SFH that reproduces simultaneously:

- the EWs of Balmer H $\alpha$  and H $\beta$  emission lines
- the EWs of Balmer H $\gamma$  and H $\delta$  absorption lines
- the slope of the observed spectral energy distribution (SED)
- the observed broad band colors

## Limitations

Simple parametrizations of the SFH (e.g., **old** + **young** stellar component, approximated, respectively, by an exponentially decreasing SFR and a single burst with varying duration and burst parameter)

# Steps towards self-consistent evolutionary synthesis involving both stellar and nebular emission in SFDGs

Guseva et al. (2001)

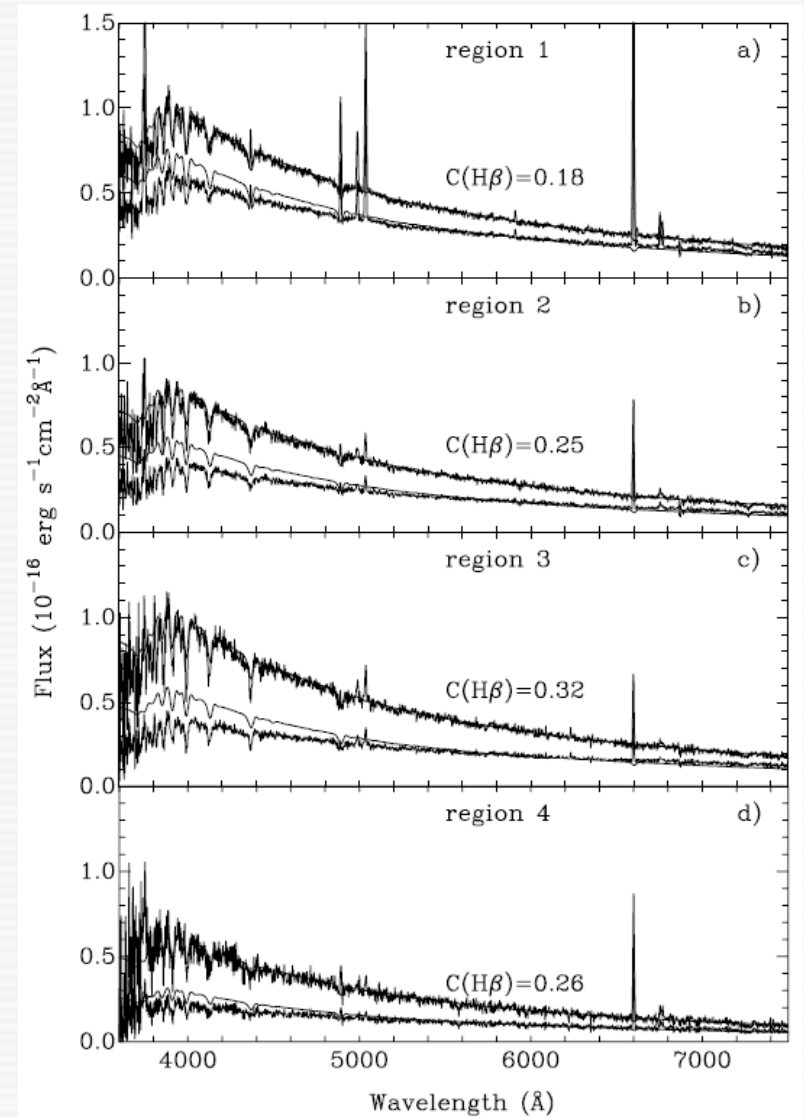
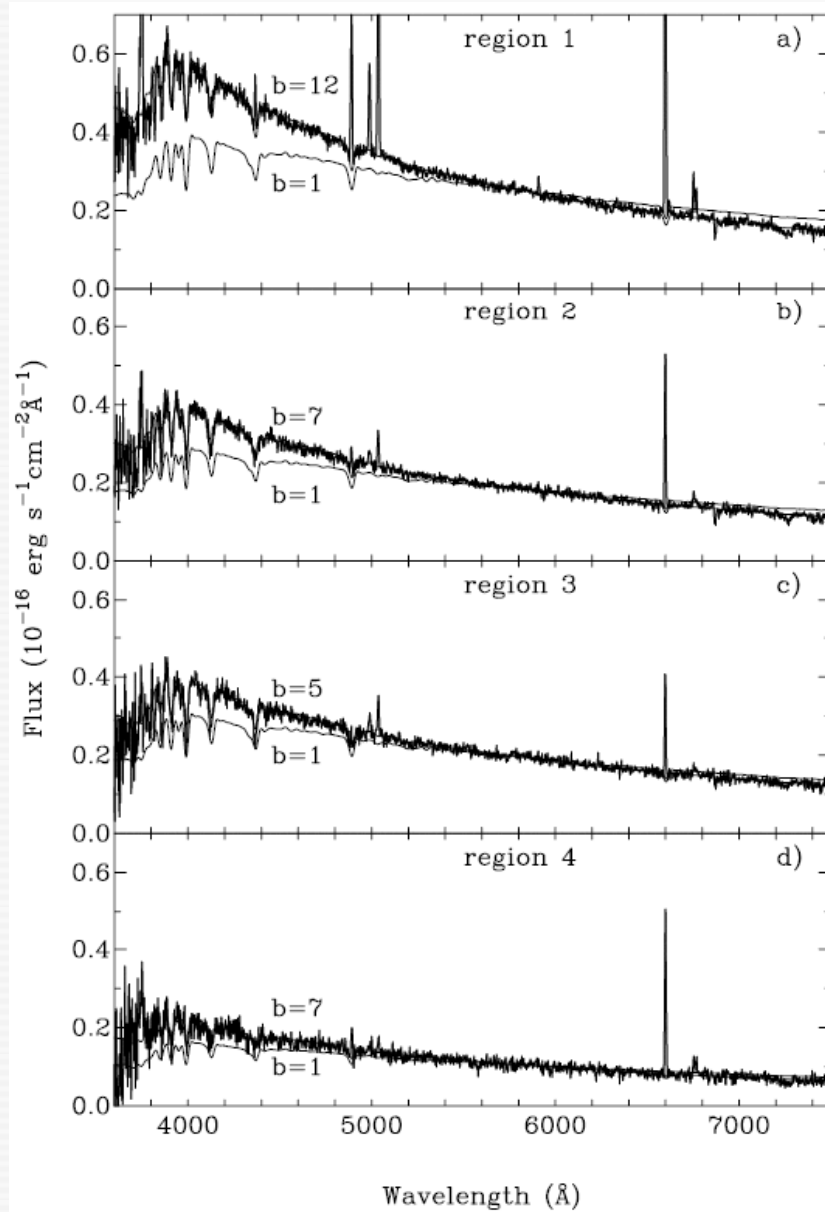


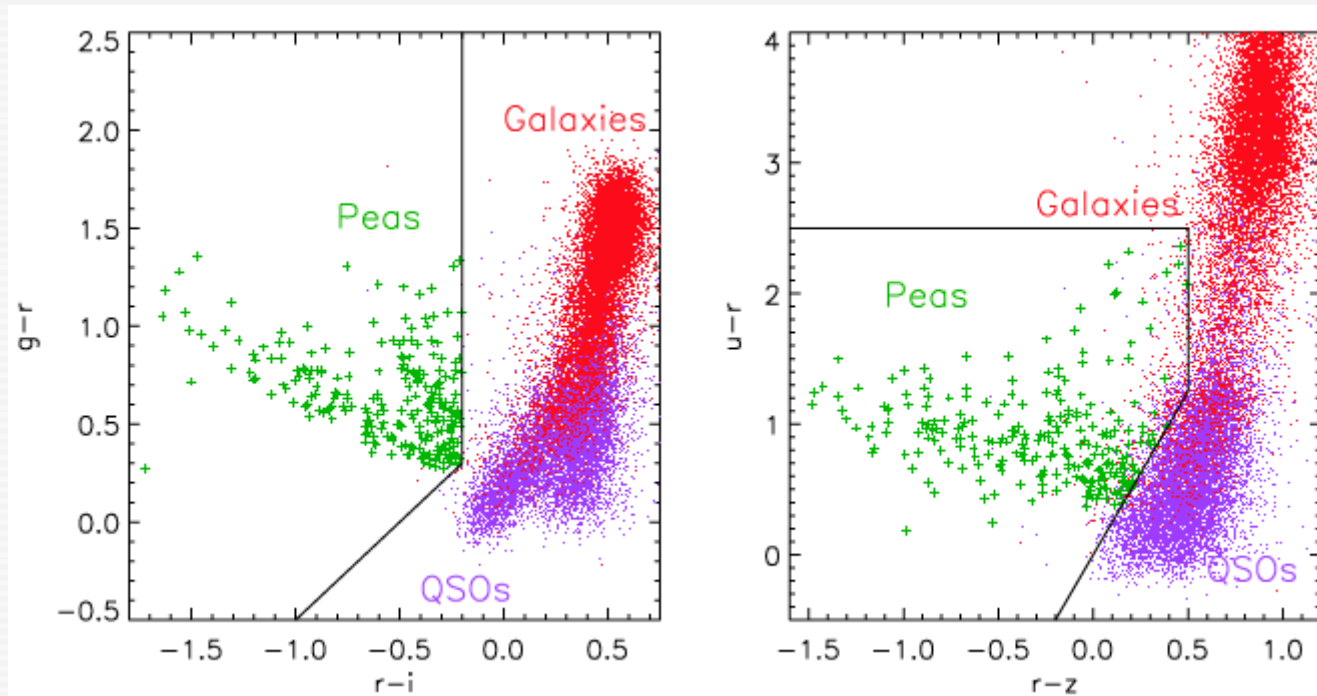
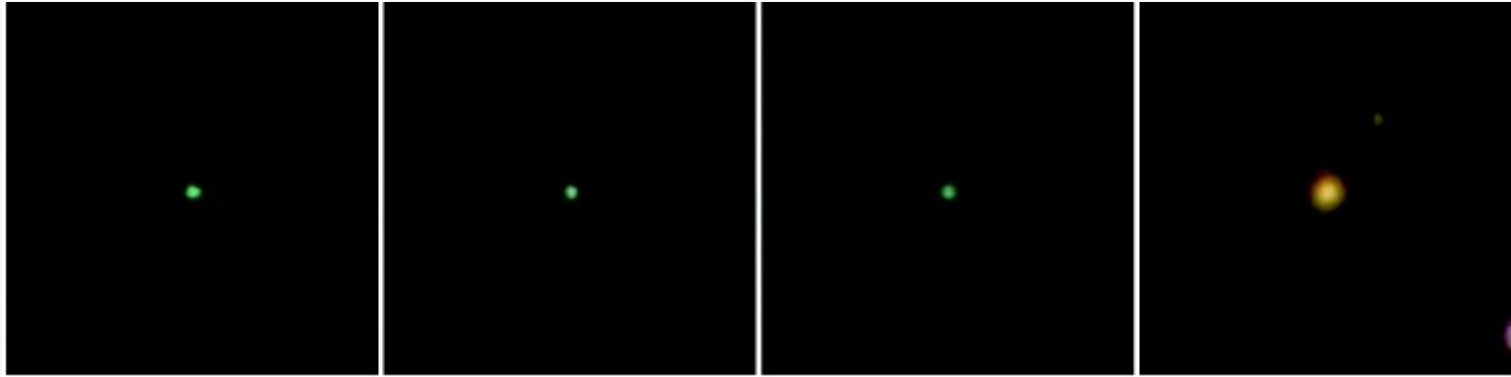
Fig. 11. Keck II telescope spectra of 4 regions in the main body of SBS 0940+544 on which synthetic continuum spectral energy distributions are superposed. Lower spectra in a)–d) are synthetic SEDs of a 20 Myr instantaneous burst stellar population superposed on the observed spectra uncorrected for extinction ( $C(H\beta) = 0$ ). Upper spectra in a)–d) are synthetic SEDs of a 20 Myr instantaneous burst stellar population superposed on the spectra corrected for extinction. Each upper spectrum is labeled by the extinction coefficient  $C(H\beta)$  which gives the best fit of the theoretical SED to the extinction-corrected observed SED.

Constraints on both burst parameter and intrinsic extinction

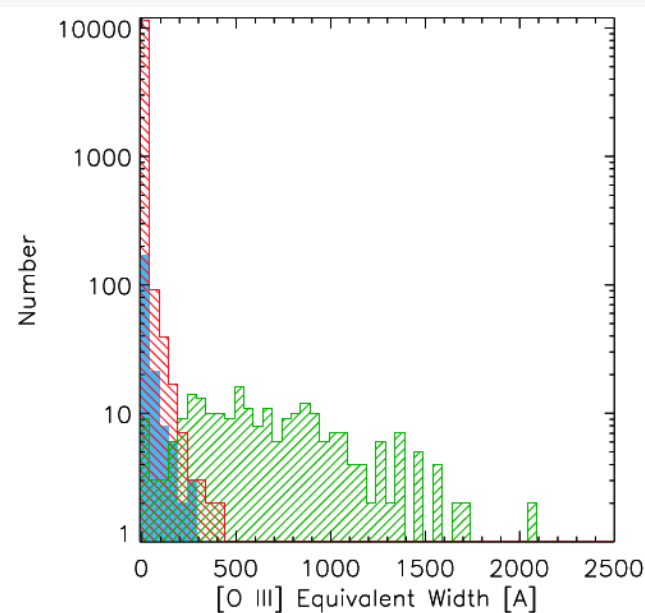
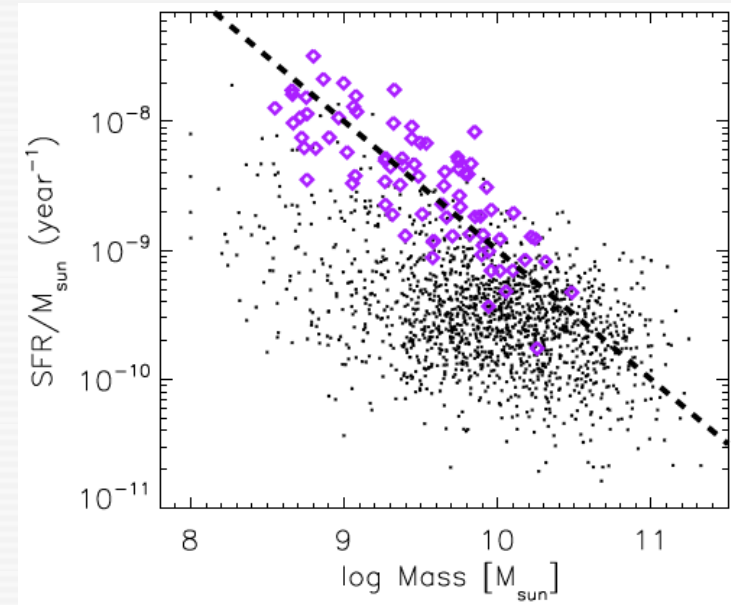
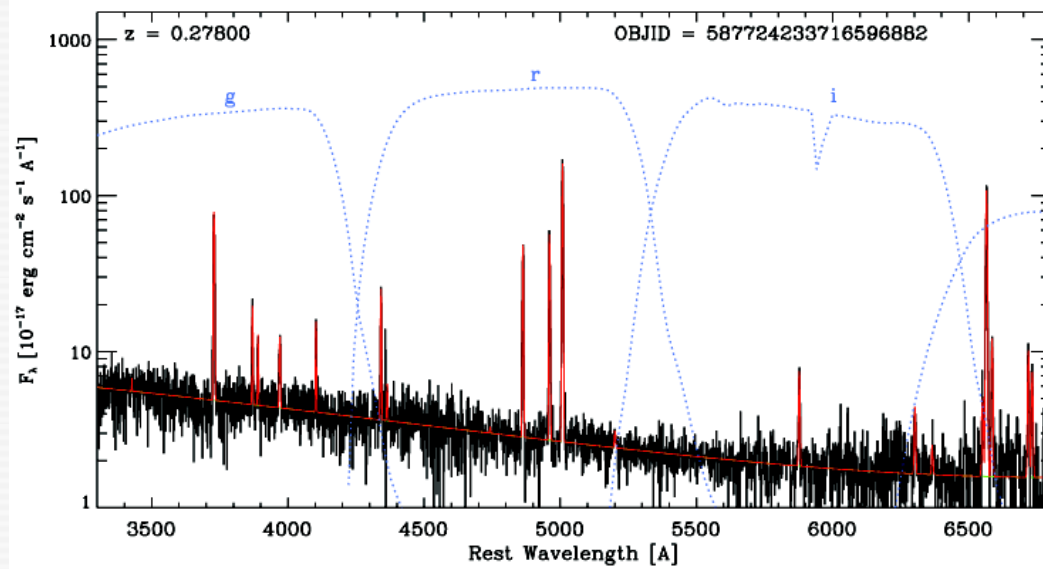


# Low-mass compact starburst galaxies at intermediate redshift

Example: “Green Pea galaxies”



# Green Pea galaxies



- Specific SFR of  $10^{-8}$  ( $\text{yr}^{-1}$ )
- i.e. mass doubling time of a few  $10^8$  yr
- Sub- $L^*$  galaxies undergoing a dominant phase in the assembly of their stellar component.
- Overabundance in nitrogen (origin ?)
- Multiple kinematically distinct components

Cardamone et al. (2010)

[OIII]5007 equivalent width of up 2000 Å, i.e. comparable to values observed in nearby XBCDs!

# Steps towards self-consistent evolutionary synthesis involving both stellar and nebular emission in SFDGs: application to **green peas**

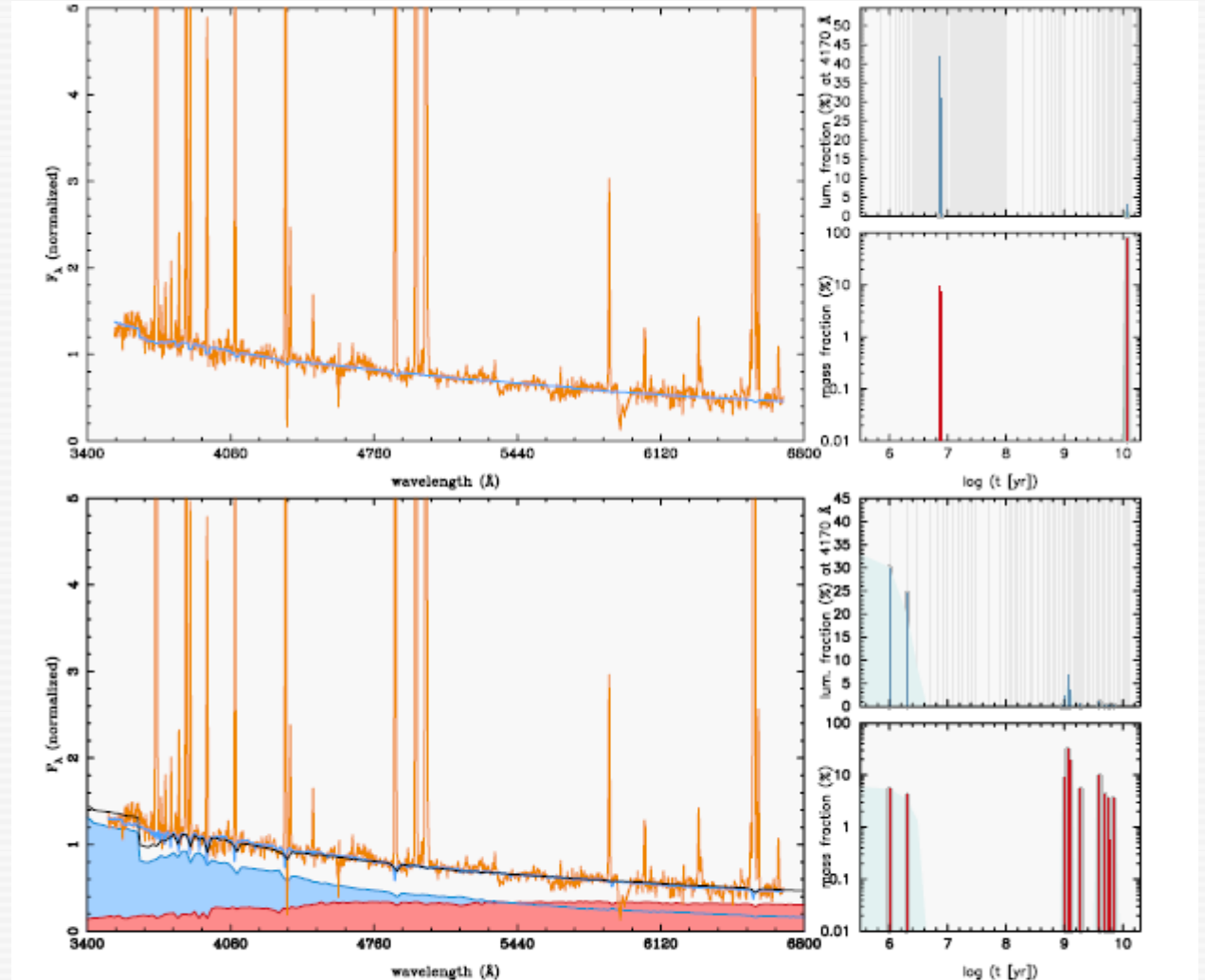
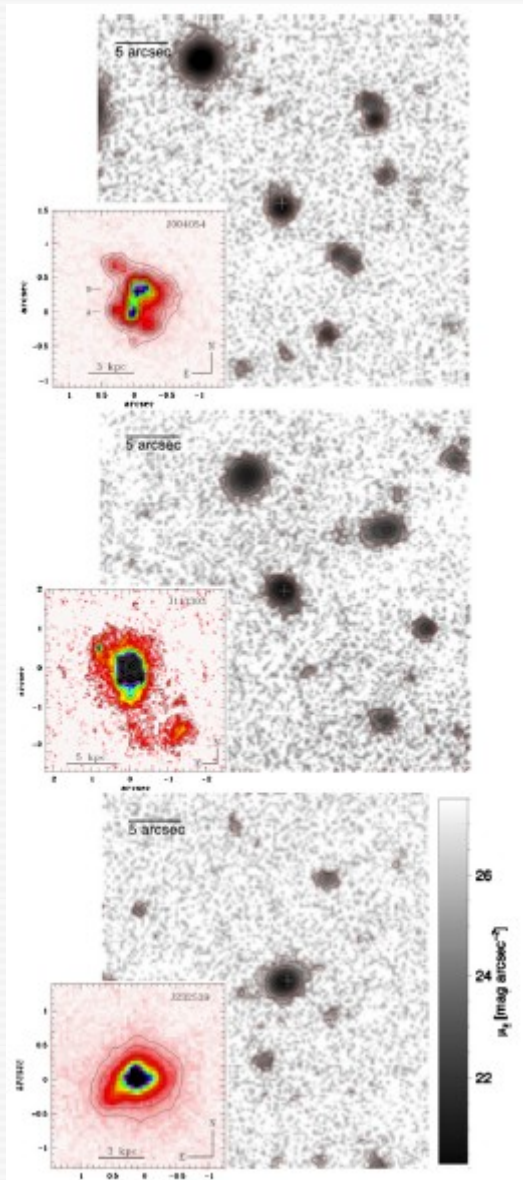


**Figure 3** Upper panel: best-fitting synthetic SED based on POPSTAR SSPs (RUN1; blue color), overlaid on the rest-frame observed spectrum of GP004054 (orange), normalized at 4170 Å. The smaller plots on the right show the luminosity and mass contribution of individual SSPs (upper and lower panel, respectively). The age distribution of the library SSPs is illustrated by thin vertical lines in the upper panel. Lower panel: fit to the observed spectrum based on purely stellar SSPs from Bruzual & Charlot (RUN2). The color coding is as in the upper large panel. Vertical strips mark regions that have been flagged prior to spectral fitting. The best-fitting synthetic SEDs from a two-component evolutionary synthesis model (RUN3) that comprises an old and a young stellar component (red and blue shaded area, respectively) and self-consistently accounts for the observed Balmer H $\alpha$  and H $\beta$  EWs are overlaid in black color.



Remarks on the biases introduced by intense and extended nebular emission in studies of high-sSFR (starburst) galaxies near and far



I Zw 18

(extremely metal-poor BCD;  $12+\log(\text{O}/\text{H})=7.2$ )

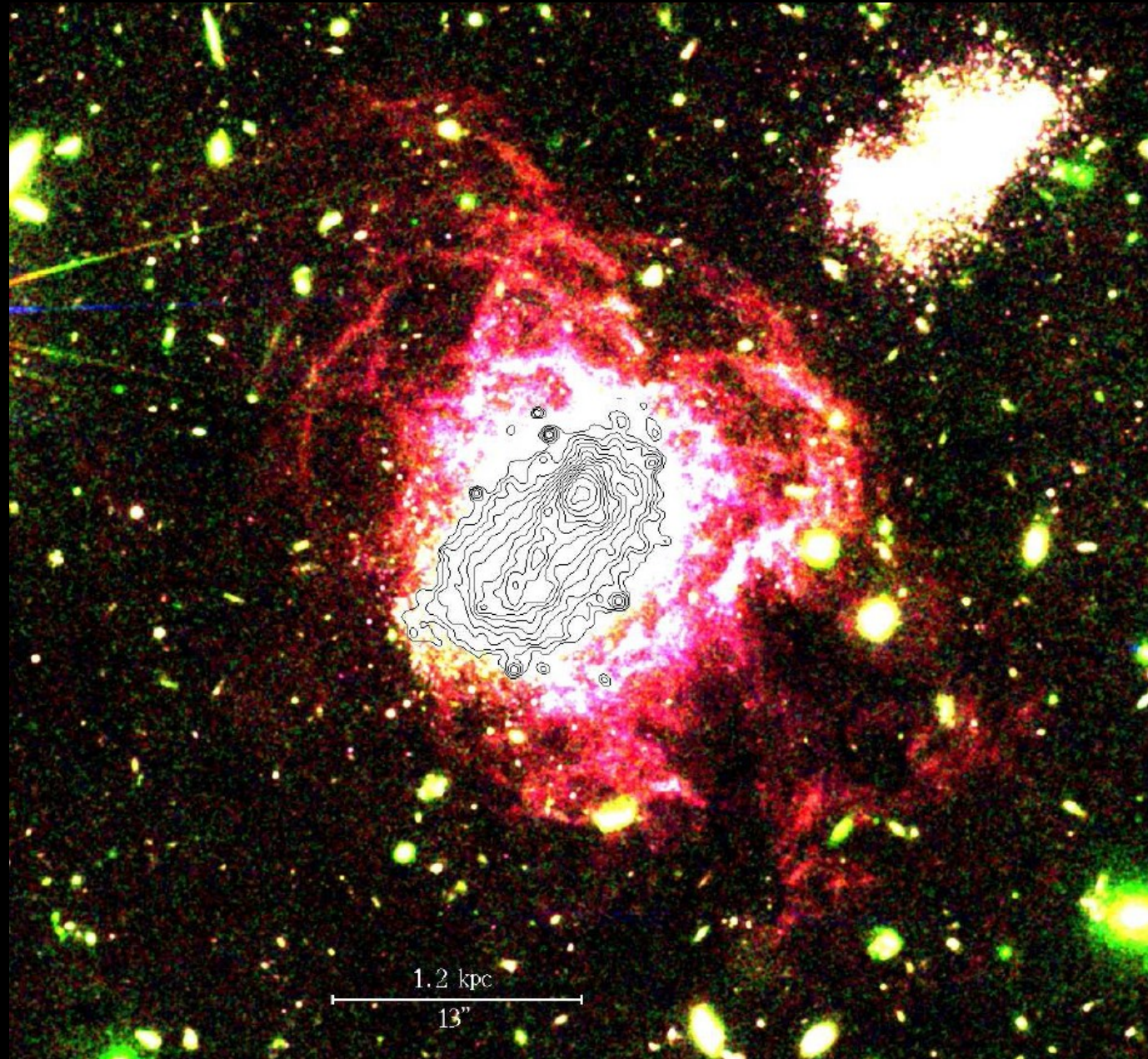
# I Zw 18: the prototypical BCD/XBCD

- 2D subtraction of nebular line emission using HST WFPC2 [OIII]5007 and H $\alpha$  narrow band images (Papaderos et al. 2002) leads to complete removal of the lower-surface brightness (LSB) envelope of I Zw 18

The LSB envelope of I Zw 18 is entirely due to extended nebular emission

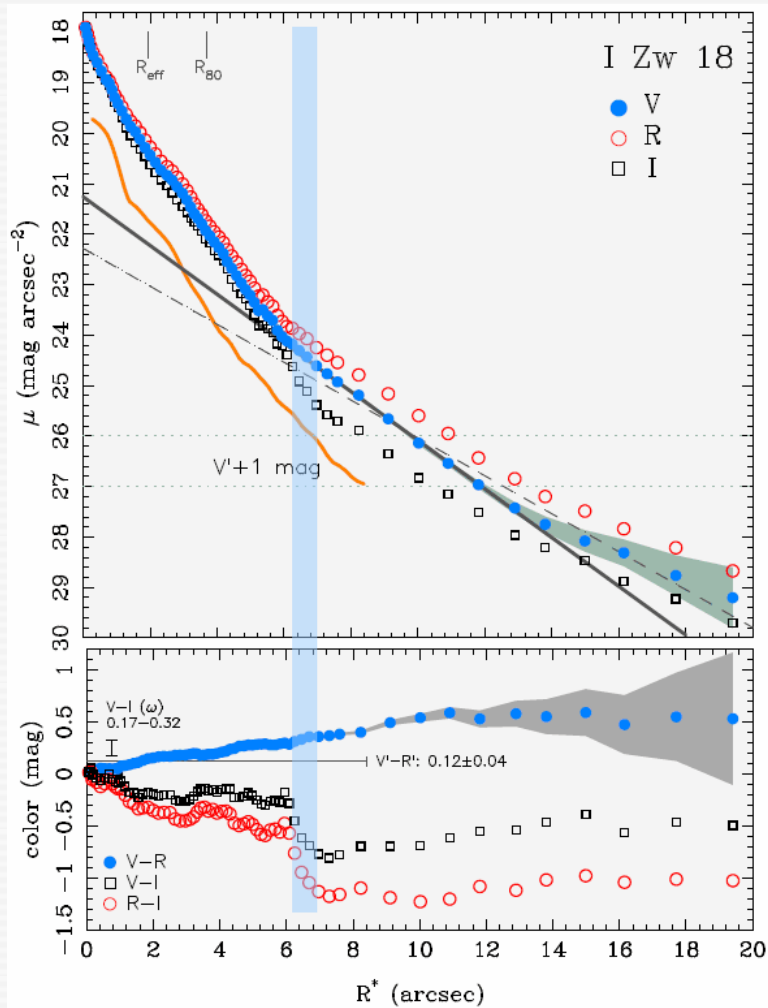
- Very deep HST ACS imaging down to  $\mu \approx 30$  mag/arcsec<sup>2</sup> (Papaderos & Östlin 2012) shows that the nebular envelope of I Zw 18 reaches out to  $R \approx 2.6$  kpc

The nebular halo of I Zw 18 extends out to **16 exponential scale lengths of the stellar component** and contributes  **$\geq 1/3$  of the total R band luminosity**





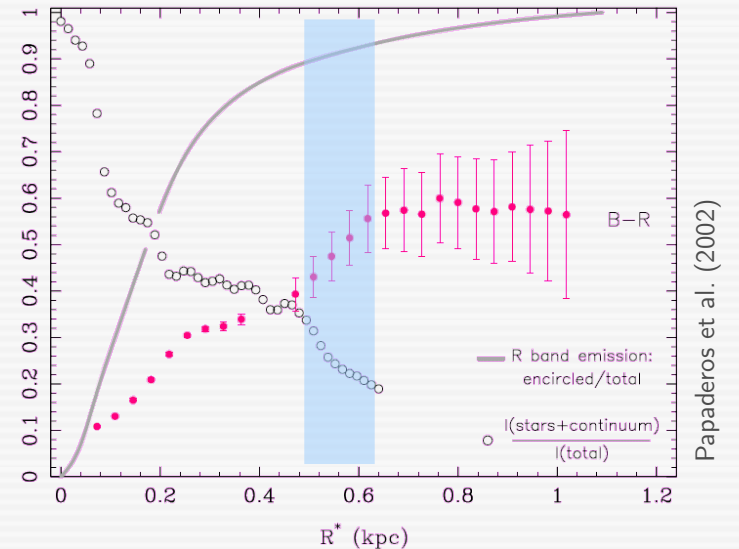
# I Zw 18: surface brightness and color profiles



Papaderos & Östlin (2012)

— Stellar + neb. continuum emission

- V-R and B-R relatively red (0.5...0.6 mag) but V-I and R-I extremely blue (-0.7 and -1.2 mag)
- There is no stellar population, regardless of SFH, age and metallicity, that can reproduce the observed combination of colors in the LSB host of I Zw 18.
- Such colors can plausibly accounted for by extended nebular emission.

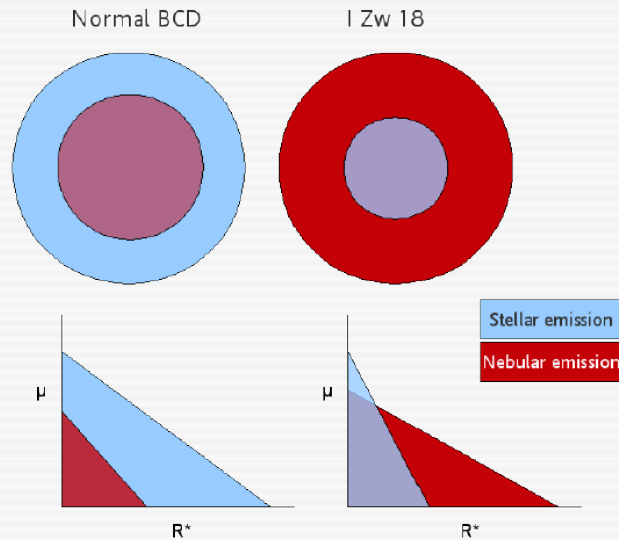


Papaderos et al. (2002)

Sudden decrease of the line-of-sight intensity contribution from the stellar component at  $\sim 6$  arcsec ( $3 R_{\text{eff}}$ ) to  $< 20\%$



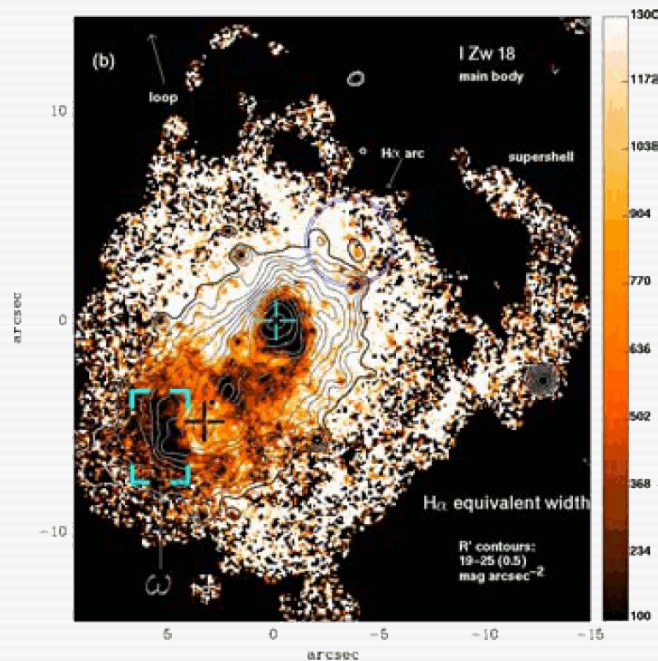
# Spatial distribution of stellar and nebular emission in I Zw 18



- Nebular emission is not necessarily cospatial with the local ionizing and non-ionizing stellar background
  - spatial anti-correlation between stellar surface density and equivalent width (EW) of nebular emission
  - important assumptions of state-of-art 0-dimensional evolutionary synthesis models are not valid

- The nebular envelope of I Zw 18 shows an exponential profile and has a relatively high surface brightness

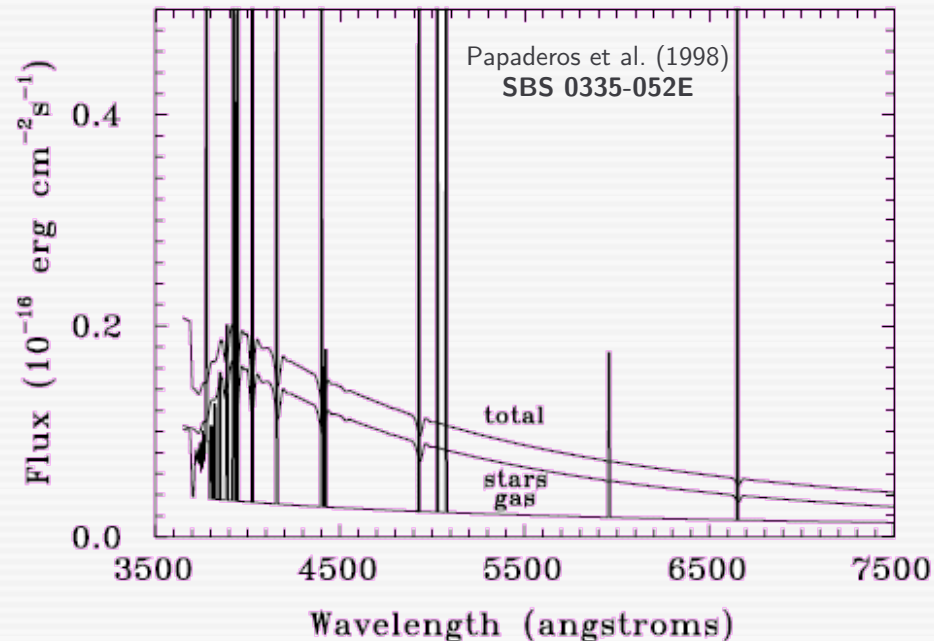
- Nebular emission contributes  $\geq 1/3$  of the optical luminosity ( $\equiv \delta_{\text{mag}} \geq 0.4 \text{ mag}$ )



Papaderos et al. (2002)

# Some biases introduced by strong nebular emission in studies of distant morphological analogs of I Zw 18 (and high-sSFR galaxies in general)

- i)** increased scatter and/or systematic error ( $\geq 0.4$  mag) in fundamental relations involving galaxy luminosities. Examples: **Tully-Fisher** relation; **luminosity vs metallicity**, **velocity dispersion**, **diameter**, **mean surface brightness**.
- ii)** errors in luminosity propagate (amplified) in  **$M_\star$  determinations** based on theoretical **M/L ratios** and **SED fitting**.



The relative contribution of nebular continuum emission increases with increasing  $\lambda$

In high-sSFR galaxies, (the reddish) nebular continuum can contribute up to 20-40% of the emission at 7000 Å → SED fitting invokes a much too high contribution from old stars →  **$M_\star$  overestimated by a factor of up to  $\sim 4$**  (Izotov et al. 2011, see also Amorin et al. 2012)

# Impact of nebular emission on photometric quantities

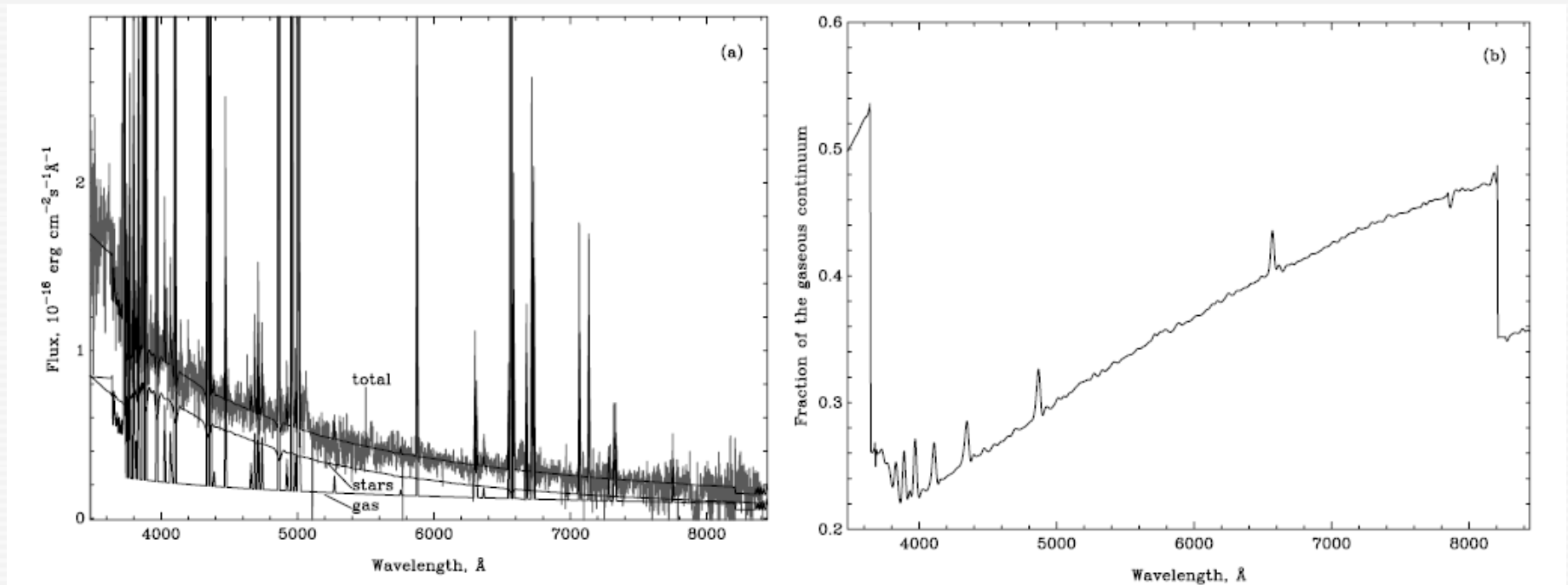


**Figure 9.** (a) Best-fit model SED (solid black line labeled “total”) superposed on the redshift- and extinction-corrected spectrum of the LCG SDSS J0851+5840 (gray line). The separate contributions from the stellar and ionized gas components are shown by black solid lines and labeled “stars” and “gas,” respectively. (b) Gaseous emission fraction vs. wavelength for the modeled spectrum of LCG SDSS J0851+5840 with  $\text{EW}(\text{H}\beta) = 303 \text{ \AA}$ . The two jumps seen at  $\sim 3660 \text{ \AA}$  and  $\sim 8200 \text{ \AA}$  are due, respectively, to the hydrogen Balmer and Paschen discontinuities in the ionized gas emission.

Izotov et al. (2011)

In high-SSFR galaxies, (the reddish) nebular continuum can contribute up to 20–40% of the emission at  $7000 \text{ \AA}$   $\rightarrow$  SED fitting invokes a much too high contribution from old stars  $\rightarrow$   **$M_{\star}$  overestimated by a factor of up to  $\sim 4$**  (Izotov et al. 2011, see also Amorin et al. 2012)